Australian Government
Geoscience Australia

Potential geologic sources of seismic hazard in the Sydney Basin

Proceedings volume of a one day workshop

Edited by Dan Clark

Record
2009/11

GeoCat # 65991

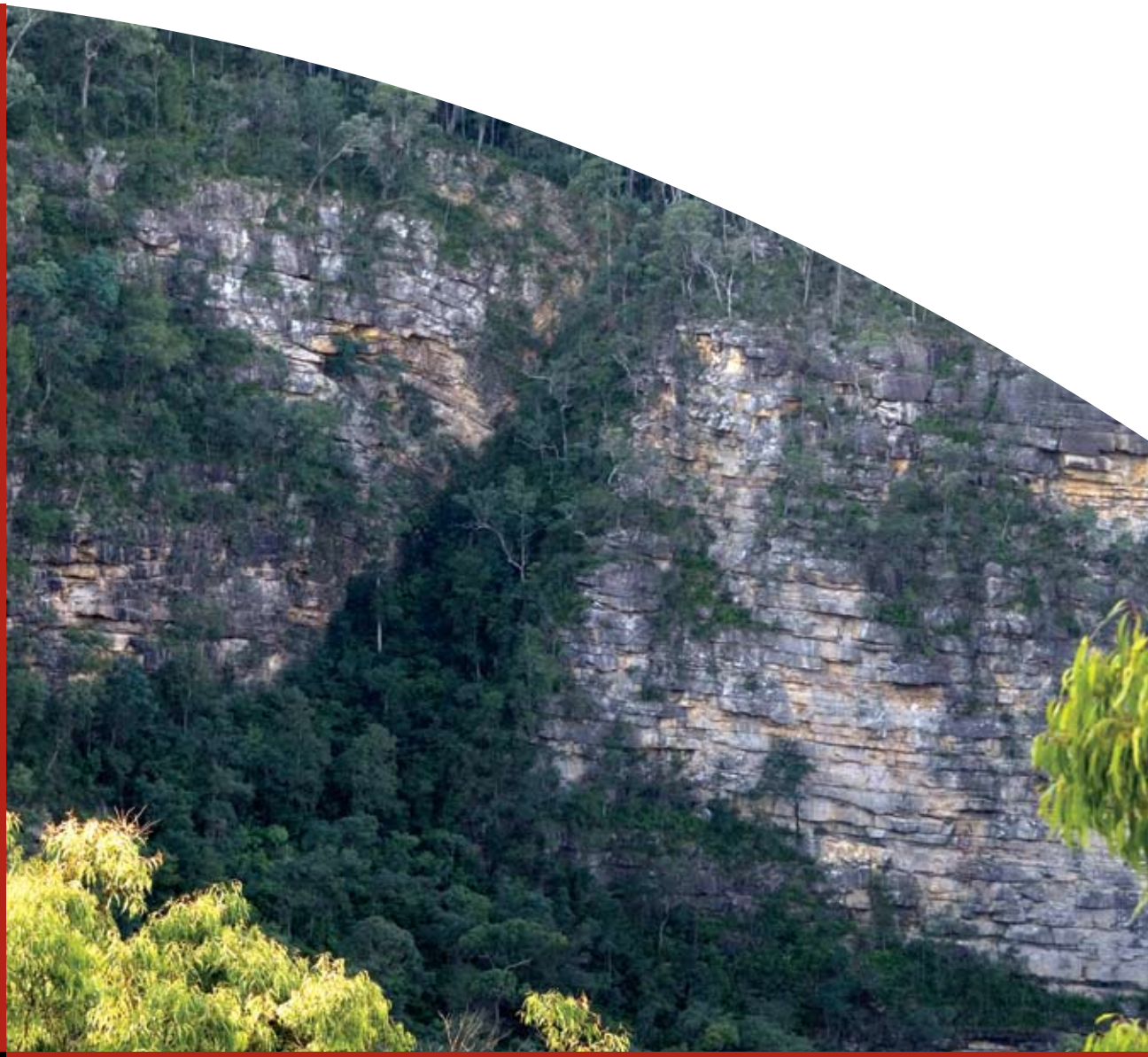

Potential geologic sources of seismic hazard in the Sydney Basin

geology

geomorphology

seismicity

hazard studies

future directions

Proceedings volume of a one day workshop:

Wednesday 13th April 2005

GEOSCIENCE AUSTRALIA
RECORD 2009/11

Workshop coordinator: Dan Clark[1]

Australian Government
Geoscience Australia

The University of Sydney

1. Natural Hazard Impacts Project, Geospatial and Earth Monitoring Division, Geoscience Australia. Email: dan.clark@ga.gov.au.

Department of Resources, Energy and Tourism
Minister for Resources and Energy: The Hon. Martin Ferguson, AM MP
Secretary: Mr John Pierce

Geoscience Australia
Chief Executive Officer: Dr Neil Williams PSM

ISSN 1448-2177
ISBN 978-1-921498-64-0 Hardcopy
ISBN 978-1-921498-63-3 Web

GeoCat # 65991

Bibliographic reference: Clark, D., (Editor), 2009. Potential geologic sources of seismic hazard in the Sydney Basin. Proceedings volume of a one day workshop. Geoscience Australia Record 2009/11. 115pp.

Foreword

The Sydney Basin encloses a significant proportion of the Australian population, and the 1989 M5.6 Newcastle earthquake demonstrated that the basin is not immune from the impact of even relatively modest earthquakes. In spite of this, few investigations have been conducted to identify and characterise potential geologic sources of strong ground shaking. A recent major study of the southern part of the basin commented that "The available data are less complete than ideal for the purposes of probabilistic seismic hazard analysis". Essentially, the extreme infrequency of large earthquake events in intraplate regions, such as Australia, means that the short historic record of seismicity is poorly suited to the task of assessing seismic hazard. Hence, geologic, geomorphic and paleoseismic knowledge has a vital role to play in obtaining constraint on the probable location and recurrence of large and damaging earthquakes near Sydney.

In April 2005 a one–day workshop at the University of Sydney brought together a diverse range of researchers with experience in the geology and geomorphology of the Sydney Basin, neotectonics and seismic hazard science. A series of seminars were presented covering geology, geomorphology, seismicity and seismic hazard. These served as a nucleation point for subsequent discussion, and the drafting of the papers presented herein. This proceedings volume contains within its covers tools for understanding large earthquake occurrence within the Sydney Basin. Hence, it represents a framework upon which future advances in our understanding of the seismic hazard posed to Australia's largest population centre may be based.

Contents

Neotectonics and landscape evolution of southeastern Australia: establishing a geologic context for contemporary seismicity

MARK C. QUIGLEY[1], MIKE SANDIFORD[1], DAN CLARK[2]
[1]SCHOOL OF EARTH SCIENCES, THE UNIVERSITY OF MELBOURNE
[2]GEOSPATIAL AND EARTH MONITORING DIVISION, GEOSCIENCE AUSTRALIA

ABSTRACT

Southeastern Australia contains a rich geologic record of Plio-Quaternary reverse faulting and associated landscape evolution that can be used to provide geologic constraints on historical seismicity. The Mt Lofty-Flinders Ranges-eastern Gawler Craton region and Eastern Highlands are characterized by high fault density, "youthful" geomorphology, and high seismic activity relative to most of Australia, including the intervening Murray Basin. Inferred ~east-west directed maximum compressive paleostress orientations derived from Plio-Quaternary faults are generally consistent with ~east-west to ~southeast-northwest maximum compressive stress orientations derived from historical earthquake focal mechanisms, providing a link between the neotectonic record, seismicity, and *in situ* stress. Plio-Quaternary fault slip rates along range-bounding reverse faults range from 20 to 150 m per million years (m Myr^{-1}). Coupled with slow bedrock erosion rates at range summits, this suggests a minimum of 100 m of surface uplift has occurred over considerable areas of southeastern Australia since the Miocene. Estimates of recurrence interval of large magnitude, surface rupturing earthquakes along individual faults range from ~ 22 000 to ≥ 83 000 years. Single-event fault displacements may have reached up to 8 m in total fault offset. The data acquired from neotectonic investigations bear heavily on the modes, mechanisms, and seismic risk associated with the active regional deformation of southeastern Australia, including the Sydney Basin.

INTRODUCTION

Although records of historical earthquakes provide cursory information on active crustal deformation and seismic risk, recurrence intervals of large earthquakes in many intracontinental regions commonly surpass the life span of these records by orders of magnitude, defining the need for fault studies over geologic time-scales. The neotectonic record of prehistoric faulting provides an important source of information on the long-term behaviour of intracontinental faults, especially where it can be linked to contemporary seismicity. Australia is particularly well-suited to study these structures as much of the continent is relatively arid and has remained immune from Quaternary glaciations, resulting in high preservation levels of faults and associated landforms.

In southeastern Australia, distribution patterns of contemporary seismicity closely overlap with topographically high regions containing increased concentrations of neotectonic faults and rugged "youthful" geomorphology, implying a casual link between active deformation and landscape evolution (Fig. 1). Considerable progress has been made towards a better understanding of the dynamics, rates, and landscape manifestations of this modern tectonic regime through recent neotectonic, geomorphic, and geodynamic studies. In this paper, we briefly summarize this progress and provide a regional geologic context for southeastern Australian earthquakes.

ACTIVE DEFORMATION OF SOUTHEASTERN AUSTRALIA

Seismicity and *in situ* stress

Southeastern Australia is one of the most seismically active parts of the continent, with distributions of historical (~1850 A.D. to present) earthquakes up to Richter Magnitude ~6.4 extending from the eastern Gawler Craton to the Eastern Highlands (Fig. 1). Approximately 7000 earthquakes were

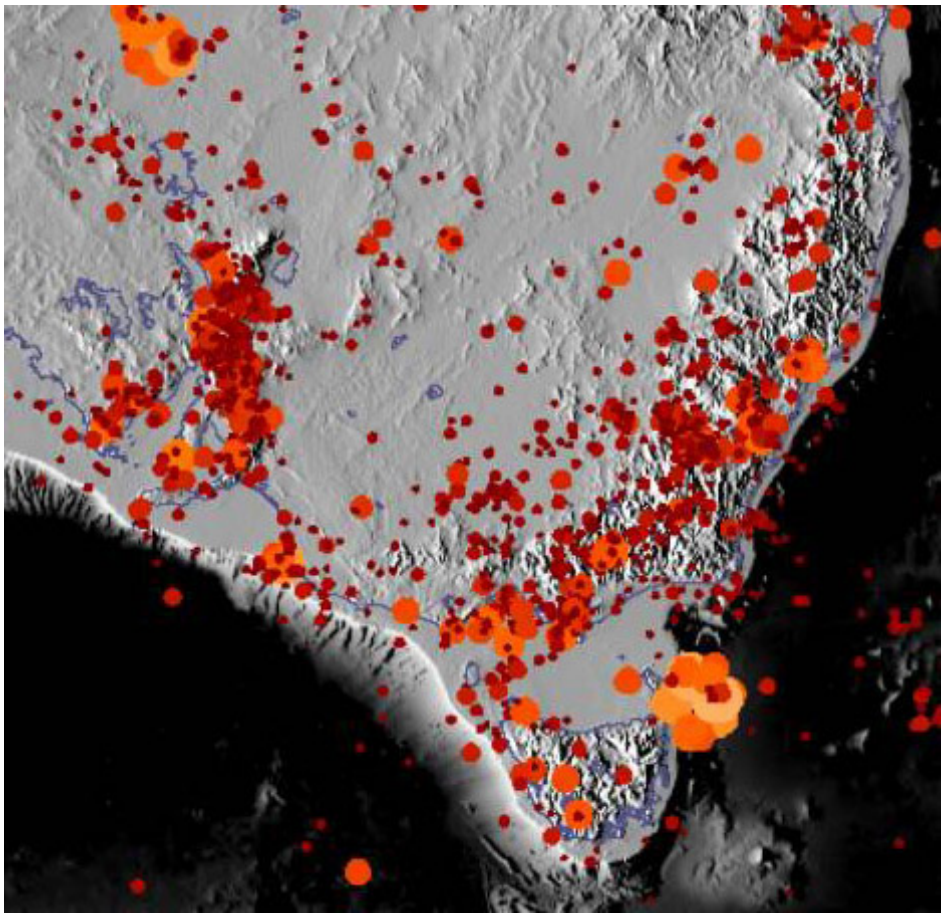

Figure 1: *Distribution of seismicity in southeastern Australia. Earthquakes concentrated in the Mt Lofty-Flinders Ranges-eastern Gawler Craton region and in a belt traversing the west coast of Tasmania through the Eastern Highlands in southeast Victoria and New South Wales.*

recorded in the region from 1958 to 1999 (Spassov and Kennett, 2000). Two distinguishable belts of enhanced seismicity are visible; the first centred within the Mt Lofty-Flinders Ranges-eastern Gawler Craton region and the second continuing from the west coast of Tasmania through the Eastern Highlands in southeast Victoria and New South Wales in the vicinity of the Sydney Basin (Fig. 1). Seismicity is considerably lower in the intervening Murray Basin and cratons to the west. Earthquake focal mechanisms in the Flinders Ranges indicate combinations of compressive strike-slip and reverse faulting along roughly north- to northeast-striking focal planes, from which a principle horizontal compressive stress orientation (S_{hmax}) of ~ 83^o was inferred (Greenhalgh et al., 1994; Hillis and Reynolds, 2000; Clark and Leonard, 2003). Reverse fault mechanisms and borehole breakouts define a roughly southeast-northwest oriented S_{hmax} azimuth (~130^o) throughout the eastern highlands in Victoria (Gibson et al., 1981; Hillis and Reynolds, 2000). The bulk of focal-mechanism data from the Sydney Basin seem to indicate a roughly northeast-southwest oriented S_{hmax} (Clark and Leonard, 2003). In summary, when historical earthquake and *in situ* stress data is considered at the scale of southeastern Australia, there seems to be a general pattern of roughly east-west oriented compression, with superimposed S_{hmax} variability a possible artefact of either seismic sampling (Clark and Leonard, 2003) and/or local geologic conditions such as topography or basin structure (Zhang et al., 1996; Hillis and Reynolds, 2000).

Quaternary faulting

Geologic studies have identified as many as 100 faults with demonstrable Quaternary displacements across southeastern Australia (Fig. 2). Recent studies have integrated ASTER and SRTM high resolution satellite imagery (Sandiford, 2003; Quigley et al., 2006), structural geology and geomorphology (Clark et al. in press), optically stimulated luminescence (OSL) dating (Quigley et al., 2006; Clark et al. in press), ^{10}Be cosmogenic nuclide dating (Quigley et al., 2007) and other techniques to provide quantitative constraints on paleoseismicity, fault slip rates, recurrence intervals, and related sedimentary and landscape responses to faulting. Several important conclusions and implications have come from this work: (1) All documented Quaternary faults involve either purely dip-slip reverse movement or oblique-reverse movement; no Quaternary strike-slip or normal faults have been found. Fault kinematic data derived from fault plane and slickenline orientations indicate a roughly east-west oriented palaeo-S_{hmax}, consistent with the S_{hmax} azimuth derived from historical seismicity (Sandiford, 2003; Quigley et al., 2006); (2) Quaternary faults commonly occur along geologic boundaries such as inherited lithotectonic boundaries (e.g., Wilkatana and Roopena / Ash Reef Faults within Lake Torrens Rift Zone) and range fronts (Flinders and Mt. Lofty Ranges) and commonly reactivate ancient fault zones (e.g., Mundi Mundi Fault, Lake Edgar Fault) (3) Estimates of prehistoric southeastern Australian earthquake magnitudes (M), based on fault rupture lengths, single-event displacements and inferred ranges of hypocentral rupture depth, range from M = 5.8 to 7.2 (Clark and McCue, 2003; Quigley et al., 2006). The data is consistent with M estimates for the largest recorded Australian earthquakes (Meeberiee, WA 1941, M=7.3; Meckering, WA 1968, M=6.8; Tennant Creek, NT 1988; M=6.7); (4) Plio-Quaternary fault slip rates derived from cumulative displacements of Pliocene and Quaternary sediments range from 20-150 m Myr^{-1} (Sandiford, 2003; Quigley et al., 2006). Fault slip rates determined from individual fault exposures are difficult to assess because of the tendency of intracontinental faulting to cluster in time and space (Crone et al., 1997, 2003). For example, faults in the Wilkatana area of the central Flinders Ranges may have incurred upwards of 15 m of cumulative slip since ~ 67 000 years ago (Quigley et al., 2006), equating to Quaternary rates of ~225 m Myr^{-1}, whereas the Lady Buxton segment of the Paralana Fault in the northern Flinders Ranges may not have moved since the Pliocene; (5) Estimates of surface-rupturing earthquake recurrence interval from Quaternary faults range from 1: 22,000 years to $\geq$ 1: 83,000 years and are also severely hampered by the sporadic nature of intracontinental faulting (Quigley et al., 2006); (6) Earthquake activity may have resulted in upwards of several 100's of meters of cumulative surface uplift in some parts of southeast Australia, such as the Flinders, Mt Lofty, and Otway Ranges (Sandiford, 2003; Tokarev et al., 1999; Bourman and Lindsay, 1989) and Eastern Highlands (e.g. Khancoban-Yellow Bog Fault, Sharp, 2004; Lake George Fault, Abel, 1985). Quaternary faulting also appears to have defeated and diverted the Murray and Goulburn River systems near Echuca in northern Victoria (Clark, 2007) and diverted the Murray River again near Morgan in South Australia. This suggests that major landscape changes have occurred in response to large earthquakes generated within the modern tectonic regime.

Modes and mechanisms of crustal deformation

Insights into the mode of active crustal deformation in southeastern Australia may be obtained by combining historical seismicity with neotectonic studies and geological and geophysical datasets. Celerier et al. (2005) suggest that two modes of active deformation have been in operation in the Flinders Ranges region over the last several million years: (1) low-amplitude (~200-500 m), long-wavelength (~200 km) elastic lithospheric flexure, as indicated by long-wavelength correlations between surface topography and gravity, and (2) active range front reverse faulting. Seismicity has been focused in the Flinders Ranges because of older (Neoproterozoic and Cambrian) tectonic structuring and thermal weakening, generated by high concentrations of heat producing elements within granite bodies that compose the regional basement (Celerier et al., 2005). Older tectonic

structuring is also likely to have played a part in localizing seismicity in the Eastern Highlands, where Miocene to Quaternary reverse faulting has in places reactivated normal faults formed during

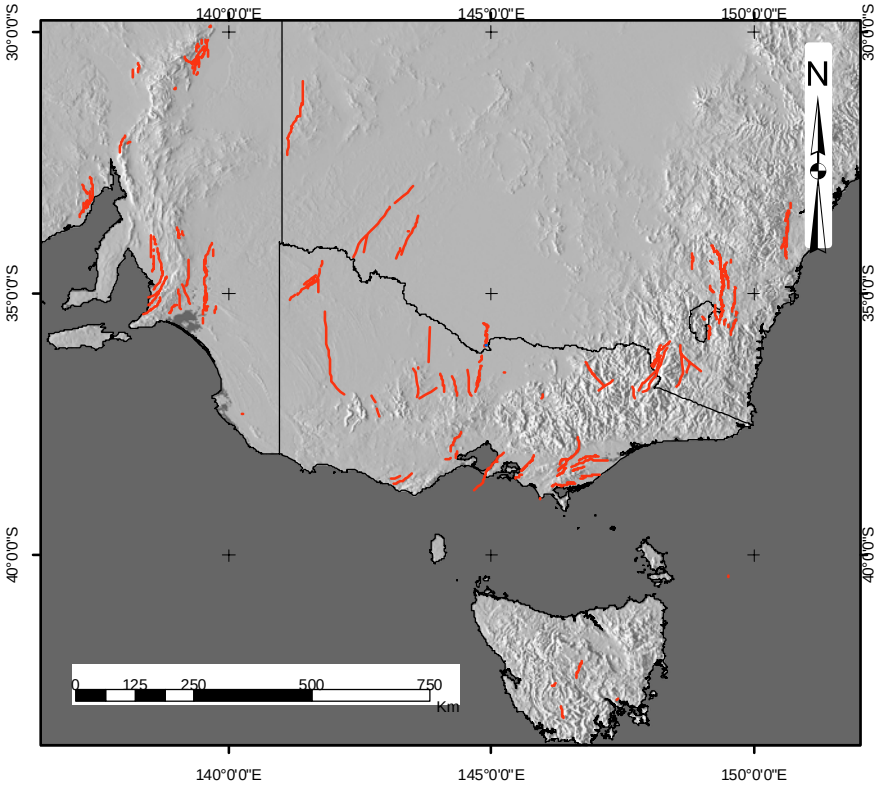

Figure 2: *Distribution of faults in southeastern Australia suspected of hosting Quaternary seismogenic displacement (from the Geoscience Australia neotectonics database*).

Mesozoic rifting. However, thermal weakening appears less relevant to the seismicity of this region, as basement rocks are characterised by significantly lower heat flows than those composing the Flinders Ranges (Cull, 1982).

The origin of the east-west compressional *in situ* stress field in southeastern Australia is controversial and attributed either to variations in density structure associated with the formation of the eastern Australian margin (Zhang et al., 1996) or interactions along the Pacific-Australian plate boundary associated with the generation of the Southern Alps of New Zealand (Coblentz et al., 1995, 1998; Sandiford, 2003; Sandiford et al., 2004). While crustal density structure must undoubtedly influence the local stress regime beneath the Eastern Highlands, it is unlikely to account for S_{hmax} trends across Victoria and in the Flinders Ranges, where there is no prominent coastal escarpment (Sandiford et al., 2004). Alternatively, the shift from a predominately strike-slip to highly transpressional regime along the Pacific-Australian plate boundary, initiating as early as 12 Ma (Sutherland 1995, 1996) but firmly entrenched by 6.4 Ma (Walcott, 1998) is thought to have progressively built the Southern Alps and consequently increased plate boundary resisting forces (Sandiford et al., 2004). Sandiford and co-workers (Sandiford, 2003; Sandiford et al., 2005; Celerier et al., 2005; Quigley et al., 2006) suggest that a small component of this stress is transferred back into the Australian plate, where it is manifested as compressional intraplate earthquakes in southeast Australia.

The geological record of southeastern Australia tentatively attests to the establishment of the modern tectonic regime during the terminal Miocene. For instance, a number of basins in southeastern Australia were inverted and eroded by up to 1 km on structurally controlled highs during the interval 8-6 Ma (Dickinson et al., 2001). Further constraints on the timing at which compressional faulting began in southeastern Australia are urgently required to better constrain temporal-spatial links between changing plate-boundary kinematics and intraplate deformation. Continued research into the evolution of Plio-Quaternary fault systems will contribute to play a vital role in developing a better understanding of contemporary seismicity in southeastern Australia.

REFERENCES

ABEL R. S. 1985. Geology of the Lake George Basin, N.S.W. Bureau of Mineral Resources, Geology and Geophysics Record 1985/4, 57p.

BOURMAN R. P. and LINDSAY J. M. 1989. Timing, extent and character of late Cainozoic faulting along the eastern margin of the Mount Lofty Ranges, South Australia. *Transactions of the Royal Society of South Australia* **113**, 63-67.

CELERIER, J., SANDIFORD, M., HANSEN, D.L., QUIGLEY, M., 2005, Modes of active intraplate deformation, Flinders Ranges, Australia, *Tectonics* **24**, doi:10.029/2004&C001679

CLARK D. and MCCUE K. 2003. Australian palaeoseismology: towards a better basis for seismic hazard estimation. *Annals of Geophysics* **46**, 1087-1105.

CLARK D. J. and LEONARD M. 2003. Principal stress orientations from multiple focal plane solutions: new insight in to the Australian intraplate stress field. *In:* Hillis R. R. and Muller D. eds. *Evolution and Dynamics of the Australian Plate*. Geological Society Australia Special Publication **22,** 85-99.

CLARK D. J., CUPPER M., SANDIFORD M., and KIERNAN, K. Style and timing of late Quaternary faulting on the Lake Edgar Fault, southwest Tasmania, Australia: implications for hazard assessment in intracratonic areas: Geological Society of America Special Publication, in press.

CLARK D., VAN DISSEN R., CUPPER M., COLLINS C. & PRENDERGAST A. 2007. Temporal clustering of surface ruptures on stable continental region faults: a case study from the Cadell Fault scarp, south eastern Australia. Proceedings of the Australian Earthquake Engineering Society Conference, 23-25 November 2007, Wollongong, Paper 17.

COBLENTZ D., ZHOU S., HILLIS R., RICHARDSON R. AND SANDIFORD M. 1998. Topography, plate-boundary forces and the Indo-Australian intraplate stress field. *Journal of Geophysical Research* **103**, 919-931.

COBLENTZ D., SANDIFORD M., RICHARDSON R. ZHOU S. AND HILLIS R. 1995. The origins of the Australian stress field. *Earth and Planetary Science Letters* **133**, 299-309.

CRONE A. J., MACHETTE M. N. AND BOWMAN J. R. 1997. Episodic nature of earthquake activity in stable continental regions revealed by palaeoseismicity studies of Australian and North American Quaternary faults. *Australian Journal of Earth Sciences* **44**, 203-214.

CRONE A. J., DE MARTINI P. M., MACHETTE M. N., OKUMURA K. and PRESCOTT J. R. 2003. Palaeoseismicity of two historically quiescent faults in Australia – implications for fault behaviour in stable continental regions. *Bulletin of the Seismological Society of America* **93**, 1913-1934.

GREENHALGH S. A., LOVE D., MALPAS K. AND MCDOUGALL R. 1994. South Australian earthquakes, 1980-92. *Australian Journal of Earth Sciences* **41**, 483-495.

HILLIS R. R. and REYNOLDS S. D. 2000. The Australian stress map. *Journal Geological Society London* **157**, 915-921.

QUIGLEY, M., CUPPER, M., SANDIFORD, M., 2006, Quaternary faults of southern Australia: palaeoseismicity, slip rates and origin, *Australian Journal of Earth Sciences* **53**, 315-331.

QUIGLEY M., SANDIFORD M., ALIMANOVIC A. & FIFIELD L. K. 2007. Landscape responses to intraplate tectonism: quantitative constraints from 10Be abundances. Earth and Planetary Science Letters 261, 120-133.

SANDIFORD M. 2003. Neotectonics of southeastern Australia: linking the Quaternary faulting record with seismicity and in situ stress. *In:* Hillis R. R. and Muller D. eds. *Evolution and dynamics of the Australian Plate*. Geological Society of Australia, Special Publication **22,** 101-113.

SANDIFORD M., WALLACE M. AND COBLENTZ D. 2004. Origin of the in situ stress field in southeastern Australia. *Basin Research* **16**, 325-338.

SHARP K. R. 2004. Cenozoic volcanism, tectonism and stream derangement in the Snowy Mountains and northern Monaro of New South Wales. Australian Journal of Earth Sciences 51, 67-83.

TOKAREV V., SANDIFORD M. and GOSTIN V. 1999. Landscape evolution in the Mount Lofty Ranges: implications for regolith development. *In*: Taylor G. and Pain C. eds. *New approaches to an old continent, 3rd Australian Regolith Conference Proceedings, Regolith '98*. Cooperative Research Centre for Landscape Evolution and Mineral Exploration, Perth, 127-134.

WALCOTT R. I. 1998. Modes of oblique compression: late Cainozoic tectonics of the
South Island of New Zealand. *Reviews of Geophysics* **36**, 1-26.

WILLIAMS G. E. 1973. Late Quaternary piedmont sedimentation, soil formation and palaeoclimates in arid South Australia. *Zeitschrift für Geomorphologie* **17**, 102–125.

The Inner Sydney Basin: Geology, Land Surface and Earthquakes

DAVID BRANAGAN
School of Geosciences, University of Sydney

ABSTRACT

The term *Sydney Basin* is often misunderstood by the general public, who think it refers to the region extending to the edge of the Blue Mountains, north to the Hawkesbury River and south to about Picton. This *Inner Sydney Basin* is the focus of discussion in this paper. While the Lapstone Structural Complex is given most attention as a possible site for strong seismicity, numerous smaller fault zones, such as the Coastal and Berowra Waters lineaments, also need to be studied. Although some geophysical evidence has been put forward that the Lapstone structures have developed by thrusting from the west, the general pattern of the complex, its extension north and south and the related structures at these extremities are more consistent with normal faulting, and down dragging of the Cumberland Basin.

INTRODUCTION

This paper discusses some aspects of what I call the *Inner Sydney Basin*, the region extending approximately north to the Hawkesbury River, south to Stanwell Park and west to the lower Blue Mountains (Figure 1).

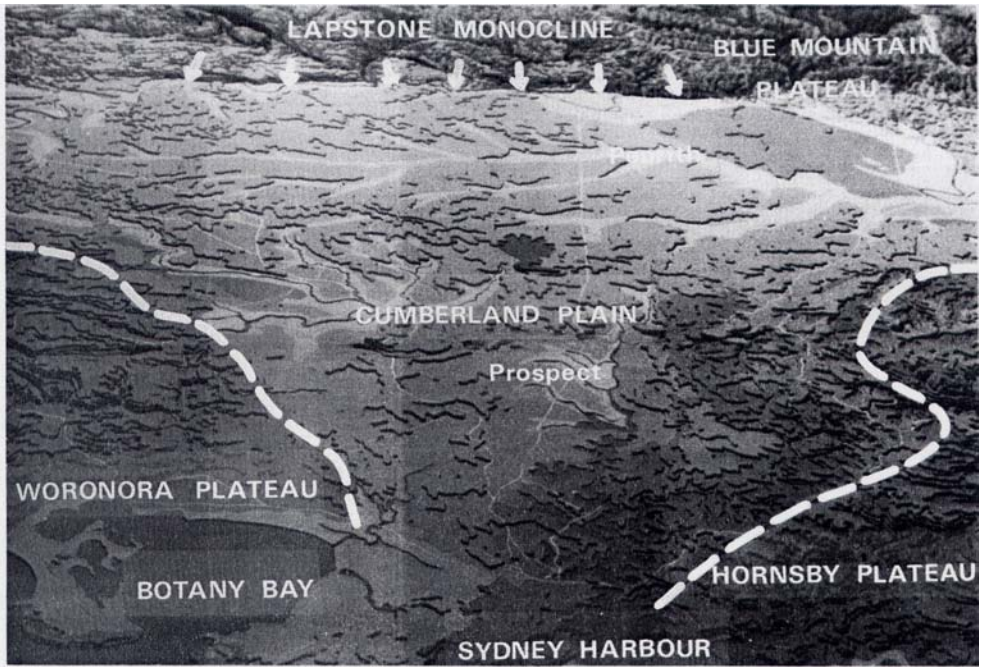

Figure 1. *The "Inner Sydney Basin", what many lay people regard as the total Sydney Basin (Branagan, 1985).*

This is what the general public think of when the term 'Sydney Basin" is used, although it is approximately what geologists define as the Cumberland Basin, with the adjacent plateaux. While the discussion of this paper focuses on this inner region, it needs to be remembered that earthquakes,

anywhere in the whole Sydney Basin, as defined by geologists, and even beyond, can affect the inner region and its man-made structures.

The region consists dominantly of sedimentary rocks deposited in the Permian and Triassic periods (about 260 – 200 million years before present (B.P.)). In the Sydney region the Triassic rocks are exposed. The underlying Permian rocks are exposed on the south coast (from Stanwell Park and south), to the north around Lake Macquarie to Newcastle and in the valleys of the western Blue Mountains. In the Sydney region the Permian rocks are at about 900m deep. In a few places these 'solid' Triassic and Permian rocks have a relatively thin cover (say 100m) of mostly unconsolidated sediments of Pleistocene to Recent age (2 million BP), notably around Botany Bay, the Penrith Lakes, and Maroota (to the north west).

Igneous activity has occurred, but is not extensive. It consists of both intrusions and extrusions. In the inner Sydney region these range in age from about 200 Ma to 15Ma. Volcanic necks such as at Hornsby, Dundas, Nortons and Bents Basins, the distinctive Prospect intrusion, and numerous dykes have been mapped. The dykes appear to be commoner in the eastern (coastal) area. This might be a matter of better exposure on the coast than across the Cumberland Plain, although dykes are certainly rare in the Blue Mountains.

While the sedimentary succession is generally flat-lying, there is clear evidence of minor folding during deposition, and there is also post-depositional folding and faulting. Some of this post-depositional deformation can be attributed to the last phases of movement of the Hunter-Bowen Thrust System (Moelle and Branagan, 1987; Mills et al, 1989; Branagan, 2000a and 2000b), but other later activity occurred, mainly in the period 80 – 20 Ma.

Even within the "inner Sydney Basin" we can recognise smaller basins and domes, which reflect these deformations. The most obvious is the Botany Basin, which is also, incidentally, the site of the thickest succession of young sediments (Tertiary – Cainozoic). These sediments will react to seismic shaking quite differently to the older, consolidated rocks, as happened in the Newcastle region during the 1989 earthquake.

Evidence indicates that both compression and tension have occurred during and after deposition, and there appear to have been two long periods of tension – at the end of major deposition (Late Triassic), and Early Tertiary (sea-floor spreading), as indicated particularly by the dyke intrusions.

POSSIBLE SITES OF SEISMIC ACTIVITY

Emphasis has been given to the Lapstone Structural Complex as a likely site of strong seismic activity (based on past seismic records**.** However it is pertinent to point out other structural weaknesses that have been mapped in the Sydney region in the past thirty years. Although these mostly show little or no signs of geologically recent activation, they should not be entirely discounted as sites of seismic activity. At the various sites mapped a variety of fault types can be recognised. They include normal, steep reverse, overthrust, strike-slip and fault breccia (crushed rock) varieties. It is not unusual to find several different fault types in close proximity. This is not to be unexpected, as once a rock mass has been weakened by faulting it is quite likely to be the locus of further faulting, and although one might expect similar movements as had taken place previously, the weak material could easily deform in a new way. Although a little removed from the "inner Sydney Basin", the fault systems mapped just east of the Mooney Mooney Creek Bridge on the F 4 Freeway, are a particularly good example of such deformation. Here reverse folding/faulting, normal and strike-slip faults have been recorded (Mills et al., op. cit.).

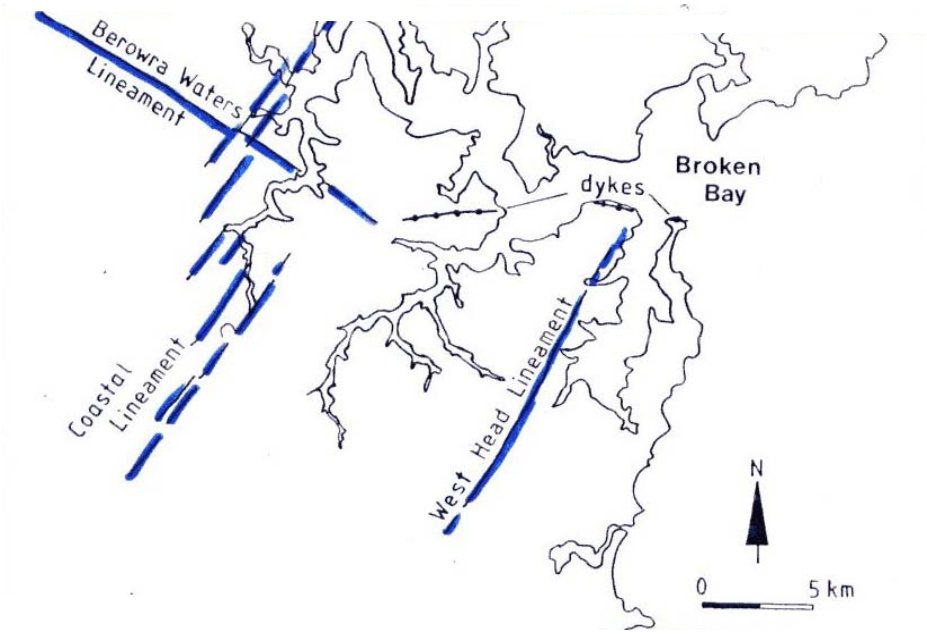

Figure 2 *Coastal, West Head and Berowra Waters Lineaments (after Mauger et al, 1984; and Norman, 1986).*

The strike-slip faults and related structures, (including strongly developed shear zones, and possibly the breccia features) have attracted some attention in recent years as they have been encountered during various large engineering projects in the region and have required special treatment. Slickensides patterning on the Mooney strike slips, and a similar fault at Normanhurst appears surprisingly fresh (Branagan & Packham 2000), but no evidence is known of any movements on these features, although such cannot be discounted. Norman (1986) and Whitehouse and Branagan (1998) discussed aspects of the "Coastal Lineament' of Mauger et al (1984), the West Head Lineament and related structures (Figure 2), and more recently Ochs et al (2004) have produced a coloured map of the Sydney CBD showing mapping by Branagan, 1985; Norman, op. cit., with additional more recent mapping. For further discussion on Sydney faulting see Branagan, 1977; 2000a, and 2000b**;** Branagan and Norman, 1984; Branagan et al., 1987; Branagan and Mills, 1990).

THE LAPSTONE STRUCTURAL COMPLEX

As mentioned earlier this structure marking the eastern edge of the Blue Mountains has been the focus of attention by geophysicists as the most likely site for a reasonably large earthquake to affect the Sydney region. Cotton (1921) presented information on the last reasonably large earthquake here, in 1919, and there are some additional notes on this earthquake in his personal papers (University of Sydney Archives).

It is not proposed to discuss the geology of this region here. It has been covered to a considerable extent in Pedram, 1983; Rawson 1989; Branagan & Pedram, 1990, 2000), which also list many of the earlier papers.

My only concern is to comment on the suggestion put forward by a number of speakers at the recent symposium on Sydney Earthquakes, and also in some papers in this volume (e.g. Fergusson, 2005) that the major movement on the Lapstone structure has been a thrust (variously suggested as high angle, and low angle) from the west. This has been based to some

degree on the suggested pattern of reverse faulting in the north-south striking faults in the Lachlan Foldbelt to the west, and on the not too detailed seismic records obtained during coal and oil exploration in the region**,** (Herbert, 1989).

.

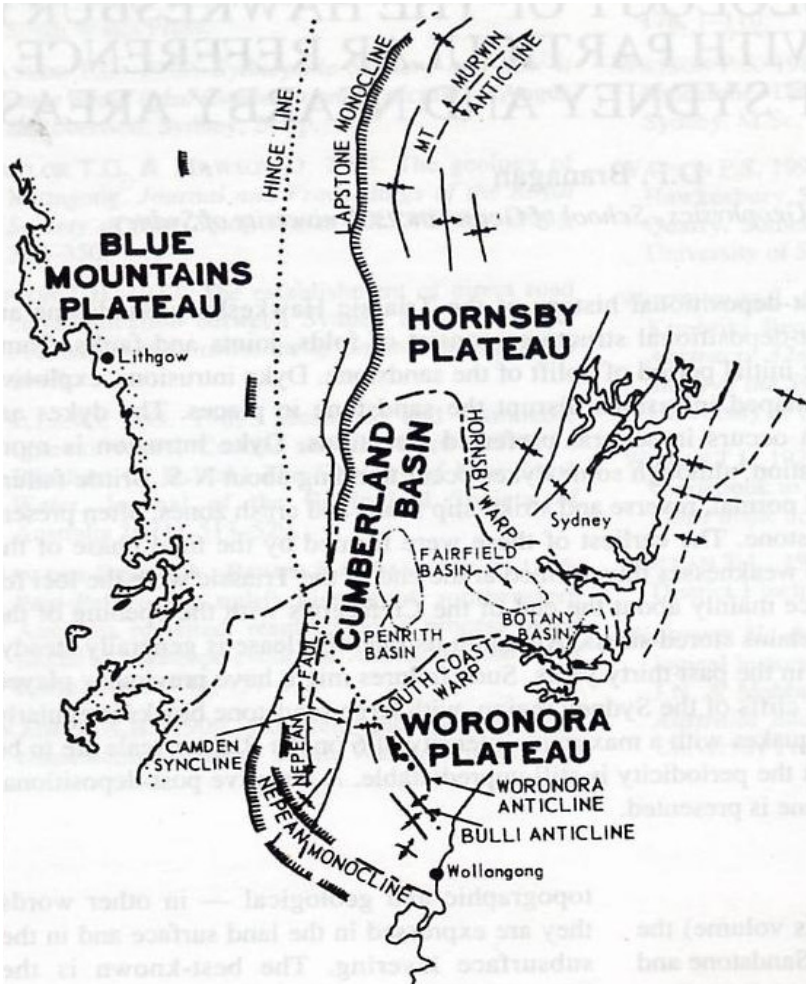

Figure 3. *The Lapstone Structural Complex and its associated faults to the north and South seem more consistent with normal down warping to the east, rather than thrust deformation from the west [after Bembrick et al, 1973].*

While the classical explanation of the formation of the originally named Lapstone Monocline required an uplift of the Blue Mountains in the Late Pliocene (The Kosciusko Uplift) (Andrews, 1910), Branagan (1975) suggested an alternative – down dragging of the Cumberland Basin during the period of sea-floor spreading at the beginning of the Tertiary. Herbert (op. cit.) attributed the origin of the faulting to a late Triassic movement, during reactivation of underlying Lachlan Foldbelt deformation, including some wrench faulting (see also Harrington, 1982).

Although the author has recognised overturning of the steep Mt. Riverview Fault (east of the Hawkesbury Lookout) and also of the Nepean Fault at Bents Basin (Branagan & Pedram, 1990) he believes these are very localised events. One problem with the west-dipping thrust suggestion is that it seems only to be looking at the north-south fault forming the main scarp of the edge of the Blue Mountains. I believe we also have to take into consideration the associated faults and flexures which

occur to the north and south and which mark the edges of the two plateaux, the Hornsby and Woronora Plateaux. To my knowledge these structures, which by my suggestion of formation are mainly contemporaneous with the major formation of the Lapstone structures, show no evidence of reverse movement on any large scale. The curvature of these structures as they swing easterly seems to conform with a fairly simple pattern of downdragging of the central basin (Figure 3).

Although it might be simplistic, one would expect a strong thrusting from the west to produce sympathetic curving of faults westerly at the north and southern extensions of a strong north-south trending thrust, rather than what we now map.

CONCLUSIONS

There is much still to learn about the structural nature and tectonic history of the inner (and total) Sydney Basin. It is pleasing that this task is being taken up with vigour by geologists and geophysicists. It will surely bear fruit and contribute to the raising of safety standards within and extending beyond the metropolis, particularly with respect to seismicity.

REFERENCES

Andrews, E.C., 1910. The Tertiary unity of eastern Australia. Journal and Proceedings of the Royal Society of New South Wales, 44, 420 - 480.

Bembrick, C.S., Herbert, C., Scheibner, E. and Stuntz, J., 1973. Structural sub-division of the New South Wales portion of the Sydney – Bowen Basin. New South Wales Geological Survey Quarterly Notes 11, 1 – 13.

Branagan, D.F., 1975. Further thoughts on the Lapstone Structure. 10th Symposium on Advances in the Study of the Sydney Basin, Abstracts. Department of Geology, University of Newcastle, 22 – 23.

Branagan, D.F., 1977. Faults in the Hawkesbury Sandstone, 1977 11th Symposium on Advances in the Study of the Sydney Basin, Abstracts. Department of Geology, University of Newcastle, 20.

Branagan, D.F., 1985. An overview of the geology of the Sydney Region. In Pells, P.J.N., (ed.) Engineering Geology of the Sydney Region. Rotterdam: Balkema, 3 – 48.

Branagan, D.F., 1991, Pyrmont Geology. 25th Symposium on Advances in the Study of the Sydney Basin. Department of Geology, University of Newcastle, 162 – 169.

Branagan, D.F., 2000a. The Hawkesbury Sandstone: its origins and later life.In G.H. McNally and B.J. Franklin (eds.) Sandstone City (Sydney's dimension stone and other sandstone geomaterials). Monograph No. 5, Environmental, Engineering and Hydrogeology Specialist Group, Geological Society of Australia, 23 – 38.

Branagan, D.F., 2000b. Structural Geology of the Hawkesbury Sandstone, with particular reference to the city of Sydney and nearby areas. In G.H. McNally and B.J. Franklin (eds.) Sandstone City (Sydney's dimension stone and other sandstone geomaterials). Monograph No. 5, environmental, engineering and Hydrogeology Specialist Group, Geological Society of Australia, 39 – 54.

Branagan, D.F., Mills, K.J. and Norman, A.R., 1987. Sydney Faults – Facts and Fantasies. 22nd Symposium on Advances in the Study of the Sydney Basin. Department of Geology, University of Newcastle, 111 – 118.

Branagan, D.F. and Mills, K.J., 1990. Some newly-exposed faults in the Sydney Region. 24th Symposium on Advances in the Study of the Sydney Basin. Department of Geology, University of Newcastle, 105 – 111.

Branagan, D.F. and Norman, A.R., 1984. Sydney Faults: More conundrums? 18th Symposium on Advances in the Study of the Sydney Basin. Department of Geology, University of Newcastle, 125 – 12.

Branagan, D.F. and Packham, 2000. Field Geology of New South Wales. NSW Department of Mineral Resources.

Branagan, D.F. and Pedram, 1990. The Lapstone Structural Complex, New South Wales. Australian Journal of Earth Sciences, 37, 23 – 36.

Branagan, D.F. and Pedram, 2000. Engineering Geology of a Sandstone Escarpment. The Blue Mountains, Sydney Basin, NSW. In G.H. McNally (ed.) Case Studies in Engineering Geology, Hydrology and Environmental Geology, third series, EEHSG of GSA. Conference Publications, Springwood, 38 – 52.

Cotton, L.A., 1921. The Kurrajong Earthquake of August 15, 1919. Journal and Proceedings of the Royal Society of New South Wales, 55, 83 – 104.

Fergusson, C.L., 2005. Review of Structure and basement control of the Lapstone Structural Complex, Sydney Basin, Eastern New South Wales. Geoscience Australia Record, 2005.

Harrington, H.J., 1982. Tectonics and the Sydney Basin. 16th Symposium on Advances in the Study of the Sydney Basin. Department of Geology, University of Newcastle, abstracts 15 – 19.

Herbert, C., 1898. The Lapstone Monocline – Nepean Fault – A high angle reverse fault system. 23rd Symposium on Advances in the Study of the Sydney Basin. Department of Geology, University of Newcastle, 179 – 186.

Mauger, J.W., Creasey, J.W. and Huntingdon, J.F. 1984. The use of pre-development data for mine design: Sydney Basin fracture pattern analysis. CSIRO Division of Mineral Physics, North Ryde.

Mills, K.J., Moelle, K.H.R. and Branagan, D.F., 1989. Faulting near Mooney Mooney Bridge. 23rd Symposium on Advances in the Study of the Sydney Basin. Department of Geology, University of Newcastle, 217 – 224.

Moelle, K.H.R. and Branagan, D.F., 1987. Thrust Faulting at Freeman's Waterholes. 22nd Symposium on Advances in the Study of the Sydney Basin. Department of Geology, University of Newcastle, 75 – 77.

Norman, A.R., 1986. A structural analysis of the southern Hornsby Plateau, Sydney Basin, New South Wales, Australia. University of Sydney, Department of Geology and Geophysics, M.Sc thesis, (unpublished).

Ochs, D., Pells, P. and Braybrooke, J.C., Geological Faults and Dykes in Sydney CBD. The Engineering Geology of the Sydney Region. Australian Geomechanics Society. Sydney Chapter Mini-Symposium, 13 October, 2004.

Pedram, H., 1983. Structure and Engineering Geology of the Lower Blue Mountains, Sydney Basin, N.S.W., Australia. University of Sydney, Department of Geology and Geophysics, M.Sc thesis, (unpublished).

Rawson, A., 1989. Fault–angle basins of the Lapstone Structural Complex – Geomorphological evidence for neo-tectonism. 23rd Symposium on Advances in the Study of the Sydney Basin. Department of Geology, University of Newcastle, 171 – 178.

Whitehouse, J. and Branagan, D.F., 1998. Geology at Kimbriki Recycling and Waste Disposal Depot. 32nd Symposium on Advances in the Study of the Sydney Basin. Department of Geology, University of Newcastle, 63 – 69.

Review of structure and basement control of the Lapstone Structural Complex, Sydney Basin, eastern New South Wales

Christopher L. Fergusson
School of Earth and Environmental Sciences, University of Wollongong, NSW 2522, Australia

ABSTRACT

In the western Sydney Basin, the Lapstone Structural Complex is a major north-trending association of monoclines and faults that forms the frontal ridge of the Blue Mountains Plateau. Palaeomagnetic data from the southern part of the Lapstone Structural Complex indicates a Late Cretaceous to Cenozoic timing of deformation. At Upper Kurrajong, the Lapstone Structural Complex is dominated by an east-facing monocline with a central limb containing several different homoclinal segments. At the Hawkesbury Lookout section, strata are steeply dipping to near vertical along the main east-facing monocline and the subsurface structure is interpreted as a moderately west-dipping thrust fault. The Lapstone Structural Complex can be regarded as related to either a west-dipping thrust at depth or formed from steep east-dipping extensional faulting. Seismicity is consistent with the first alternative. The eastern Lachlan Fold Belt is basement to the Sydney Basin and includes moderately west-dipping faults that may also have been reactivated as thrust faults in the present-day stress regime. These structures provide an analogue for a structure in the basement that controlled development of the Lapstone Structural Complex.

INTRODUCTION

This account presents a brief review of the structure of the Lapstone Structural Complex in the western Sydney Basin with two cross sections shown across the structure at Upper Kurrajong and the Hawkesbury Lookout. These cross sections complement the structural outline of the Lapstone Structural Complex given by Branagan and Pedram (1990, 1997). Additionally, the issue of basement control of the Lapstone Structural Complex is considered with reference to potentially active faults in the Lachlan Fold Belt to the west and south of the Sydney Basin.

BACKGROUND

The Lapstone Structural Complex consists of an association of east-facing monoclines, high-angle faults, and fracture zones that form the frontal ridge of the Blue Mountains Plateau in the Permian to Triassic Sydney Basin to the west of Sydney (Branagan & Pedram 1990, 1997). Development of the Lapstone Structural Complex has been related to the Late Permian – Early Triassic Hunter-Bowen Orogeny (Pickett & Bishop 1992). This argument was based on the inference that the Jurassic Nortons Basin diatreme postdated local development of the monocline near Wallacia and from suggestions that stratigraphic units thicken from west to east as they cross the Lapstone Structural Complex and it is therefore a syndepositional feature. Eastward thickening of units begins well to the west of the Lapstone Structural Complex and therefore this structure may not have been active during deposition (Mayne *et al.* 1974). Palaeomagnetic data indicate that the Lapstone Structural Complex has affected the widespread mid-Cretaceous overprint magnetisation in the Sydney Basin and therefore that the structures formed later than mid Cretaceous (Schmidt *et al.* 1995). This is consistent with an Early Tertiary age for the Lapstone Structural Complex advocated by Branagan and Pedram (1990) and also with studies of sub-basalt topography and modelling of uplift in the Blue Mountains (van der Beek *et al.* 2001). Numerous earthquakes have occurred in the Blue Mountains and indicate that the Lapstone Structural Complex may still be active (Brown & Gibson 2004) despite the lack of tilting of Miocene magnetisation along the monocline at Lapstone (Bishop

et al. 1979). Elsewhere in the Sydney Basin, for example, to the north of Wollongong, the high modern-day stress regime has reactivated pre-existing fracture systems (Memarian & Fergusson 2003).

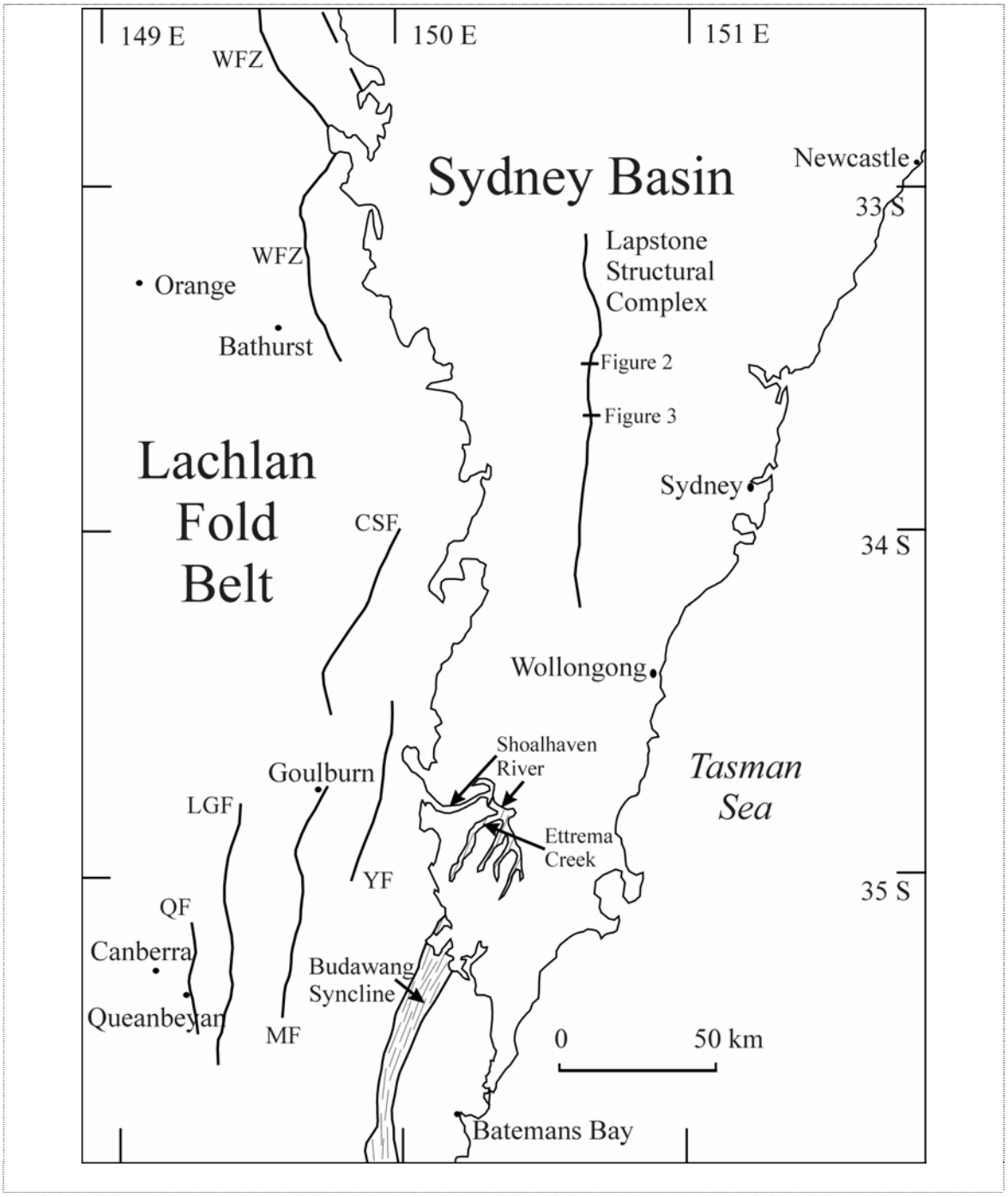

Figure 1 *Sydney Basin and major structures in the adjoining Lachlan Fold Belt (after Scheibner 1997). Lapstone Structural Complex is marked along with locations of Figures 2 and 3. Faults in Lachlan Fold Belt: CSF = fault on western margin of Cockbundoon Syncline, LGF = Lake George Fault, QF = Queanbeyan Fault, MF = Mulwaree Fault, YF = Yarralaw Fault, WFZ = Wiagdon Fault Zone.*

STRUCTURE OF THE LAPSTONE MONOCLINE

The Lapstone Structural Complex varies along its length with monocline(s), high-angle faults and minor structures such as thrusts, minor folds, tectonic breccias and joints (Branagan & Pedram 1990, 1997). An east-facing monocline is well developed along much of the Complex and this is shown in a west-east cross section at Upper Kurrajong where the central limb of the monocline consists of several segments with different dips to the east (Figure 2). Monoclines, such as in the Colorado Plateau, have been attributed to contractional deformation along thrust faults at depth (Bump & Davis 2003) but they are also related to deformation in rock strata overlying steeply dipping extensional faults in underlying basement (Withjack & Callaway 2000).

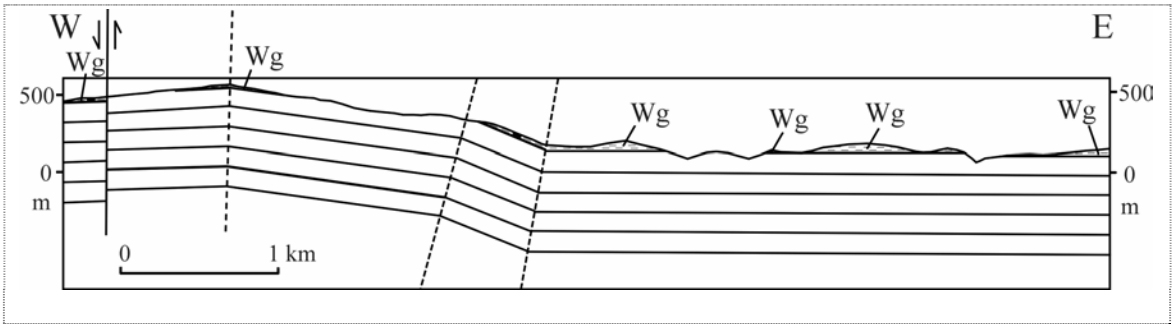

Figure 2 *West to east cross section through the Lapstone Structural Complex at Kurrajong Heights. Wg = Wianamatta Group (underlying units not labelled). Vertical scale = horizontal scale. Cross section is constrained by the contact between the Wianamatta Group and the underlying Hawkesbury Sandstone as shown on the Penrith 1:100 000 Geological Sheet (Clarke & Jones 1991). The cross section has been drawn using the kink-band method of construction (Suppe 1985).*

The steepest dips on the monocline associated with the Lapstone Structural Complex occur below the Hawkesbury Lookout. Here, strata west of the monocline are flat and gradually increase in dip up to *ca* 15º to the east before crossing a fault onto the steeply dipping near vertical central limb (Branagan & Pedram 1990, figure 7). A cross section is shown along a west-east line through the monocline at Hawkesbury Lookout in Figure 3. The zone of ductile deformation at the surface associated with the central limb of the monocline is replaced at depth by a moderately west-dipping thrust fault in the lower part of the Sydney Basin and presumably the underlying basement with approximately 500 m of net slip.

BASEMENT CONTROL

It has been suggested that the Lapstone Structural Complex was controlled by reactivation of the western margin of the Budawang Syncline (the Eden-Comerong-Yalwal Rift) in the underlying Lachlan Fold Belt especially where this was intersected by elements of the east-trending Lachlan Lineament (Branagan & Pedram 1990). The structure of the Budawang Syncline exposed at the Shoalhaven River and Ettrema Creek has been described by Cooper (1992); the western margin of the Syncline is locally faulted and other faults occur within the structure although no evidence has been found to indicate that any of these faults have been reactivated in the present-day stress field. South the Sydney Basin, Ordovician turbidites and black shales dominate the Lachlan Fold Belt either side of the Budawang Syncline. These rocks are complexly deformed with multiple deformation and are also affected by common late brittle structures (Fergusson 1998; Fergusson & Frikken 2003). Moderate to intense deformation with widespread folding, cleavage development and numerous faults occur in the Lachlan Fold Belt to the west of the Sydney Basin (Glen 1992). Faults in this region are west dipping and include structures such as the Wiagdon Fault Zone, Mulwaree Fault, Yarralaw Fault and other structures (Fergusson & VandenBerg 1990). The Lake George Fault,

northeast of Canberra, has spectacular topographic expression and has been related to Tertiary normal faulting (Abell 1991). Other faults in the region show less evidence for Tertiary reactivation although some have limited topographic expression with subdued fault scarps consistent with some local neotectonic activity in addition to topographic variations caused by differential weathering. It is considered that a pre-existing west-dipping thrust in the basement under the western Sydney Basin, analogous to structures further west, provided control for development of the Lapstone Structural Complex. Such a structure may have been reactivated in the east-west Late Neogene contractional regime that has affected southeastern Australia (Sandiford 2003; Brown & Gibson 2004). The cross section for Hawkesbury Lookout in Figure 3 is consistent with this interpretation.

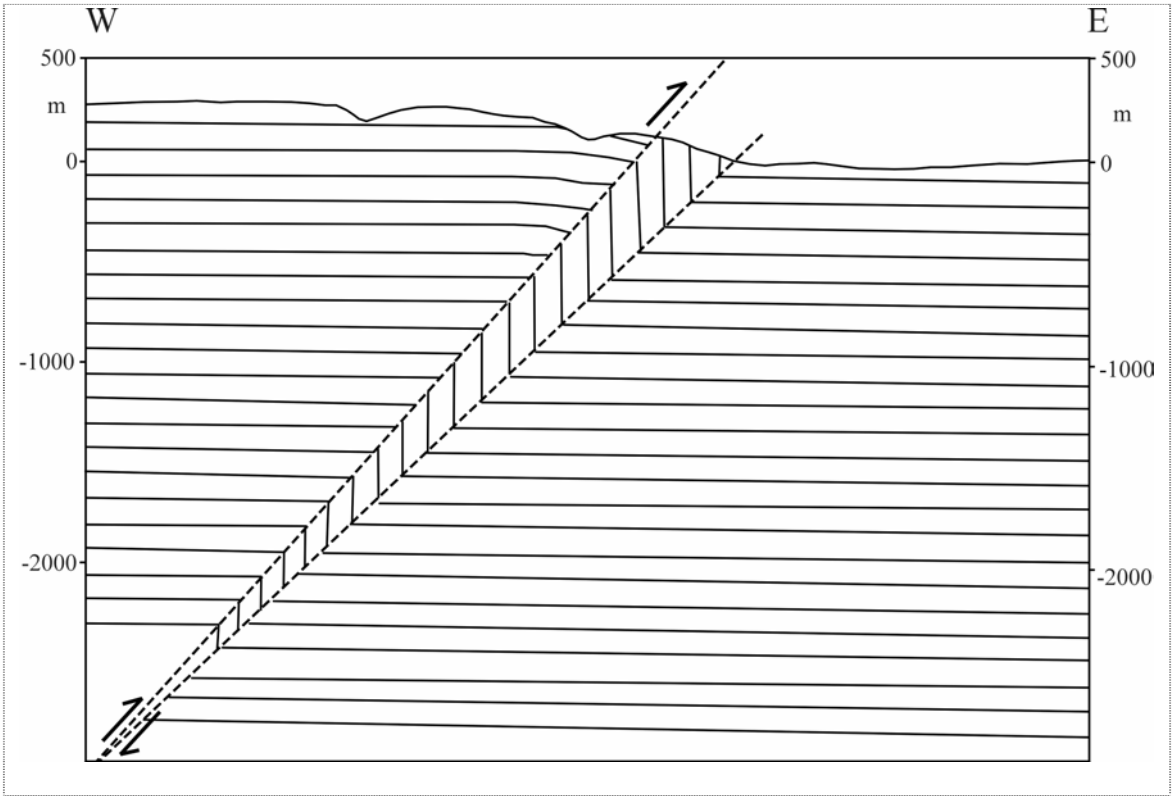

Figure 3 *West to east cross section through the Lapstone Structural Complex at the Hawkesbury Lookout (note that stratigraphy is omitted but the surface exposure is in the Hawkesbury Sandstone). Vertical scale = horizontal scale. Cross section was drawn using the kink-band method of Suppe (1985).*

DISCUSSION AND FUTURE DIRECTIONS

Earthquake activity in southeastern Australia is concentrated in a broad zone between Sydney and Melbourne in the southeastern highlands as well as in other regions such as the Mt Lofty and Flinders Ranges and Tasmania (Brown & Gibson 2004). Seismicity has been related to a contractional regime reflecting east-west convergence across the Australian-Pacific plate boundary in the South Island of New Zealand that has developed in the Late Neogene (Sandiford 2003). Slip rates along faults are low (metres per million years, Brown & Gibson 2004) and it is therefore not surprising that neotectonic faulting remains difficult to establish and many earthquakes cannot be tied to source faults. Given the clear topographic expression of the Lapstone Structural Complex and faults such as the Lake George Fault these structures may be at least partly related to the Late Neogene contractional tectonic setting. Suggestions of an extensional origin for both these structures need to be critically re-evaluated. A Late Neogene age for the Lapstone Structural Complex is

apparently contradicted by untilted Miocene magnetisation at Lapstone (Bishop *et al.* 1979) but it does provide a plausible explanation for the problematic Rickabys Creek Gravel at Glenbrook (cf. Pickett & Bishop 1992).

Given the great antiquity of much of the landscape in eastern Australia, the lack of evidence for notable tectonic events in the latest Cretaceous to latest Palaeogene and recent evidence of Late Neogene deformation and uplift in southeastern Australia (Sandiford 2003), it is important to re-evaluate the role of reactivation and neotectonic activity on structures such as the Lake George Fault, Mulwaree Fault and Lapstone Structural Complex. The present-day seismicity of southeastern Australia indicates that thrust faulting is active and therefore west-dipping structures with potential evidence for neotectonic activity should be carefully examined. More cross sections drawn to depth incorporating seismic and borehole data are needed to determine if these structural geometries are viable.

ACKNOWLEDGEMENTS

Dr Dan Clark is thanked for organising the symposium on the Lapstone Structural Complex. Dr David Branagan kindly commented on a draft of this manuscript. Dr Hossein Memarian is thanked for many discussions on Sydney Basin structure. I am most grateful to the late Professor Peter Coney for showing me the Colorado Plateau and it's monoclines in 1993.

REFERENCES

Abell, R. S., 1991. Geology of the Canberra 1:100 000 Sheet area, New South Wales and Australian Capital Territory. *Bureau of Mineral Resources, Geology & Geophysics, Bulletin*, **233**, 116pp.

Bishop, P., Hunt P. and Schmidt, P. W., 1982. Limits to the age of the Lapstone Monocline, N.S.W.— a palaeomagnetic study. *Journal of the Geological Society of Australia*, **29**, 319–326.

Branagan, D. F. and Pedram, H., 1990. The Lapstone Structural Complex, New South Wales. *Australian Journal of Earth Sciences*, **37**, 23–36.

Branagan, D. F. and Pedram, H., 1997. Engineering geology of a sandstone escarpment: the Blue Mountains. Sydney Basin NSW. In: McNally G. (Ed.) Collected Case Studies in Engineering Geology, Hydrogeology and Environmental Geology. Third Series. *Environmental, Engineering and Hydrogeology Specialist Group, Geological Society of Australia and Conference Publications*, pp. 38–52.

Brown, A. and Gibson, G., 2004. A multi-tiered earthquake hazard model for Australia. *Tectonophysics*, **390**, 25–43.

Bump, A. P. and Davis, G. H., 2003. Late Cretaceous–early Tertiary Laramide deformation of the northern Colorado Plateau, Utah and Colorado. Journal of Structural Geology, 25, 421–440.

Clarke, N. R. and Jones, D. C., (Eds.), 1991. Penrith 1:100 000 Geological Sheet 9030. *New South Wales Geological Survey, Sydney.*

Cooper, G. T., 1992. Early Carboniferous back-arc deformation in the Lachlan Fold Belt, Shoalhaven River–Ettrema Creek area, NSW. *Australian Journal of Earth Sciences*, **39**, 529–537.

Fergusson, C. L., 1998. Thick-skinned folding in the eastern Lachlan Fold Belt: an example from the Shoalhaven River Gorge, New South Wales. *Australian Journal of Earth Sciences*, **45**, 677–686.

Fergusson, C. L. and Frikken, P., 2003. Diapirism and structural thickening in an Early Palaeozoic subduction complex, southeastern New South Wales, Australia. *Journal of Structural Geology*, **25**, 43–58.

Fergusson, C. L. and VandenBerg, A. H. M., 1990. Middle Palaeozoic thrusting in the eastern Lachlan Fold Belt, southeastern Australia. *Journal of Structural Geology,* **12**, 577–589.

Glen, R. A., 1992. Thrust, extensional and strike-slip tectonics in an evolving Palaeozoic orogen—a structural synthesis of the Lachlan Orogen of southeastern Australia. *Tectonophysics,* **214**, 341–380.

Mayne, S. J., Nicholas, E., Bigg-Wither, A. L., Rasidi, J. S. and Raine, M. J., 1974. Geology of the Sydney Basin—A review. *Bureau of Mineral Resources, Geology and Geophysics, Bulletin,* **149**, 229pp.

Memarian, H. and Fergusson,C. L., 2003. Multiple fracture sets in the southeastern Permian-Triassic Sydney Basin, New South Wales. *Australian Journal of Earth Sciences,* **50**, 49–61.

Pickett, J. W. and Bishop, P., 1992. Aspects of landscape evolution in the Lapstone Monocline area, New South Wales. *Australian Journal of Earth Sciences,* **39**, 21–28.

Sandiford, M., 2003. Neotectonics of southeastern Australia: linking the Quaternary faulting record with seismicity and *in situ* stress. *Geological Society of Australia Special Publication,* **22**, and *Geological Society of America Special Paper,* **372**, 107–119.

Scheibner E. 1997. Stratotectonic map of New South Wales, scale 1:1 000 000. *Geological Survey of New South Wales, Sydney.*

Schmidt, P. W., Lackie, M. A. and Anderson, J. C., 1995. Palaeomagnetic evidence for the age of the Lapstone Monocline, NSW. *Australian Coal Geology,* **10**, 13–22.

Suppe, J., 1985. Principles of Structural Geology. *Prentice-Hall, New Jersey,* 537pp.

van der Beek, P., Pulford, A. and Braun, J., 2001. Cenozoic landscape development in the Blue Mountains (SE Australia): lithological and tectonic controls on rifted margin morphology. *Journal of Geology,* **109**, 35–56.

Withjack, M. A. and Callaway, S., 2000. Active normal faulting beneath a salt layer: an experimental study of deformation pattern in the cover sequence. *American Association of Petroleum Geologists Bulletin,* **84**, 627–651.

Geomorphological evidence for neotectonic activity on the northern Lapstone Structural Complex.

ANDREW RAWSON[1] AND DAN CLARK[2]
1. NSW DEPT. OF NATURAL RESOURCES, C/O FACULTY OF SCIENCE AND AGRICULTURE, CHARLES STURT UNIVERSITY, LEEDS PDE, ORANGE PO BOX 883 NSW 2800
2. GEOSCIENCE AUSTRALIA, GPO BOX 378, CANBERRA ACT 2601

ABSTRACT
The results of morphometric analysis of drainage lines crossing the northern Lapstone Structural Complex west of Sydney show that there are indicators of recent and possibly ongoing tectonic deformation. Stream long-profiles oversteepen as they cross major faults, valley cross sections narrow to 'V-notches' where streams enter the upthrown side of fault blocks, and several streams have been partially dammed, forming swamps and lakes. These indicators are consistent with a model of periodic deformation of the Kurrajong Fault System, near to the threshold conditions of uplift/incision. The most pronounced example of tectonic modification of stream morphology is Burralow Creek, which has been partially dammed to form Burralow Swamp. Sandy sediments underlying an extensive lacustrine clay deposit, potentially relating to the last fault movement, obtained Late Pleistocene ages.

INTRODUCTION
The Lapstone Structural Complex (LSC) consists of a series of related faults and folds bounding the western edge of the Cumberland Basin approximately 50 kilometres west of the Sydney CBD (**Fig. 1**). It is one of the most prominent tectonic and topographic features of the Sydney Basin. The eastern margin of the complex is an escarpment, rising some 200-400 metres above the surrounding plain, known as the Lapstone Monocline. The western edge consists of a series of overlapping en-echelon faults known as the Kurrajong Fault System (KFS, Pedram 1983, Branagan and Pedram, 1990). The maximum vertical displacement of the Kurrajong Fault System is approximately 130 metres at Cut Rock (near Kurrajong Heights), with progressively smaller displacements to the south.

The LSC has undoubtedly had a long and complex history, and there seems little doubt that it is related in part to basement structures that were active during deposition of the Sydney Basin sediments (Qureshi, 1984, Harrington and Korsch, 1985, Branagan and Pedram, 1990; Pickett & Bishop, 1992). Several lines of evidence suggest a Cenozoic age for a significant portion of the relief generation across the LSC, including: a) Miocene basalts west of the LSC appear to have erupted onto a low-relief pre-incision land-surface (Van Der Beek, 2001), and b) deeply weathered and sometimes lateritised Tertiary Rickaby's Creek Gravels, which show an internal structure consistent with deposition in a braided stream environment (Bishop & Hunter, 1990), occur on both uplifted and downthrown sides of the LSC (Bishop, 1986; Branagan & Pedram, 1990). Opinions are divided regarding whether this relief generation is temporally related to the deformation which crafted the LSC in its present form (e.g. Branagan & Pedram, 1990; Van Der Beek et al., 2001; Schmidt et al., 1995), or relates to passive erosive exhumation of a structure which formed largely during Mesozoic syn-depositional deformation (Pickett & Bishop, 1992). Apparent truncation of the 18.8 Ma Green Scrub Basalt by the Kurrajong Fault (Crook, 1956, Wellman and McDouga11, 1974; Pedram, 1983; Branagan & Pedram, 1990) has been taken as evidence for the former, while the fact that Rickabys Creek gravels unconformably overlie Hawkesbury Sandstone on the face and upthrown side of the Lapstone Monocline, and Wianamatta Shale on the downthrown side, has been

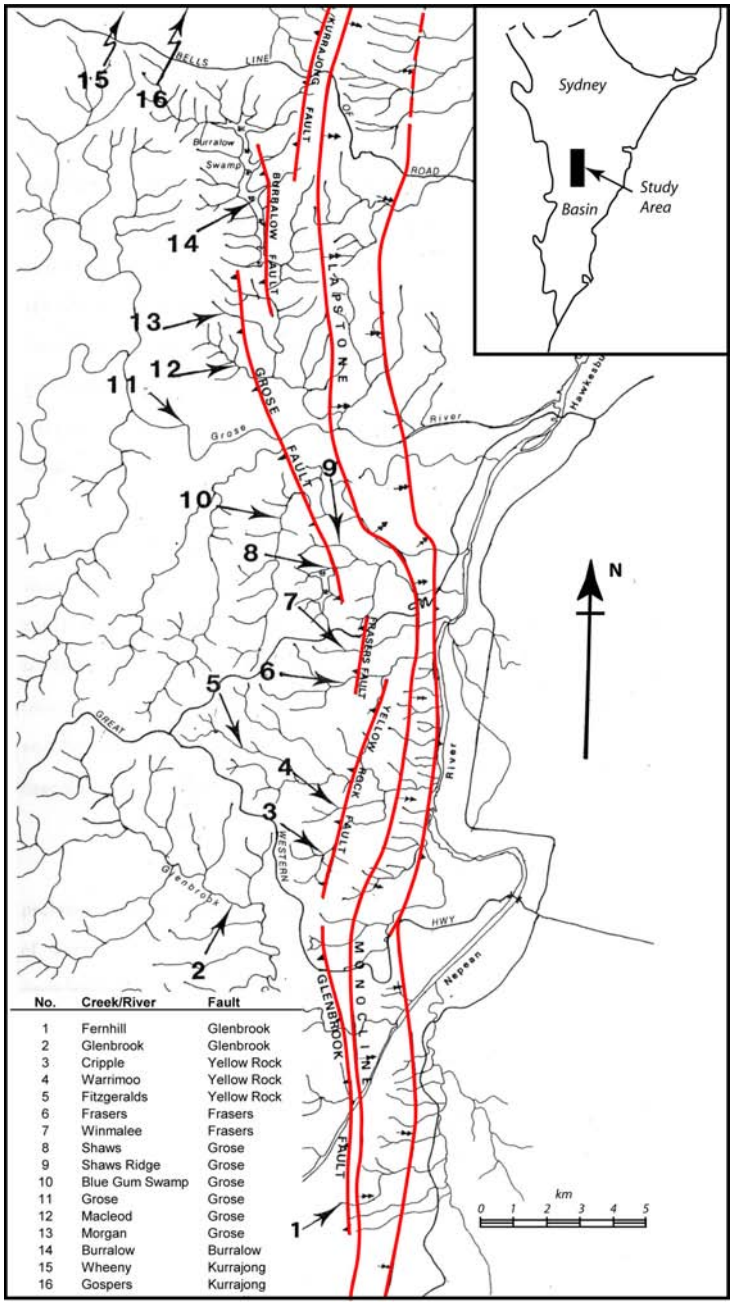

Figure 1: *The northern Lapstone Structural Complex showing the east facing Lapstone Monocline and west-facing scarps relating to the en echelon faults of the Kurrajong Fault System (modified after Branagan & Pedram, 1990).*

used to argue for the latter (Pickett & Bishop, 1992). Paleomagnetic data showing that rotation of strata on the limb of the Lapstone Monocline occurred after the mid-Cretaceous (~90 Ma, Schmidt et al., 1995) and prior to 8 ± 5 Ma (Bishop et.al., 1982 with ages recalculated by Pillans, 2003) suggests that the Lapstone Monocline might have formed during rifting of the Tasman Sea (e.g. Schmidt et al., 1995), and was fully formed by the Pliocene. However, a spatial association between the LSC and the historic catalogue of earthquake epicentres (Gibson, this volume), and the neotectonic indicators discussed herein, suggest the potential for ongoing deformation.

Tectonic activity can significantly control stream patterns and behaviour (e.g. Schumm et al., 2000). One of the most sensitive indicators of change is the longitudinal profile and valley floor profile of a stream (e.g. Bendefy et al., 1967; Zuchiewicz, 1979). In alluvial environments, changes in valley slopes may be accommodated by changes in stream sinuosity. However, in areas of resistant alluvium or bedrock, which tend to confine the channel and retard meander shift and bank erosion, deposition in areas of reduced gradient and incision in areas of increased gradient may dominate stream response. Streams crossing the LSC pass over the Hawkesbury Sandstone and sandstone rocks of the Narrabeen Group, upon which only skeletal soils are typically developed (Jones & Clark, 1991; Bannerman, 1990). Hence, the latter condition might be expected to pertain.

The degree to which disequilibrium is preserved consequent of uplift, and its longevity, depends upon the relative rates of uplift and erosion (including knickpoint retreat, valley incision and plateau lowering rates). A reconstruction of the *ca.* 20 Ma palaeo-topography west of the Kurrajong Fault based upon the elevation of the bases of a number of basalt flows suggests that the landscape had a low relief (predominantly <100 m) and dipped ~1º towards the northeast (van der Beek et al., 2001). This is in stark contrast to the current relief of over 700 m, and was used to infer plateau lowering and river incision rates of <14 and <40 m/Ma respectively. The former results are consistent with surface lowering rates calculated from in situ cosmogenic isotope abundances elsewhere in the Blue Mountains (13.2 m Myr^{-1} in heath and 11.4 m Myr^{-1} in forest, Wilkinson et al. 2003). These rates of denudation are of the same order as the rate of relief generation that might be expected from the limited data on eastern Australian fault slip rates (e.g. Clark & McCue, 2003; Sandiford, 2003) with the consequence that evidence for recent faulting might be difficult to recognise. Evidence for faulting might be even more difficult to recognise if activity is temporally clustered, as has been suggested for intraplate faults elsewhere (Crone et al., 1997, 2003; Clark et al., in press).

This paper presents an analysis of the morphology of streams crossing the northern LSC, focussing on Burralow Creek as the most pronounced example of a stream in disequilibrium. The study aims to provide insight on the fundamental question of whether recent or ongoing uplift must be invoked to explain the current relief of the LSC.

NEOTECTONIC INDICATORS

Longitudinal profiles of 16 streams (ranging in catchment area from 0.51 sq. km to 569 sq. km) crossing the six primary faults of the Kurrajong Fault System were digitised and plotted from 1:25,000 topographic sheets. Geological boundaries were transferred from the Penrith 1:100,000 Geological sheet (Jones & Clark, 1991) and the Sydney 1:250,000 sheet (ie. Rh:- Hawkesbury Sandstone, Rwa:- Ashfield Shales, Rno:- Burralow Formation, Rnw:- Banks Wall Formation, Bryan, 1966). Each long profile has also been plotted on semi-logarithmic axes to control for exponential decay of elevation from source to base level. Hack (1973), in developing the ideas of Mackin (1948), showed that any stream which is in dynamic equilibrium (ie. having sufficient slope to adequately transport supplied sediments) exhibited this concave upward profile form, thus plotting as a straight line on semi-log axes. Streams which flowed over differing lithologies plotted as a series of straight line segments on semi-log axes, with steeper segments corresponding to more resistant rocks. Profiles disturbed by tectonic activity could become markedly convex upward. A further morphometric test for tectonic activity is the examination of valley cross-sectional profiles on either side of the fault zones, following the procedure of Bull and McFadden (1977). The index of valley floor width : valley wall height (Vf) is an indication that in actively uplifting regions stream base levels are continually changing, hence vertical incision of valleys could outpace lateral erosion, as evidenced by a V-shaped cross-section with a minimal valley floor width.

Stream Profiles

The most obvious result upon examination of the longitudinal profiles (**Fig. 2**) is the remarkable similarity between them. Almost all streams exhibit a reach of low gradient immediately upstream of the Kurrajong Fault System, and a corresponding over-steepened reach downstream. The exception to this rule is the Grose River, and to a lesser extent Wheeny and Glenbrook creeks, which appear to be largely unaffected by the fault. In most cases this disruption is entirely independent of lithology, and largely independent of catchment size. Creeks to the north of the Grose River exhibit similar drainage disruption. However, the picture here is complicated by lithological variation. Most importantly, the steeper reaches downstream of the fault correspond with the supposedly less resistant rocks of the Narrabeen Group, in direct conflict with expectations (cf. Hack, 1960; 1973a). It could be argued therefore, that these anomalous over-steepened reaches indicate tectonic, and not lithological, control of the profiles in this area.

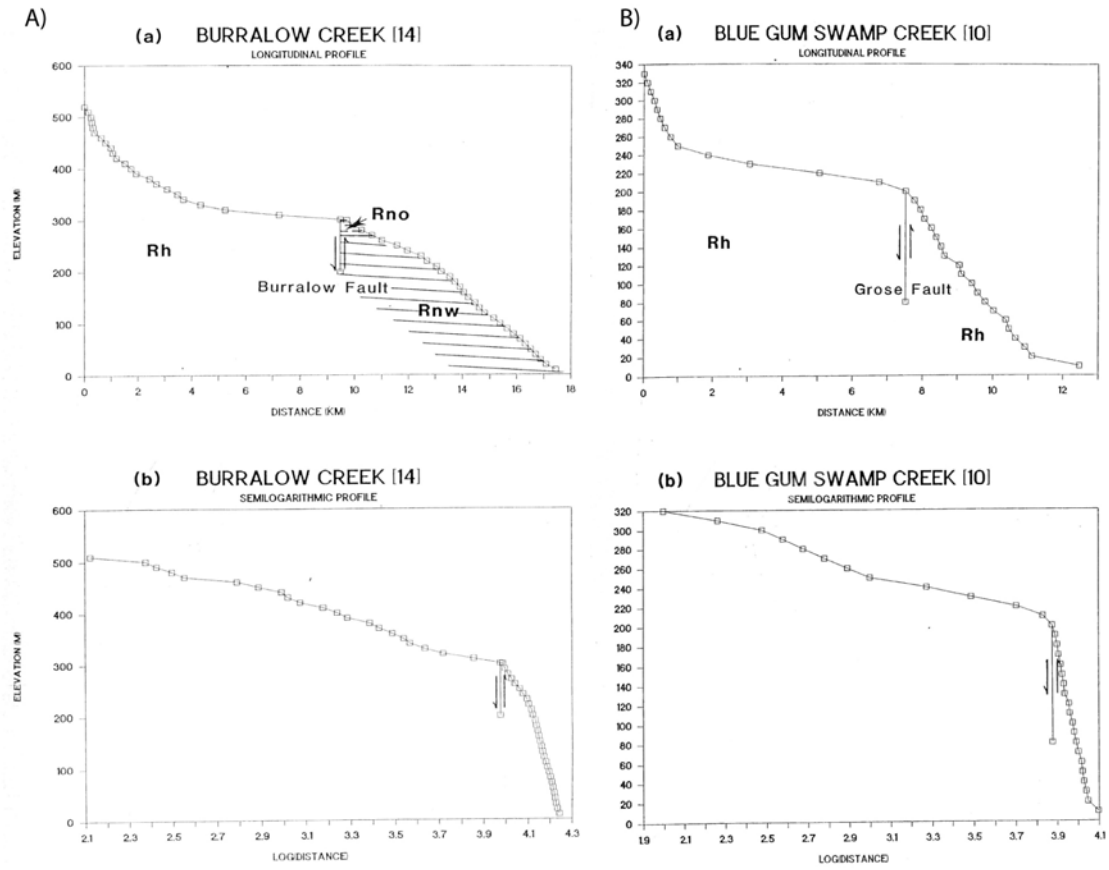

Figure 2: *Long profiles for selected easterly flowing streams passing through the northern Lapstone Structural Complex. a) Burralow Creek, b) Blue Gum Swamp Creek.*

The Stream Gradient (SL) Index is defined as the change in elevation of a stream reach normalised for the exponential decay of elevation along a typical stream length (**Fig. 3**). It is particularly sensitive to anomalous changes in slope, and can therefore be used to determine whether long profile shape is controlled by lithology or by tectonic deformation. For all streams crossing the Lapstone Structural Complex, SL values were found to be at least an order of magnitude greater between the KFS and Lapstone Monocline than in upstream reaches. This cannot be sufficiently explained by lithological variation across the fault zone, and is indicative of recent or ongoing deformation.

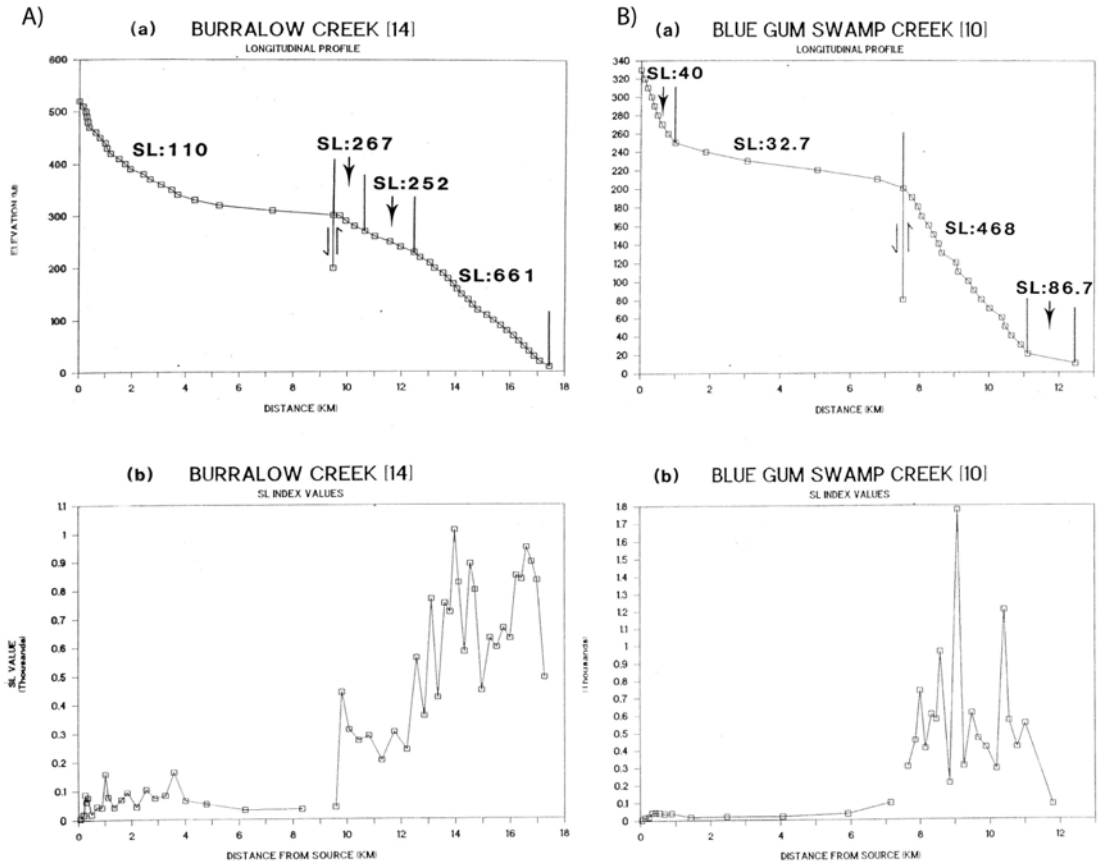

Figure 3: *Stream Gradient Index (SL) for selected easterly flowing streams passing through the northern Lapstone Structural Complex. a) Burralow Creek, b) Blue Gum Swamp Creek*

Valley Cross Sections

The valley cross-sections of 13 of the streams crossing the KFS show a marked difference as the streams pass into the deformed area (**Fig. 4**). The three largest streams (i.e. Wheeny Creek, Grose River and Glenbrook Creek) appear to be largely unaffected. Two representative examples are given to illustrate changes in valley shape. Those of Burralow Creek are shown in **Fig. 4a**, while nearby Morgan Creek cross sections appear in **Fig. 4b**.

The cross-sections of both Burralow Creek and Morgan Creek exhibit a wide valley floor on the upstream (downthrown) side of the fault, and V-shaped profiles immediately downstream of the fault. This is consistent with uplift between the KFS and the Lapstone Monocline (cf. Bull and McFadden, 1977). Downstream of the Kurrajong fault-line vertical incision appears to be outpacing lateral erosion, whereas the upstream side is controlled by the local base-level produced by the fault, therefore lateral erosion is dominant.

FAULT ANGLE DEPRESSIONS

An overwhelming result of the long profile analysis is the fact that drainage modification is evident for all streams with catchment sizes up to and including that of Glenbrook Creek. This modification is usually in the form of a marked reduction in stream gradient upstream of fault zones. Field evidence shows that this reduction in gradient is coincident with many swamps and lakes (eg.

Mountain Lagoon, Burralow Swamp, Blue Gum Swamp, Shaws Creek Swamp and Warrimoo Swamp). Other smaller unnamed swamps are also juxtaposed with the Kurrajong Fault System.

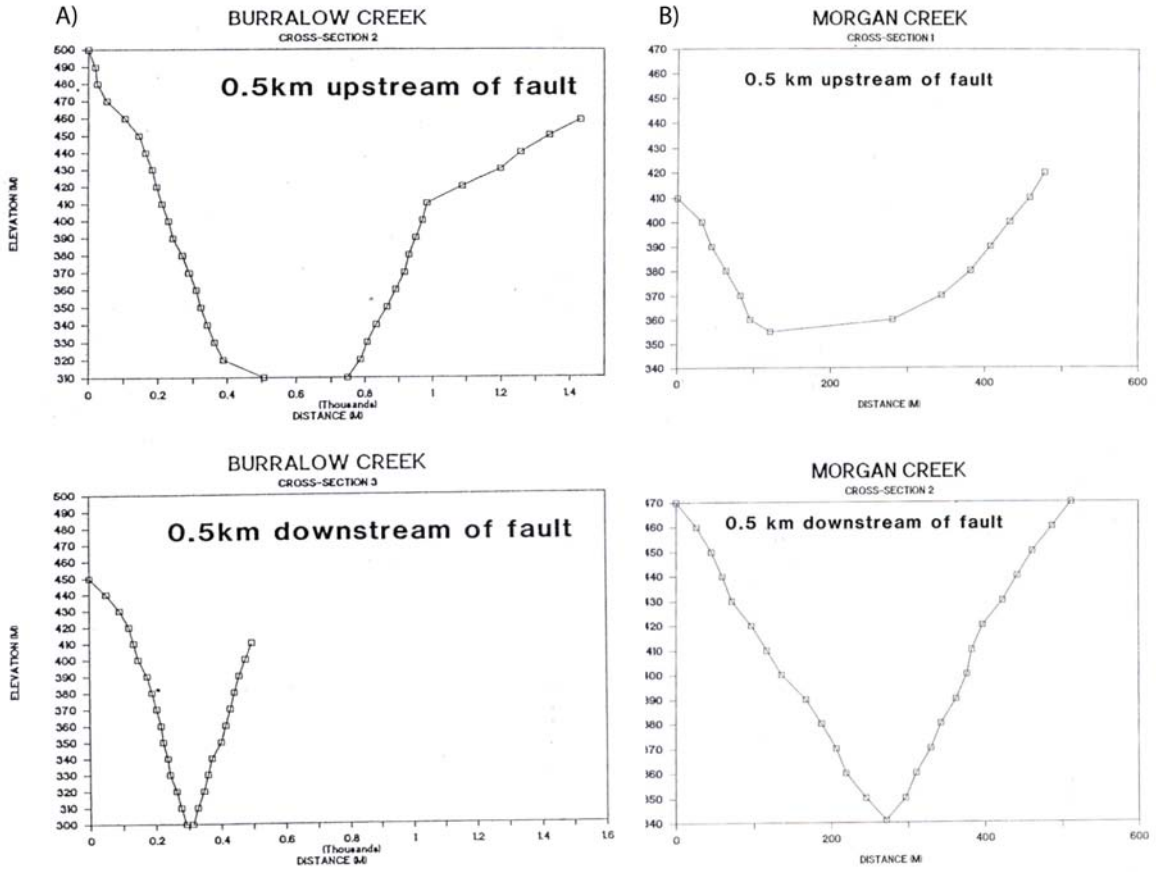

Figure 4: *Valley cross sections across selected easterly flowing streams passing through the northern Lapstone Structural Complex. a) Burralow Creek, b) Morgans Creek.*

Smaller Basins

Most of the smaller basins investigated were found to have a marked paucity of sediment accumulation at the fault, the exceptions being Burralow Swamp, Blue Gum Swamp, and possibly Shaw's Creek Swamp. Morgan Creek Swamp was found to contain no more than 3 metres of sediment at the fault, Winmalee Creek only 5 metres, and Warrimoo Creek only about 3.5 metres. Sediments are generally organic fine to medium sands, with minimal clay or silt fraction. In each case the maximum sediment depths were found in localised regions adjacent to a very narrow swamp. Away from the swamp axes, bedrock depth decreases sharply and sandy surface sediments are considered to be primarily slope wash deposits. Wide, flat floored basins first identified from air photos as large accumulations of sediment are in fact largely bedrock controlled.

These reaches of low gradient are considered to be caused by the imposition of a local base level at the fault, and it seems that the only effect of fault displacement is to maintain this perched base level and thus hinder incision upstream. Sedimentation could only have taken place immediately following major uplift events, whereas incision into the uplifted zone would act against the accumulation of sediments. The lack of sediments in the fault angle depressions, combined with the "neotectonic" features of the basin morphology suggests a long term average condition where incision largely matches uplift. This is an indication of slow and persistent uplift along the Kurrajong Fault System.

Burralow Swamp

Burralow Swamp (**Figs. 1, 5**) is an exceptional fault angle depression of the Kurrajong Fault System because it contains a considerable sediment accumulation which has both lateral and stratigraphic complexity. Seismic tests on the cleared ground bordering the Burralow Fault (the "Paddock Sands") show up to 20 metres of consolidated sediment with seismic velocities less than those expected for sandstone bedrock (Rawson, 1990). The swamp surface itself is far larger in extent than any other basin of the Lapstone Structural Complex, with valley wide swamp sedimentation in the upstream half of the basin. The downstream half of the swamp is inset into and onlaps the Paddock Sands unit, which appears to be a deep and coherent deposit most likely related to colluviation at the toe of the Burralow Fault scarp, which forms its eastern margin.

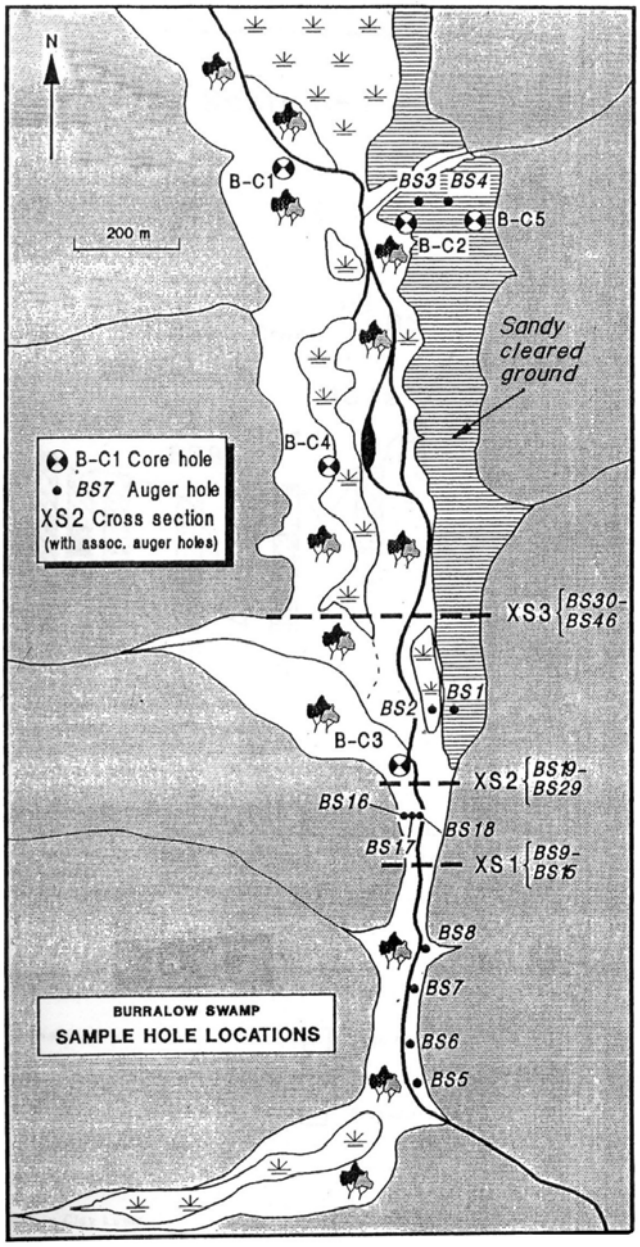

Figure 5: *Plan of Burralow Swamp showing the distribution of sedimentary units at the surface, and the locations of boreholes and coreholes from Rawson (1990).*

Drilling carried out on the downstream end of the valley floor has shown that although the present surficial sediments are dominated by sands, there is evidence of a persistent large swamp or lake in the past. This is indicated by an extensive deposit of organic clay/silt sediment (denoted the Tabaraga Unit, Rawson 1990) which locally reaches up to 6-7 metres thick and extends down to depths in excess of 10 metres (**Fig. 6**). The unit rapidly thins in a downstream direction and pinches out against a steeply rising bedrock bar relating to the Burralow Fault. We contend that this deposit is the result of tectonic rejuvenation whereby movement of the Burralow Fault has imposed a new, relatively higher, perched base-level leading to disruption of drainage. Sandy strata extending from the top of the fines to the surface are interpreted to have been deposited during the progressive restoration of the creek to pre-faulting conditions.

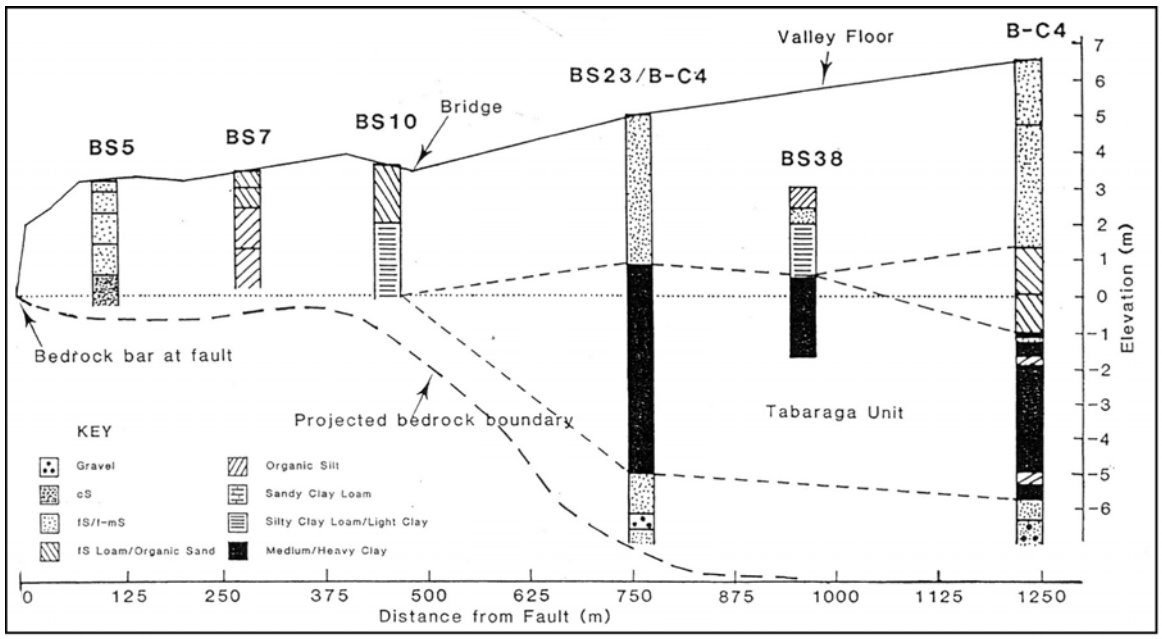

Figure 6: *Longitudinal section through Burralow swamp showing the distribution of the clay-rich Tabaraga Unit, inferred to be related to uplift of 6-7 m on the Burralow Fault.*

Timing of Sedimentation in Burralow Swamp

Having established that sedimentation within Burralow Swamp has been markedly affected by displacement on the Burralow Fault, the age of sediments within it should reflect the onset of at least the most recent phase of activity. Two radiocarbon ages were obtained from small charcoal samples from borehole B-C4 (**Fig. 5; Rawson, 1990**). The first, at a depth of 12.90 metres, came from coarse sandy sediments beneath the organic clays/silts of the Tabaraga Unit. This should indicate the age of pre-deformation fluvial sedimentation. The age obtained was 28200 (+900/-800) BP (SUA-2873). The second sample, from within the clayey unit at 8.80 metres, was dated at 35400 (+2400 -1990) BP (SUA-2874). The inversion of the dates is problematic, and might relate either to contamination of one or both of the samples, or redeposition of the top sample. The fact that both dates lie close to the limit of the dating technique also reduces the confidence that can be placed in them.

Sedimentological evidence does, however, mitigate in favour of accepting the dates, or at least a late Pleistocene age for the sediments. Both dates came from samples of clean, unindurated charcoal, which had no obvious contamination (eg. coatings, recrystallisation, or evidence of

humic acids) (Colin Murray-Wallace, verbal communication). The rest of the sediments within B-C4 also exhibited no iron induration, regardless of sediment type. This is unusual, considering that deep weathering profiles of only late Pleistocene age have been identified in alluvium on the nearby Nepean floodplain (Young et.al., 1987). Furthermore, the sediments were not cemented in any way, were not compacted, and there was no evidence of secondary crystallisation (diagenesis). In short, no indicator could be found to suggest that these sediments were Tertiary in age.

Eight samples were selected for pollen analysis from the Tabaraga Unit in boreholes B-C3 and B-C4 (Rawson, 1990). All of the samples indicate a Eucalyptus and Casuarina dominated sclerophyllous forest with a heath understorey. Significantly, this forest is seen to be dry, having few ferns and virtually no rainforest component. *Nothofagus* pollen is also noticeably absent. This pattern is essentially modern in character i.e. definitely Late Pleistocene - Holocene, with no Tertiary or early Pleistocene evident (J. Dodson, personal communication). The presence of some `small spined' *Asteraceae* grains perhaps indicates a pre-Holocene age for the sediments, as this particular taxon became extinct during the latest Pleistocene (cf. D'Costa et.al., 1989).

The sediments within the basin show gross characteristics consistent with a rapid change in flow regime caused by a rise in local base level at the fault, followed by a gradual re-establishment of equilibrium conditions. The dating results and sedimentology indicate that this change in flow regime occurred during the late Pleistocene.

DISCUSSION

Both the morphometric analysis of regional drainage and sedimentological evidence from fault angle depressions imply a significant influence of the Lapstone Structural Complex on landscape evolution in the Lower Blue Mountains. The majority of stream reaches downstream of the KFS exhibit marked oversteepening which, for the most part, cannot be explained by lithological control. It is postulated therefore that the majority of streams have not had sufficient stream power to keep pace with uplift focused on the KFS and Lapstone Monocline. The incision rate estimated for the Grose River (<40 m/Ma, Van Der Beek, 2001), which demonstrates an equilibrated long profile (Rawson, 1990), provides an upper limit on this time averaged rate of uplift.

Aspects of the character of activity of the Kurrajong Fault System can be inferred from these results. The Kurrajong fault system is approximately 40 km long (Bryan, 1966). The maximum magnitude earthquake that might be hosted on a fault system of this length is in the order of moment magnitude 7.0, which would involve 2.5 m to 3 m of uplift (Wells & Coppersmith, 1994). If it is assumed that the 6-7 m thickness of the Tabaraga Unit reflects an equivalent uplift across the KFS, two or three maximum magnitude earthquake events, or a greater number of smaller events, are required. The age and apparently homogeneous nature of the Tabaraga Unit suggests that these events were closely spaced in time in the Late Pleistocene.

The paucity of sedimentary fill in most of the fault angle basins associated with the Kurrajong Fault System suggests that this episode of activity was preceded by a long period of seismic quiescence. This pattern is consistent intraplate fault behaviour deduced from other sites within Australia, where active periods of earthquake activity comprising a finite number of large events are separated by much longer periods of seismic quiescence (Crone et al., 1997, 2003; Clark, 2007; Clark et al., in press). It is plausible in the case of the LSC that large earthquake frequency may have been in the order of several thousand to a few tens of thousand years in the late Pleistocene, but that this active period was not preceded by a rupture for a million years or more. Thus, the long-term rates of relief generation are likely to be of the same order or less than the rates of plateau lowering (cf. Wilkinson et al., 2003), and be much less than the rates of incision of the major streams (cf. Van Der Beek et al., 2001), with the result that neotectonic indicators are typically subtle (especially in stream profiles), and largely related to the most recent active period.

There is an apparent conflict between this evidence for recent activity and the palaeomagnetic data indicating that folding related to the Lapstone Monocline occurred prior to 8 ± 5 Ma (Bishop et.al., 1982 with ages recalculated by Pillans, 2003). Given that the Kurrajong Fault System and the Lapstone Monocline form part of the same structure (Herbert, 1989; Fergusson, this volume), deformation on the one might be expected to be accompanied by deformation on the other. One possibility, which is testable by careful field observation, is that the blind fault underlying the Lapstone Monocline (see Gibson, this volume) reached the surface in the Pliocene and deformation since then has been accrued by sliding along the fault rather than by folding. Alternatively, the recent active period may have been the first since the late Tertiary (cf. Branagan & Pedram, 1990) or Mesozoic (cf. Pickett & Bishop, 1992; Schmidt et al., 1992).

Given the very low uplift rates postulated for the LSC, passive exhumation (cf. Pickett and Bishop 1992) is likely to have played a significant role in the development of the contemporary landscape. In particular, the fact that the Tertiary Rickabys Creek Gravels overly Wianamatta Group shales on the Cumberland Plain, and Hawkesbury Sandstone on the face and top of the Lapstone Monocline, implies that erosional lowering of the landsurface had stripped shale from many areas west of the syn-depositional warp (proto-Lapstone Monocline) by the time of gravel deposition, but not to the extent that significant relief was generated [as indicated by structure within the gravels suggesting a braided stream depositional environment, Bishop & Hunter (1990)]. However, we demonstrate a significant tectonic imprint in the geomorphology of streams crossing the LSC, as distinct from the lithologic control that would be expected to dominate in a scenario only involving passive exhumation. Additional research, guided by new erosion rate data obtained on streams with catchment areas significantly smaller than the Grose River, is required to determine definitively whether this tectonic imprint relates only to the last active period identified in the sediments of Burralow Swamp, or to periodic activity throughout the late Tertiary.

Intuitively, the prominent 'V-notch' valley profiles of streams between the Kurrajong Fault System and the Lapstone Monocline suggest a recent tectonic history extending beyond the last active period. Furthermore, it is tempting to speculate that the apparent associations between the LSC and Miocene volcanics (Pedram, 1983; Branagan and Pedram, 1990; Van Der Beek et al., 2001) relate to late Tertiary development of the complex, synchronous with the establishment of the current crustal stress field, and a pulse of tectonic activity recorded in all southeast Australian basins (Dickinson et al., 2002; Sandiford et al., 2004). A terrestrial analogue to this pulse of deformation is seen in the Lake George Fault, which has accumulated up to 200 m of throw since the late Miocene (Abel, 1985).

CONCLUSIONS

The results of morphometric analysis of drainage lines crossing the northern Lapstone Structural Complex show indicators of geologically recent, and potentially ongoing tectonic deformation. Stream long-profiles oversteepen as they cross major faults, valley cross sections narrow to 'V-notches' where streams enter the upthrown side of fault blocks, and several streams have been partially dammed, forming swamps and lakes. While these indicators are consistent with a model of periodic (perhaps temporally clustered) deformation of the Kurrajong Fault System, near to the threshold conditions of uplift/incision, additional erosion rate data is required to determine the relative contribution of passive exhumation of syn-depositional basin structure in forming the present landscape.

The important question to ask relating to seismic hazard is whether faults of the LSC are still within an active period, or whether we are now in a quiescent period that might last many hundreds of thousands to a million years or more (cf. Crone et al., 2003). Earthquake epicenters located at depth to the west of the LSC (Gibson, this volume) potentially indicate that the most recent active period has not yet finished.

REFERENCES

ABEL, R.S., 1985. Geology of the Lake George Basin, N.S.W. Bureau of Mineral Resources, Geology and Geophysics Record 1985/4, 57p.

BANNERMAN S. M., 1990. Soil landscapes of the Penrith 1:100 000 sheet. Soil Conservation Survey of New South Wales 1:100 000 Soil Landscape Series Explanatory Notes, 122 pp.

BENDEFY L., DOHNALIK J. & MIKE K. 1967. New methods for genetic study of streams. International Association of Scientific Hydrology 75, 64-73.

BISHOP P. & HUNTER T. 1990. Pebble fabrics in the Rickabys Creek Gravel and their implications for the relationships between the Lapstone Monocline and the Rickabys Creek Gravel. Geological Survey of New South Wales Report GS 1990/281.

BISHOP, P., 1986: Horizontal stability of the Australian continental drainage divide in South Central New South Wales during the Cainozoic. Aust. J. Earth Sciences, 33, 295-307.

BISHOP, P., HUNT, P., and SCHMIDT, P.W., 1982: Limits to the age of the Lapstone Monocline, N.S.W. - a palaeomagnetic study. J. Geol. Soc. Aust., 29, 319-326.

BRANAGAN D. F. & PEDRAM H. 1990. The Lapstone Structural Complex, New South Wales. Australian Journal of Earth Sciences 37, 23-36.

BRYAN, J. H., 1966. Geology of the Sydney 1:250 000 sheet. Geological Survey of New South Wales 1:250 000 Geological Series Explanatory Notes, 46 pp.

BULL, W.B., and MCFADDEN, L.D., 1977: Tectonic geomorphology north and south of the Garlock fault, California. In: Doehring, D.O. (ed.) Geomorphology in arid regions. Publ. Geomorphol. Proc.,8th Annu. Geomorphol. Symp.,State Univ. N.Y.,BinQhamton, 118-138.

CLARK D., 2007. Temporal clustering of surface ruptures on stable continental region faults: a case study from the Cadell Fault scarp, south eastern Australia. Proceedings of the Australian Earthquake Engineering Society Conference, Wollongong, Australia, November 2007, pp17.

CLARK, D.J., & MCCUE, K., 2003. Australian Palaeoseismology: towards a better basis for seismic hazard estimation. Annales of Geophysics 46, 1087-1105.

CLARK, D.J., CUPPER, M., SANDIFORD, M., & KIERNAN, K., in press, Style and timing of late Quaternary faulting on the Lake Edgar Fault, southwest Tasmania, Australia: implications for hazard assessment in intracratonic areas. Geological Society of America Special Publication.

CRONE, A.J., DE MARTINI, P.M., MACHETTE, M.N., OKUMURA, K., & PRESCOTT, J.R., 2003. Paleoseismicity of aseismic Quaternary faults in Australia: Implications for fault behaviour in stable continental regions. Bulletin of the Seismological Society of America 93, 1913-1934.

CRONE, A.J., MACHETTE, M.N., & BOWMAN, J.R., 1997. Episodic nature of earthquake activity in stable continental regions revealed by palaeoseismicity studies of Australian and North American Quaternary faults. Australian Journal of Earth Sciences 44, 203-214.

CROOK, K.A.W., 1956: The geology of the Kurrajong-Grose River district. M.Sc. Thesis, University of Sydney, (Unpubl.).

D'COSTA D. M., EDNEY P., KERSHAW A. P. & DE DECKKER P. 1989. late Quaternary palaeoecology of Tower Hill, Victoria, Australia. Journal of Biogeography 16, 461-482.

DICKINSON, J.A., WALLACE, M.W., HOLDGATE, G.R., GALLAGHER, S.J. & THOMAS, L., 2002. Origin and timing of the Miocene–Pliocene unconformity in southeast Australia. Journal of Sedimentary Research 72, 288-303.

HACK J. T. 1960. Interpretation of erosional topography in humid temperate regions. American Journal of Science 258-A, 80-97.

HACK J. T. 1973. Stream-profile analysis and stream-gradient index. Journal of Researchof the United States Geological Survey 1, 421-429.

HARRINGTON H. J. & KORSCH R. J. 1985. tectonic model for the Devonian to middle Permian of the New England Orogen. Australian Journal of Earth Sciences 32, 163-179.

HERBERT C. 1989. The Lapstone Monocline - Nepean Fault; a high angle reverse fault system. In: R.L. Boyd and K. Allen (eds). Proceedings of the Twenty Third Newcastle Symposium: Advances in the study of the Sydney Basin, Newcastle, NSW, 217-224.

JONES D. C. AND CLARK N. R., 1991. Geology of the Penrith 1:100 000 sheet. Geological Survey of New South Wales 1:100 000 Geological Series Explanatory Notes, 202 pp.

MACKIN J. H. 1948. Concept of the graded river. Bulletin of the Geological Society of America 59, 463-512.

PEDRAM, H., 1983: Structure and engineering geology of the lower Blue Mountains, Sydney Basin, N.S.W., Australia., M.Sc. Thesis, University of Sydney, (Unpubl.).

PICKETT J. W. & BISHOP P. 1992. Aspects of landscape evolution in the Laptsone Monocline area, New South Wales. Australian Journal of Earth Sciences 39, 21-28.

PILLANS, B. 2003. Dating ferruginous regolith to determine seismic hazard at Lucas Heights, Sydney. In: Ian C. Roach, (Editor) Advances in Regolith: Proceedings of the CRC LEME Regional Regolith Symposia, 2003 CRC LEME, 324-327.

QURESHI, LR., 1984: Wollondilly - Blue Mountains gravity gradient and its bearing on the origin of the Sydney Basin. Aust. J. Earth Sciences, 31, 293302.

RAWSON, G. A., 1990. Drainage modification associated with the Lapstone Structural Complex, New South Wales – Geomorphological evidence for neotectonism. Unpublished Masters thesis, University of Sydney, 179pp.

SANDIFORD, M., 2003. Neotectonics of southeastern Australia: linking the Quaternary faulting record with seismicity and in situ stress: In: eds Hillis R.R. & Muller D, Evolution and dynamics of the Australian Plate. Geological Society of Australia Special Publication 22, 101-113.

SANDIFORD, M., WALLACE, N., & COBLENTZ, D., 2004. Origin of the in situ stress field in southeastern Australia. Basin Research 16, 325-338.

SCHMIDT P. W., LACKIE M. A. & ANDERSON J. C. 1995. Palaeomagnetic evidence fro the age of the Lapstone Monocline, NSW. Australian Coal Geology 10, 14-18.

SCHUMM S. A., DUMONT J. F. AND HOLBROOK J. M., 2000. Active tectonics and alluvial rivers. Cambridge University Press, Cambridge, 276 pp.

VAN DER BEEK, P., PULFORD, A., AND BRAUN, J. 2001. Cenozoic Landscape Development in the Blue Mountains (SE Australia): Lithological and tectonic Controls on Rifted Margin Morphology. The Journal of Geology 109, 35-56.

WELLMAN, P. and MCDOUGALL, L, 1974: Potassium-argon ages on the Cainozoic volcanic rocks of New South Wales. J. Geol. Soc. Aust., 21, 247-272.

WELLS, D.L., & COPPERSMITH, K.J., 1994. New Empirical relationships among magnitude, rupture length, rupture width, rupture area, and surface displacement. Bulletin of the Seismological Society of America 84, 974-1002.

WILKINSON M. T., HUMPHREYS G.S., CHAPPELL J., FIFIELD K. & SMITH B., 2003. Estimates of soil production in the Blue Mountains, Australia, using cosmogenic 10Be. Advances in Regolith: Proceedings of the CRC LEME Regional Regolith Symposia, 2003. pp 441-443.

YOUNG R. W., NANSON G. C. & JONES B. G. 1987. Weathering of late Pleistocene alluvium under a humid temperate climate: Cranebrook Terrace, southeastern Australia. Catena 14, 469-484.

ZUCHIEWICZ W. 1979. A possible application of a theoretical longitudinal river profile analysis to an investigation of young tectonic movement. Annales de la Societe Geologique de Pologne 49, 327-342.

New field observations pertaining to the age and structure of the northern Lapstone Structural Complex, and implications for seismic hazard

DAN CLARK[1] AND ANDREW RAWSON[2]
1. GEOSCIENCE AUSTRALIA, GPO BOX 378, CANBERRA ACT 2601
2. NSW DEPT. OF ENVIRONMENT AND CLIMATE CHANGE, C/O FACULTY OF SCIENCE AND AGRICULTURE, CHARLES STURT UNIVERSITY, LEEDS PDE, ORANGE PO BOX 883 NSW 2800

ABSTRACT

A structural transect along a ridge entering Wheeny Gap from the west provides important insight into the nature of faults comprising the northern Lapstone Structural Complex (LSC). Sheared sandstone outcropping along the ridge east of the Kurrajong fault scarp suggests that the Kurrajong Fault is a steeply east-dipping reverse fault, in accordance with the interpretation of seismic profiles further to the south. A previously unrecognised west-dipping reverse fault (Wheeny Gap Fault) with at least several tens of metres of displacement was observed in a cliff face on the northern side of Wheeny Gap, several hundred metres east of the Kurrajong Fault. Relatively recent activity is suggested on the Wheeny Gap Fault as it laterally displaces the cliff face formed during the passage of a knickpoint up Wheeny Creek relating to initial relief generation across the Lapstone Monocline. Earthquake hypocentres recorded over the last few decades occur predominantly at depth to the west, and have been used to suggest the presence of a blind west-dipping reverse fault, into which the Kurrajong and Wheeny Gap faults link at depth. We present an evolutionary model for the LSC based upon this architecture which reconciles evidence for late Cenozoic uplift across the LSC and the observation that the Rickaby's Creek Gravels overlie shale on the Cumberland Plain and sandstone on the Lapstone Monocline. This model suggests that the findings of a major seismic hazard assessment of the Sydney Basin, which concludes that magnitude M_W7.0 and greater earthquake events might be expected on the LSC on average every 15-30 ka, should be treated with caution. This expectation of regular recurrence must be tempered by the possibility that a large part of the relief relating to the LSC may have formed in the late Miocene or earlier, and evidence from other Australian intraplate faults suggesting that large earthquake occurrence is markedly temporally clustered.

Keywords: Lapstone Structural Complex, reverse fault, seismic hazard, seismicity

INTRODUCTION

Faults of the Lapstone Structural Complex (LSC - Mauger *et al.* 1984) underlie the eastern range front of the Blue Mountains west of Sydney over a distance of at least 100 km, and perhaps as much as 160 km (e.g. Branagan 1969; Branagan and Pedram 1990). More than a dozen major faults and monoclinal flexures have been mapped in the region where relief relating to the complex is most prominent, between Bargo and the Colo River north of Mountain Lagoon (**Fig. 1**). While these structures have been known for more than 100 years (Branagan, this volume and references therein) very little is known about their subsurface geometry and faulting history, particularly in the Cenozoic. The latter uncertainty stems in a large part from a paucity of readily dateable Cenozoic units associated with faulting (e.g. Wellman and McDougall 1974; Bishop *et al.* 1982; Rawson 1990; Pickett and Bishop 1992).

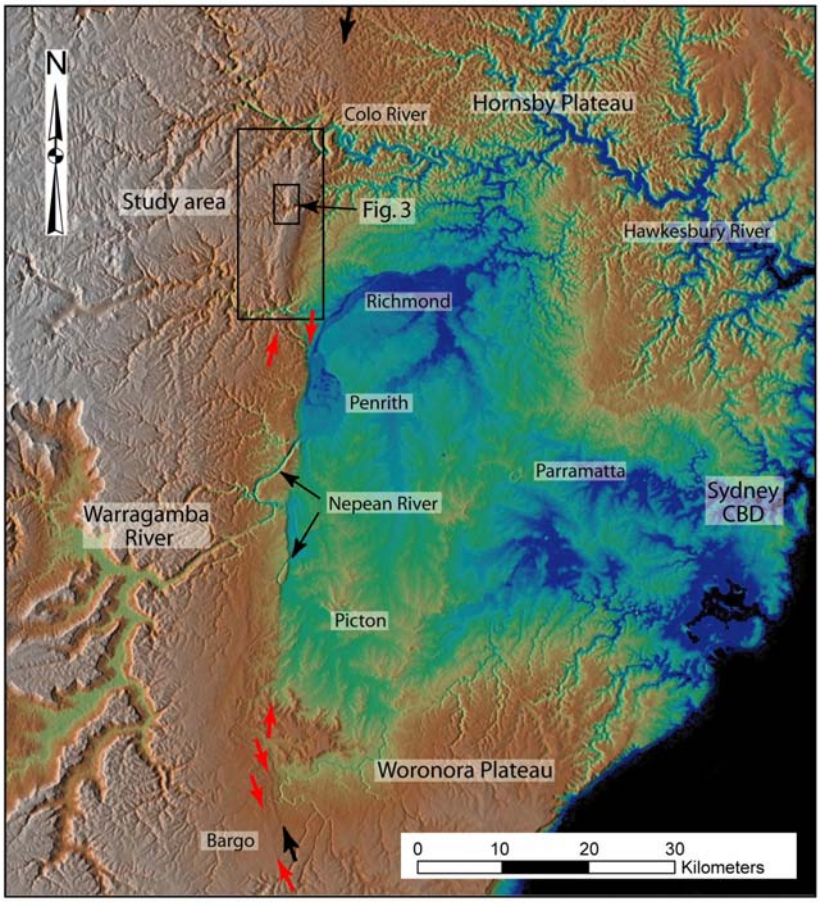

Figure 1: *Colour-draped and hill-shaded SRTM DEM (90m) image of the Lapstone Structural Complex west of Sydney. The region covered by this article is indicated with a box, as is the area of Fig. 3. Illumination is from the west. Red arrows highlight scarp segments. Black arrows indicate the extents of the profiles in Fig. 2.*

Over the last few decades the most significant concentration of earthquake hypocentres in the Sydney Basin has occurred at depth west of the LSC (Gibson, this volume). This relationship has been used to suggest that the surface expression of the LSC reflects displacement across a low angle reverse fault, emergent at the surface south of Penrith, and underlying the Lapstone monocline to the north. Based upon this model, a recent study of seismic hazard in the Sydney Basin identified the LSC as a potential source for large and damaging earthquakes, and estimated a recurrence of 15-30 ka for events exceeding M_W 7.0 (Berryman *et al.* 1999). As this analysis was necessarily based upon limited geochronological and structural data the results must be treated as highly uncertain. In particular, the authors contend that deformation resulting in the development of the Lapstone Monocline postdates the 18.8 Ma (Wellman and McDougall 1974) extrusion of the Green Scrub Basalt, which appears to have been truncated by the Kurrajong Fault (Branagan and Pedram 1990) but might just as plausibly have been emplaced against an extant fault scarp. Alternative views contend that fold development was largely complete by the Early Jurassic (Pickett and Bishop 1992), the Late Jurassic (Herbert 1989), post-mid Cretaceous (Schmidt *et al.* 1995), the Early Tertiary (Branagan and Pedram 1990; van der Beek *et al.* 2001), and the Late Tertiary (Bishop *et al.* 1982 with age recalculated by Pillans 2003). Furthermore, seismic reflection data acquired along several lines across the Nepean Fault (the southern range bounding fault) have been interpreted to suggest steep westerly dips, in the range of 50-70°, to at least 2.5 km depth (Herbert 1989).

This contribution briefly reviews existing geologic information for the northern LSC and presents new structural data from a preliminary traverse through Wheeny Gap. The implications of the new data for landscape evolution and seismic hazard assessment are discussed.

GEOMORPHIC CHARACTER AND STRUCTURE OF THE LAPSTONE STRUCTURAL COMPLEX

The range front scarp relating to the LSC rises monotonically from zero near Bargo to a relief of approximately 400 m immediately south of the Colo River (**Fig. 2**). The expression of the range front south of the confluence of the Nepean and Warragamba rivers is sharp and linear, and is defined over much of its length by a line of cliffs developed in Hawkesbury Sandstone. This expression reflects the emergence at the surface of the range front fault, the Nepean Fault, as evidenced by exposures in major cross-cutting drainage lines (Branagan and Pedram 1990). Further north the east-facing scarp is broader (up to 2 km) and is underlain by a flexure called the Lapstone Monocline (e.g. Bryan 1966; Branagan and Pedram 1990). West-facing scarps are prominently developed a couple of kilometres to the west of the monocline (e.g. David 1896, 1902). Interpretation of seismic reflection profiles acquired south of the Grose River suggest that high angle reverse faults with a geometry suggestive of a significant wrench component underlie these west facing scarps in the north, and the east facing scarps in the south (Herbert 1989). Herbert (1989) further contends that in contrast to the continuous and sinuous nature of the faults as mapped (c.f. Bryan 1966), they are in fact composed of much shorter, discontinuous, straighter *en echelon* segments; namely the Kurrajong, Burralow, Grose, Frasers, Yellow Rock and Glenbrook faults (Branagan and Pedram 1990).

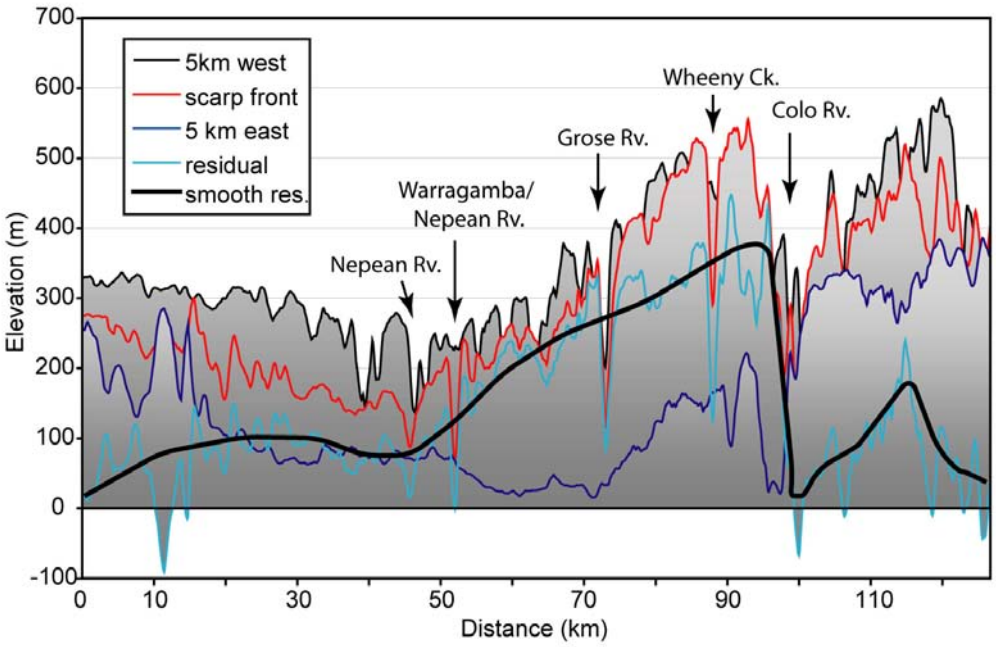

Figure 2: *Scarp-parallel topographic profiles along the LSC. "Residual" represents values from the scarp front minus those 5 km east. The residuals are depressed south of the Nepean River as some deformation is accommodated on the Oakdale Fault, west of the range front Nepean Fault. Location of profiles is shown on Fig. 1.*

The nature of the faulting which gave rise to the Lapstone Monocline is the subject of debate. Sedimentary units thin to the west across the Lapstone Monocline, indicating that the structure was active during Permian and Mesozoic sedimentation and rifting, and hence may be underlain by an

east-dipping normal fault (e.g. Bryan 1966; Branagan and Pedram 1990; Pickett and Bishop 1992; Australian Oil and Gas Corporation Ltd 1966). Pickett and Bishop (1992) argue that monocline development was complete by the time of the Early Jurassic intrusion of the Norton's Basin Diatreme, and that the high angle reverse faulting, at least in part, postdates this. While more recent palaeomagnetic evidence requires that the majority of flexure post-dates the mid-Cretaceous (Schmidt *et al.* 1995), the hypothesis that monocline development and high angle reverse faulting are temporally separate remains plausible.

Herbert (1989) implies that monocline development is related to displacement on the high angle west-dipping reverse faults imaged in seismic reflection profiles. This structural relationship is supported by Fergusson (this volume) who relates the structures exposed in the central section of the Lapstone Monocline, at the Hawkesbury Lookout, to a 50° west-dipping reverse fault at depth. An alternative interpretation of the main physiographic features is presented by Berryman *et al.* (1999), who envisage the high angle reverse faults of Herbert (1989) linking into a low angle master reverse fault at depth. The existence of this master fault is inferred from a spatial clustering of earthquake hypocentres at depth to the west of the LSC (cf. Gibson, this volume). Berryman *et al.* (1999) postulate that a shallowing of the underlying master fault dip relative to the Nepean Fault accounts for the monoclinal shape of the range front north of Penrith, and that both monocline and west-facing scarps are a consequence of post mid-Miocene movement on this blind thrust system.

AGE OF MAJOR DISPLACEMENT ACROSS THE LAPSTONE STRUCTURAL COMPLEX

Blue Mountains basalts cap relatively flat hilltops, suggesting that they may be remnants of an initially continuous subhorizontal sheet and predate river incision (Carne 1908; Wellman 1979). A reconstruction of the *ca.* 20 Ma palaeotopography west of the Kurrajong Fault based upon the sub-surface elevation of a number of basalt flows suggests that the landscape had a low relief (predominantly <100 m) and dipped ~1º towards the northeast (van der Beek *et al.* 2001). This is in stark contrast to the current relief of over 700 m. These authors attribute the difference to the passage of major knickpoints up river valleys due to base level lowering, either initiated during rifting of the Tasman Sea (*ca.* 100 Ma), or by rejuvenation of structures of the LSC (*ca.* 40-50 Ma). Detailed numerical modelling of landscape evolution conducted as part of the same study reproduced the main physiographic features of the Blue Mountains only when post-rifting passive erosional exhumation of the Sydney Basin was influenced by tectonic uplift of the LSC. While these model results provide evidence to support a Cenozoic age for the uplift across the Lapstone Structural Complex (including development of the Lapstone Monocline), the geologic evidence is equivocal.

The base of the 18.8 Ma (Wellman and McDougall 1974) Green Scrub basalt flow unconformably overlies Wianamatta Group shale at an elevation of 560-580 m. The outcrop occurs 12 km to the east of Mt Tootie, which has a sub-basalt elevation of 750 m (van der Beek *et al.* 2001). It is therefore plausible that the Green Scrub flow erupted onto the same pre-dissection, low relief Miocene surface as other Blue Mountains Plateau basalts (cf. Pulford 1997; van der Beek *et al.* 2001). As the eastern margin of the Green Scrub outcrop defines the trace of the Kurrajong fault (Bryan 1966; Branagan and Pedram 1990) it is likely that dissection of the Blue Mountains Plateau via knickpoint retreat up the major drainage lines had not progressed west of the LSC at *ca.* 20 Ma. The implications, supported by the apparent truncation of the Green Scrub flow by the Kurrajong Fault, are that knickpoint initiation is predominantly related to uplift across the LSC, and that uplift largely post-dates *ca.* 20 Ma (see also Berryman *et al.* 1999). However, stratigraphic relationships between the Tertiary Rickaby's Creek Gravel and the Triassic rocks forming the Lapstone Monocline appear to contradict this thesis.

The Rickaby's Creek Gravel is a fluvial unit disconformably overlying the Triassic rocks of the Sydney Basin (e.g. David 1897; Branagan and Pedram 1990). Clast lithology, size and sedimentary structures within the gravel point to a provenance identical to the present Warragamba-Nepean River system (Bishop 1986; Pickett and Bishop 1992). Near Penrith the gravels occur on the Cumberland Plain, as well as on the face of the Lapstone Monocline and to its west as far as Glenbrook (e.g. Branagan and Pedram 1990). On the plain the gravels overlie Wianamatta Group shales whereas they overlie Hawkesbury Sandstone in elevated regions (Chesnut 1982; Pickett and Bishop 1992). This evidence casts doubt on the widely accepted view that the gravel originally formed a continuous sheet that predates the monocline (e.g. David 1897), as shale has apparently been stripped from elevated regions prior to deposition of the gravel (Pickett and Bishop 1992). Pickett and Bishop (1992) contend that this relationship is best explained if the monocline is an 'old' structure (early Jurassic) that has been progressively exhumed during deposition of the Rickaby's Creek Gravel, which is postulated to be a composite diachronous unit.

STRUCTURAL RELATIONSHIPS EXPOSED IN WHEENY GAP

A reconnaissance structural traverse was conducted down an easterly-trending ridge that approaches Wheeny Gap from the west and crosses the trace of the Kurrajong Fault (**Fig. 3**). This unnamed ridge is hereafter referred to as Wheeny Gap Ridge for ease of reference. The initial 300 m of the traverse descends steeply through several cliff-lines formed in undeformed and horizontally-bedded blocky Hawkesbury Sandstone (Rh, **Fig. 3**). Thereafter the ridge flattens and is developed in poorly exposed Narrabeen Group sandstone and shaley fine sandstone (Rn). At grid location 279623mE/6292172mN (GDA94/MGA56) shaley fine sandstone was observed to dip 45-50º towards the west (**Fig. 4a**). Bedding at this location strikes roughly parallel to the Kurrajong Fault escarpment (~10º strike). A potential down-dip slickenside (~110º rake) was observed on one dipping bedding plane and is interpreted to reflect flexural slip (**Fig. 4a**). Within ~100 m to the east the sandstone is again sub-horizontally bedded. At grid reference 279691mE/6292198mN the ridge descends into a 20 m wide saddle ~5 m below the ridge level. The sandstone within the saddle contains sub-vertical (to steeply east-dipping) fractures and is sheared in several zones up to a metre wide (**Fig. 4b**). Fractures are open and are typically associated with pale clayey sand. We consider it probable that this saddle represents an eroded fracture zone, potentially relating to a steeply dipping fault inferred on the basis of a conspicuous ridge and associated drainage line on the southern side of the gap (**Figs. 3b, 5**).

Beyond the saddle blocky cliff-forming sandstone is again encountered. The change in lithology is associated with a rise in topography of ~10-15 m. Shaley fine sandstone intercalations suggest that these rocks belong to the Narrabeen Group. Fifty metres east of the saddle a relatively elevated subsidiary saddle occurs. The sandstone in this saddle is sub-vertically sheared with a 5 cm fracture spacing aligned with the Kurrajong Fault escarpment (~10º strike). Fractures are typically open and are variably filled with white clayey sand similar to that found further west (e.g. **Fig. 4a**).

A reverse fault is visible on the northern cliff face of Wheeny Gap from the eastern end of the ridge, immediately before it drops steeply into Wheeny Gap (**Fig. 4c**). The fault, herein referred to as the Wheeny Gap Fault, dips at between 45º and 50º to the west and appears from its intersection with the topography to be north striking (**Figs. 5a, b**). The sandstone bedding in the hanging wall has been dragged into the fault plane forming a monoclinal fold (**Fig. 4c**). Bedding dips approximately 30º towards the east immediately above the fault plane, and is shallowly dipping to flat-lying on the eastern side (footwall) of the fault. The amplitude of the roll suggests a minimum of several tens of metres of displacement. A band of foliage several metres wide occupying the fault plane on the cliff face suggests a well-developed gouge or crush/fracture zone. The vertical displacement estimate from the monoclinal roll alone might therefore be a significant underestimate. This supposition is

supported by the observation that the cliff face is laterally displaced by ~20-30 m across the fault (**Fig. 5a – circled area**).

South of Wheeny Creek, the Wheeny Gap Fault is inferred to follow a gully-line to the top of the escarpment. The intersection of the fault with Wheeny Creek could not be easily accessed from the ridge to check for displacement in the creek bed relating to recent displacement. However, a sandstone bench developed at the top of the cliff face in which the fault is exposed appears, albeit from a significant viewing distance, to be displaced by a few metres (**Fig. 4c**).

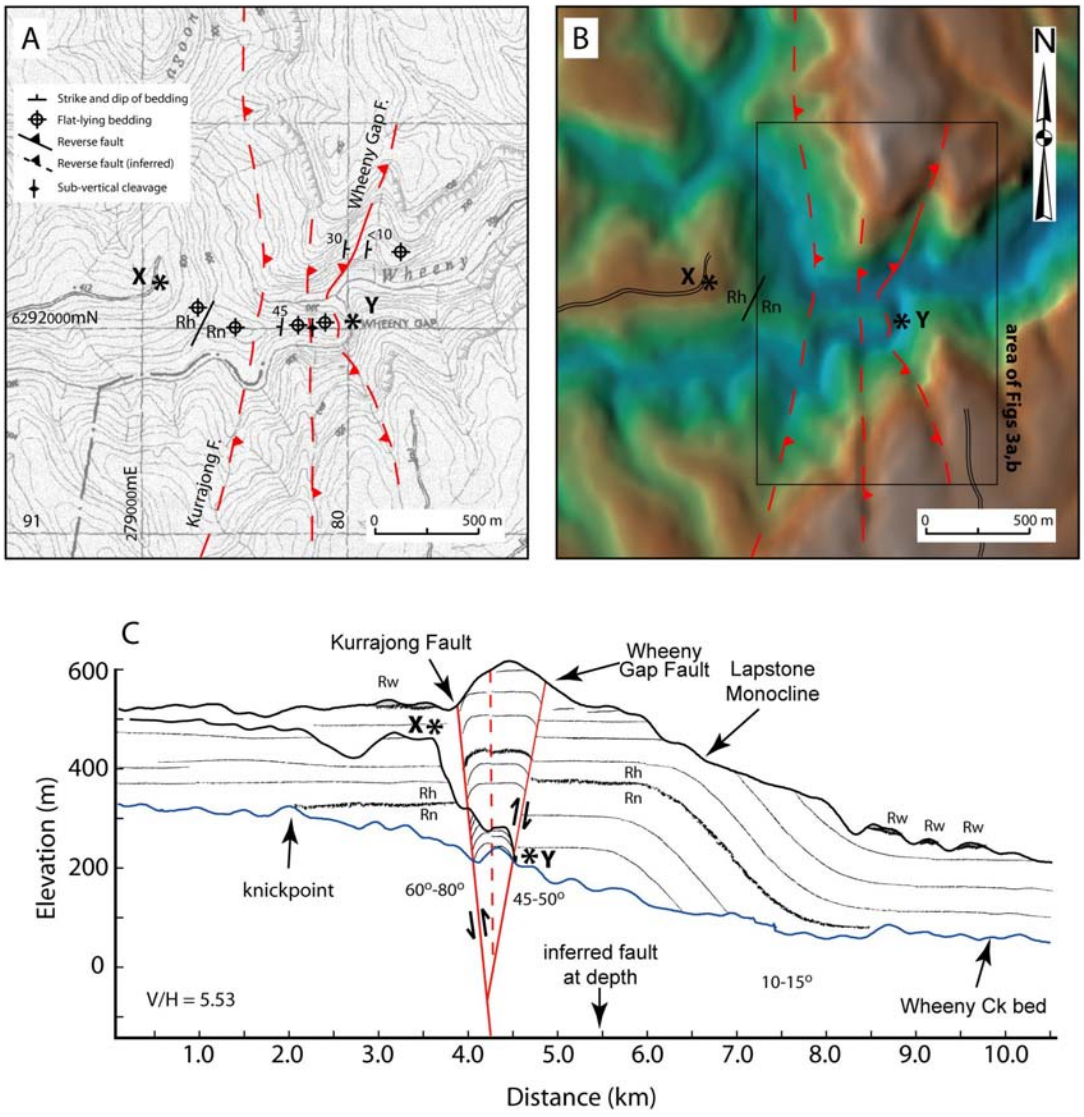

Figure 3: *Topography and structure of Wheeny Gap. (a) location of the structural traverse (marked by asterisks) transposed onto the Mountain Lagoon 1:25,000 topographic map. Fault traces are inferred - ticks are on the hanging wall. Rh=Hawkesbury Sandstone, Rn=Narrabeen group sandstone. (b) hillshaded and colour draped DEM (LPI 25 m) with fault traces inferred. (c) topographic profiles along the ridge top at Mountain Lagoon and Wheeny Creek (location as for Fig. 6), and the Wheeny Gap Ridge along the line X-Y indicated in part (b). The faulting observed in Wheeny Gap is superposed. Throw of the Kurrajong Fault and dip of strata on the face of the monocline from Branagan and Pedram (1990).*

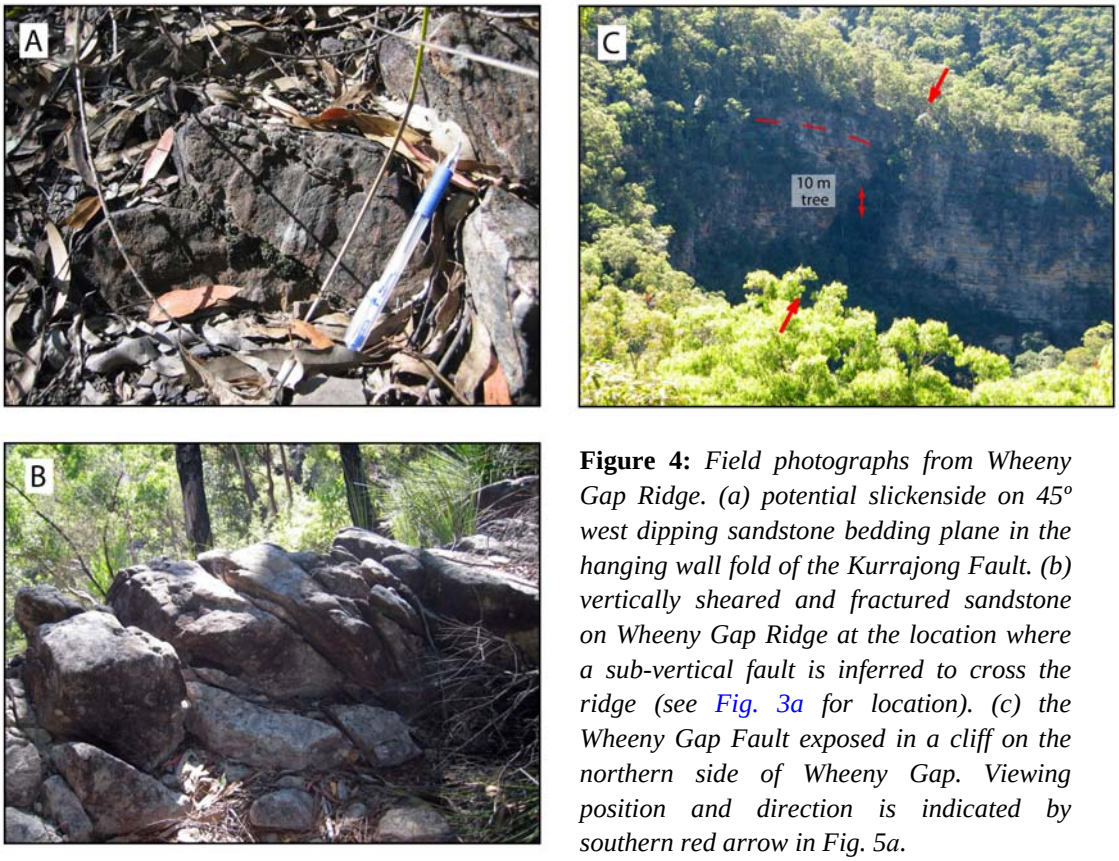

Figure 4: *Field photographs from Wheeny Gap Ridge. (a) potential slickenside on 45º west dipping sandstone bedding plane in the hanging wall fold of the Kurrajong Fault. (b) vertically sheared and fractured sandstone on Wheeny Gap Ridge at the location where a sub-vertical fault is inferred to cross the ridge (see Fig. 3a for location). (c) the Wheeny Gap Fault exposed in a cliff on the northern side of Wheeny Gap. Viewing position and direction is indicated by southern red arrow in Fig. 5a.*

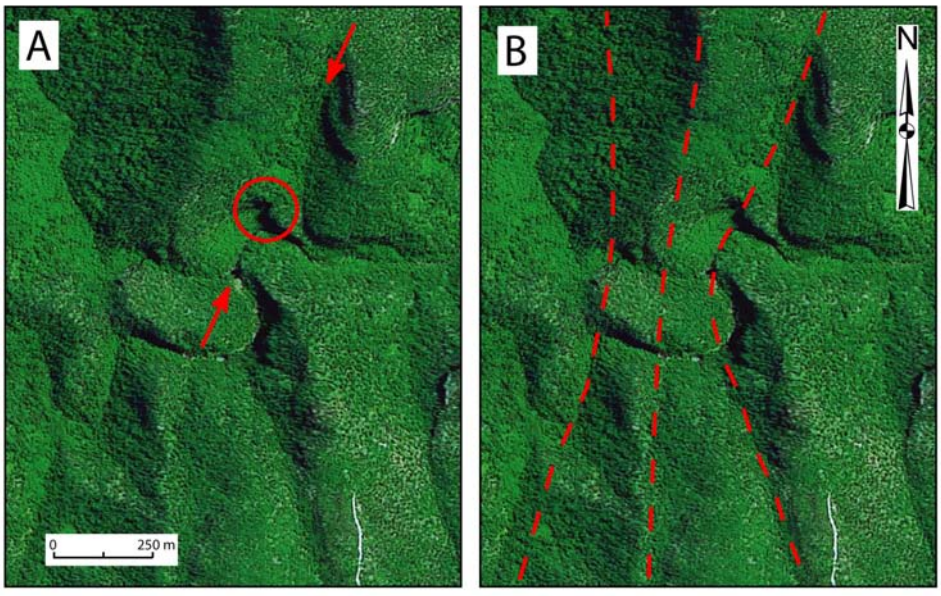

Figure 5: *SPOT 5 images of Wheeny Gap. (a) northern extension of Wheeny Gap Fault is indicated by arrows. Displaced cliff face is circled. (b) same as a, but with fault traces inferred as per Fig. 3.*

We consider the west-dipping sandstone bedding seen on Wheeny Gap Ridge to be analogous to that found in the hanging wall of the Wheeny Gap Fault and associate this zone with a steeply east-dipping Kurrajong Fault (**Figs. 3a, b**). This is consistent with the 80º east dip measured on a 3-4 m wide fault zone interpreted to relate to the Kurrajong Fault at Cut Rock on the Bells Line of Road 3.7 km to the south (Branagan and Pedram 1990). The spatial relationships between the Kurrajong and Wheeny Gap faults suggest that they merge less than 300 m below the level of Wheeny Creek.

The structural relationships exposed in Wheeny Gap are consistent with the interpretation of seismic profiles further south (Herbert 1989); the faults underlying the west facing scarps (e.g. Glenbrook, Kurrajong, Burralow) are steeply east-dipping reverse faults, which in places, such as Wheeny Gap, link into moderately steep west-dipping reverse faults with clear evidence for wrench displacement.

WHEENY CREEK STREAM MORPHOLOGY

Hack (1973) showed that any stream which is in dynamic equilibrium (i.e. having sufficient slope to adequately transport supplied sediments) exhibits a concave upward long(itudinal) stream profile that plots as a straight line on semi-logarithmic axes. Streams which flow over differing lithologies plot as a series of straight line segments, with steeper segments corresponding to more resistant rocks. Disequilibrium may be demonstrated by a change in slope unrelated to lithology.

The Wheeny Creek long profile demonstrates a grossly convex-upward form (**Fig. 6**). In detail, this form apparently comprises two concave upward sections which join near to the mapped boundary between the Hawkesbury Sandstone and Narrabeen Group sandstone (**Fig. 6b**). The gross profile form might therefore be explained in terms of this lithological change. This interpretation is supported when the profile is plotted on semi-log axes (**Fig. 6c**), with straight line segments of differing slope coinciding closely with the lithological boundaries. However, the slope relating to the Narrabeen Group sandstone is steeper than that of the Hawkesbury Sandstone, which is counter intuitive given the finer bedding and abundance of shale in the Narrabeen Group.

The digital elevation data contains insufficient detail to resolve with certainty any perturbation of the channel slope across the Kurrajong and Wheeny Gap faults. However, there is an indication of a jump in the profile in this area (**Fig. 6b**). Also, a small perturbation of the profile is associated with the passage of the stream through eastern margin of the Lapstone Monocline (**Fig. 6c**).

AN EVOLUTIONARY MODEL FOR THE LAPSTONE STRUCTURAL COMPLEX

We have constructed an evolutionary model for the Lapstone Structural Complex that attempts to reconcile the apparently contradictory evidence for the age of major deformation (**Fig 7**). The computer program *Trishear 4.5* (Allmendinger 1998; Zehnder and Allmendinger 2000; http://www.geo.cornell.edu/geology/faculty/RWA/FF_DL.html) was used to forward model a simple basin geometry subjected to faulting. Fault-related folds are modelled by the program using trishear kinematics for deformation at the tipline and fault-bend folding over trailing ramps. Growth strata are entered manually into the developing model. The effects of erosion have been schematically added to the finished model using Adobe Illustrator 11.

The observed thickening of strata across the LSC (Bryan 1966; Branagan and Pedram 1990; Pickett and Bishop 1992; Australian Oil and Gas Corporation Ltd. 1966) is reproduced by introducing an east-dipping syn-depositional normal fault into the model (**Fig. 7a**). Steep dips are developed in strata proximal to the fault tip but the near surface strata are only gently warped, consistent with the palaeomagnetic results of Schmidt *et al.* (1995) who contend that significant rotation of strata post-dates the mid Cretaceous. The large offset produced in the basement relating to the fault coincides with a marked deepening of the basin east of the LSC (SRK, 2006).

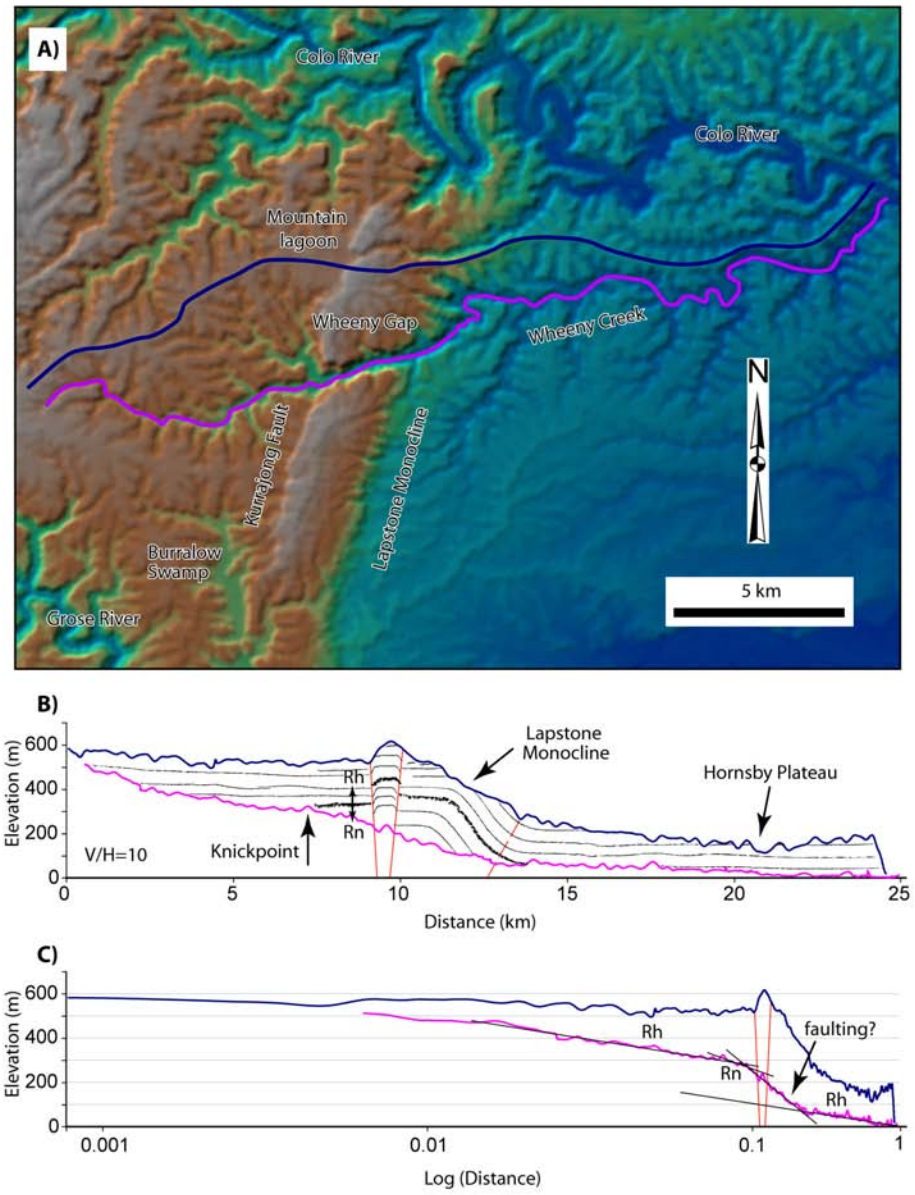

Figure 6: *(a) Hillshaded and colour draped DEM (LPI 25 m) of the northern LSC showing Wheeny Gap, the Lapstone Monocline, the prominent west facing scarp relating to the Kurrajong Fault, and Burralow Swamp. (b) topographic profiles constructed along the lines marked in part (a) with faulting and stratigraphy superposed as per Fig 3c. (b) topographic profiles in part (b) marked on semi-log axis to highlight streambed disequilibrium. Stream longitudinal profiles are shown in pink.*

The landscape is then subject to erosion, and develops a slight easterly slope as beds of Wianamatta Group shales with progressively greater dips are exhumed (**Fig. 7b**). We speculate that the scarp parallel (longitudinal) course of the Nepean River may have developed when a proto-river, flowing in an easterly direction down this developing slope, was captured by the developing rift shoulder relating to the opening of the Tasman Sea (ca. 95–100 Ma, Colwell *et al.* 1993).

Between 15 Ma and 20 Ma (e.g. Pulford 1997; Pickett 1984; van der Beek *et al.* 2001) extensive sub-horizontal sheets of basalt were extruded onto this gently dipping, low relief surface (**Fig. 7b**). The observation that these basalts overly both Wianamatta Group shales and Hawkesbury/Narrabeen sandstones (Bryan 1966) suggests that erosional lowering of the landsurface had stripped shale from many areas west of the syn-depositional warp by the time of basaltic volcanism, but not to the extent that significant relief was generated (cf Pickett and Bishop 1992). Subsequent erosion strips shale from the face and most of the crest of the syn-depositional warp (**Fig. 7c**). Rickaby's Creek Gravels are deposited on a sandstone substrate on the crest and face. The Nepean River is entrenched where it flows across exhumed sandstone (e.g. Nepean Gorge and Bents Basin).

A change in the crustal stress regime, perhaps between 10 and 5 Ma (e.g. Sandiford *et al.* 2004), initiates reactivation of a low-angle west-dipping basement fault causing uplift across the LSC and the propagation of faults into Sydney Basin strata. Refraction of one of these faults as it propagates into the basin results in the formation of a prominent east facing monocline (the Lapstone Monocline) and west facing scarps (the Kurrajong/Glenbrook fault system) (**Fig. 7d**). Benches of Rickaby's Creek Gravel are progressively stranded on the crest and face of the monocline as it grows. The entrenched meanders of the Nepean River deeply incise as the uplift proceeds. Major knickpoints retreat westward across the LSC forming deep gorges (e.g. the Grose River, Wheeny Creek). Almost all the shale is stripped from west of the LSC as these knickpoints migrate to the west. Relicts of shale are preserved beneath basalt caps.

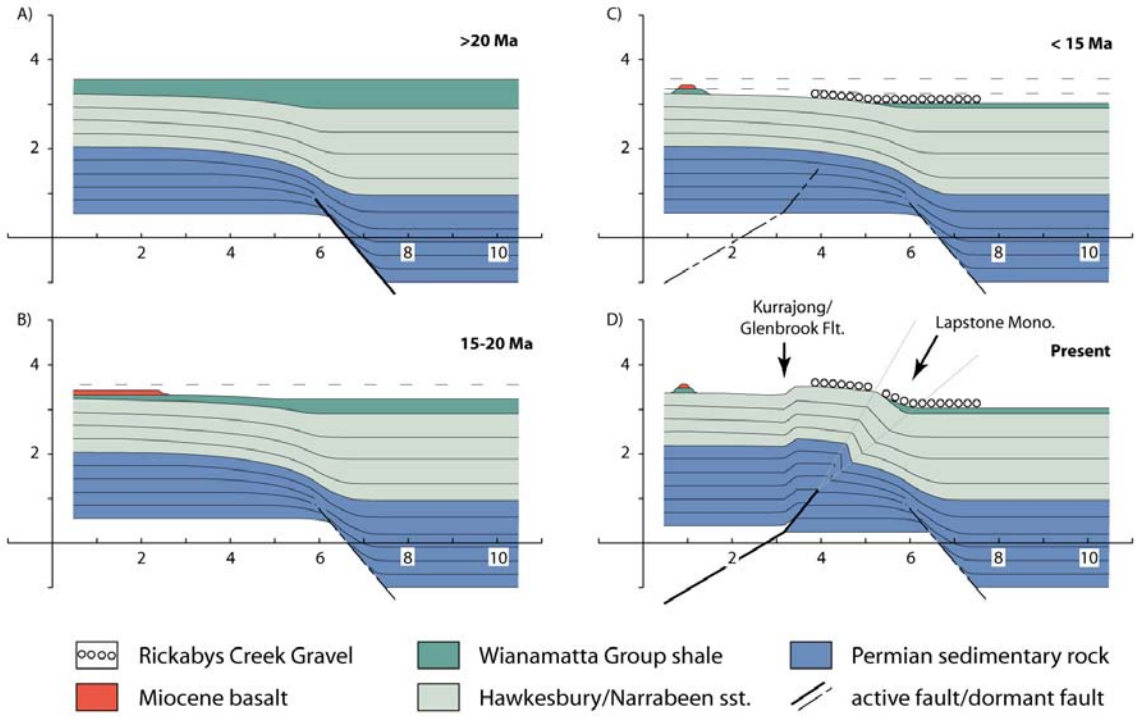

Figure 7: *Cartoons depicting our proposed model for the evolution of the Lapstone Structural Complex looking north at an E-W section through Penrith (see text for explanation). The thickness of lithological units is schematic. Axes units approximate kilometres. Note that by refracting a low-angle (30º) basement fault to 50º as it propagates into the basin the geometric features seen in Fig. 3c and 6b can be accurately reproduced (ie. sharp west-facing scarp 2 km west of the east facing monocline). The structural geometry in frame A may have formed as early as the Jurassic (Pickett and Bishop, 1992).*

DISCUSSION

Age of uplift across the LSC

In order to reconcile the stratigraphic position of the Rickaby's Creek Gravels and the apparent lack of incision of the landscape west of the LSC at *ca.* 15-20 Ma the above model proposes that significant uplift across the LSC postdates *ca.* 15 Ma. This is consistent with the ages of palaeomagnetic samples collected from the flexure of the Lapstone Monocline suggesting that rotation relating to flexure post-dates the mid Cretaceous (*ca.* 90 Ma, Schmidt *et al.* 1995) and pre-dates 8±5 Ma (Bishop *et al.* 1982 with age recalculated by Pillans 2003). Our model stands in contrast to the contemporary interpretation that monocline development and faulting is Mesozoic to mid Cenozoic in age (Pickett and Bishop 1992; Herbert 1989; Branagan and Pedram 1990), and downplays the role that opening of the Tasman Sea has had on landscape evolution in the Sydney Basin (cf. van der Beek *et al.* 2001).

The new model is attractive in that it places the main phase of deformation across the LSC at a time of significant re-organisation of the crustal stress field in southeast Australia. A major unconformity related to uplift, gentle folding and reverse faulting of Late Miocene strata in all southeastern Australian basins formed during the period 10-5 Ma (Dickinson *et al.* 2002; Sandiford 2003; Sandiford *et al.* 2004). Pliocene and Quaternary strata overlying this unconformity contain deformational structures (i.e. faults and folds) consistent with the current stress field. This time interval also corresponds to the initiation of the current phase of uplift in the Southern Alps of New Zealand (e.g. Sutherland 1996) and in Papua New Guinea (e.g. Hill and Raza 1999). The Lake George Fault in southern NSW might be considered as analogous in that almost 200 m of sediment has been deposited in the related fault angle basin, underlying an up to 200 m high scarp, in the last *ca.* 10 Ma (e.g. Singh *et al.* 1981; Abel 1985).

Evidence for recent and ongoing fault movement

The evidence suggesting that the Wheeny Gap Fault laterally displaces the northern cliff wall of Wheeny Gap indicates deformation postdating the passage of the initial uplift-induced knickpoint through Wheeny Gap (see van der Beek *et al.* 2001), which we would place at < *ca.* 15-20 Ma. Recent movement on these structures is further supported by the *ca.* 30 - 40 ka impedance of Burralow Creek, to form Burralow Swamp (**Fig. 6a**), and by the oversteepening of most easterly flowing stream profiles as they cross the LSC (Rawson 1990; Rawson and Clark, this volume). Ongoing movement is circumstantially supported by concentrations of earthquake epicentres, which cluster at depth to the west of the LSC (Gibson, this volume). In addition to this instrumental evidence, isoseismal maps constructed for the 1919 ML4.6 Kurrajong and the 1986 ML4.0 Upper Colo earthquakes (Collins and Dhu 2003) are consistent with significant rupture having occurred on structures of the LSC in recent times.

This hypothesis of a youthful Lapstone Structural Complex may be quantitatively verified with a program of targeted cosmogenic exposure dating along one (or several) of the streams demonstrating a disequilibrium longitudinal profile, such as Wheeny Creek. The age of sedimentary fill within fault angle basins such as Mountain Lagoon, Burralow Swamp, Glenbrook Lake and Blue Gum Swamp might also provide insight into the recent faulting history, with preliminary dating in Burralow Swamp indicating at least one significant phase of displacement in the late Pleistocene (Rawson 1990; Rawson and Clark, this volume).

Implications for seismic hazard

From a seismic hazard perspective, the main question is whether activity on the LSC has been regular and continuous over the last ca. 15-20 Ma, as assumed by Berryman *et al.* (1999) in their assessment, or episodic. The main evidence against a continuous evolution hypothesis are the ages of palaeomagnetic samples collected from the flexure of the Lapstone Monocline (northern LSC), which suggest that rotation relating to flexure occurred prior to 8±5 Ma (Bishop *et al.* 1982 with age recalculated by Pillans, 2003). Rapid relief-building in the late Miocene followed by little deformation from Pliocene to present is consistent with evidence of a pulse of deformation in southeast Australian offshore basins (cf. Dickinson *et al.* 2002; Sandiford 2003; Sandiford *et al.* 2004). However, the significant offset of the cliff wall in Wheeny Gap across the Wheeny Gap Fault (presumably relating to a significant number of individual earthquake events and several tens of metres displacement) and the abundant disequilibrium stream long profiles suggest continuing deformation.

The palaeomagnetic data of Bishop *et al.* (1982) is not necessarily inconsistent with significant continuing deformation on the LSC. Assuming the structural architecture proposed above, displacement might continue to accumulate without significant rotation once the fault controlling the flexure becomes emergent, or nearly so. At present there is no robust field evidence to support an emergent master fault at the foot of the Lapstone Monocline. However, the emergence of the Mount Riverview Fault over almost 10 km of strike length in the central part of the monocline (e.g. Branagan and Pedram 1990) suggests that the faulting beneath the monocline, if not emergent, is not deeply buried.

A second possible scenario relates to the folding mechanism extant during formation of the Lapstone Monocline. In the case that the monocline is amplifying largely as a result of eastward migration of the fold hinge (cf. Dahlstrom 1990; Saint-Bezar *et al.* 1999; Ahmadi *et al.* 2006), rather than by limb rotation around a fixed hinge axis, significant rotation of strata will be temporally restricted to the time when the hinge line migrated through the area of interest. Easterly fold hinge migration, and consequent easterly rotation, might plausibly be invoked to explain the formation of the anomalous Mellong Plateau immediately north of the study area (cf. Henry 1987).

Irrespective of whether or not a large portion of the relief relating to the Lapstone Monocline formed in the late Miocene, there is an emerging body of evidence to suggest that large earthquake occurrence on intraplate faults is highly temporally clustered (e.g. Crone *et al.* 1997, 2003; Clark 2007; Clark *et al.* in press). Consequently, dividing a total displacement by the total time over which that displacement accrued (cf. Berryman *et al.* 1999) is likely to provide a misleading estimate of the recurrence for large earthquakes on the LSC. Evidence of very shallow sedimentary fills (relative to the relief of the damming fault scarp) in fault angle basins juxtaposed against the Kurrajong Fault System (Rawson 1990; Rawson and Clark, this volume) is consistent with a model of temporally clustered rupture. Brief active periods of earthquake activity comprising a finite number of large events, such as those which formed Burralow Swamp in the Late Pleistocene (Rawson and Clark, this volume) are separated by much longer periods of seismic quiescence (cf. Clark 2007), such that fault dams are significantly eroded or completely removed between active periods.

CONCLUSIONS

A structural traverse conducted in the northern Lapstone Structural Complex through Wheeny Gap identified a previously undocumented west-dipping reverse fault exposed in the northern cliff face. The cliff face, related to retreat of a knickpoint up Wheeny Creek consequent of initial relief generation across the LSC, is displaced laterally by the fault, suggesting relatively youthful activity.

Evidence for recent and continuing activity on faults of the northern LSC is also provided by the impedance of Burralow Creek by the Burralow Fault, and by disequilibrium stream profiles where easterly flowing drainage crosses the LSC (Rawson 1990; Rawson and Clark, this volume). An evolutionary model for the LSC is proposed which reconciles this evidence for late Cenozoic uplift across the LSC and the observation that the Rickaby's Creek Gravels overlie shale on the Cumberland Plain and sandstone on the Lapstone Monocline. This model, while preliminary, suggests that the findings of a major seismic hazard assessment of the Sydney Basin which suggests magnitude M_W7.0 and greater earthquake events might be expected on the LSC on average every 15-30 ka should be treated with caution. This expectation of regular recurrence must be tempered by the possibility that a large part of the relief relating to the complex may have formed in the late Miocene (e.g. Sandiford *et al.* 2004), and evidence from other Australian intraplate faults suggesting that large earthquake occurrence is markedly temporally clustered (e.g. Crone *et al.* 1997, 2003; Clark 2007; Clark *et al.*, in press).

ACKNOWLEDGMENTS

Thanks to John Pickett for a very constructive critique of the model presented herein. He and Kerrie Tomkins are also thanked for animated discussions related to the evolution of the LSC. This manuscript benefited from constructive reviews by Dr. Andrew McPherson and Dr Clive Collins. This paper is published with the permission of the Chief Executive Officer, Geoscience Australia

REFERENCES

ABEL R.S. 1985. Geology of the Lake George Basin, N.S.W. *Bureau of Mineral Resources, Geology and Geophysics Record* **1985/4**, 57p.

AHMADI R., OUALI J., MERCIER E., MANSY J.-L., VAN-VLIET LANOE B., LAUNEAU P., RHEKHISS F. AND RAFINI S. 2006. The geomorphologic responses to hinge migration in the fault-related folds in the Southern Tunisian Atlas. *Journal of Structural Geology* **28**, 721-728.

ALLMENDINGER R. W. 1998. Inverse and forward numerical modelling of trishear fault-propagation folds. *Tectonics* **17**, 640-656.

AUSTRALIAN OIL AND GAS CORPORATION LTD, 1966. Putty-Oakdale Seismic Survey, Section A-B-C-D through Kurrajong Heights No. 1 Well, Map.

BERRYMAN K., *ET AL.* [INSTITUTE OF GEOLOGICAL AND NUCLEAR SCIENCES LIMITED], 1999. Seismic hazard analysis, Lucas Heights, site of the high flux Australian reactor. Australian Nuclear Science and Technology Organisation (ANSTO) report (http://www.ansto.gov.au/info/library/wnaugust2004.html), Call number: 621.039.583/16.

BISHOP P., HUNT P. AND SCHMIDT P.W. 1982. Limits to the age of the Lapstone Monocline, N.S.W. - a palaeomagnetic study. *Journal of the Geolical Society of Australia*, **29**, 319-326.

BISHOP P. 1986: Horizontal stability of the Australian continental drainage divide in South Central New South Wales during the Cainozoic. *Australian Journal of Earth Sciences* **33**, 295-307.

BRANAGAN D. F. AND PEDRAM H. 1990. The Lapstone Structural Complex, New South Wales. *Australian Journal of Earth Sciences* **37**, 23-36.

BRANAGAN D. F., 1969. The Lapstone Monocline and associated structures. Advances in the Study of the Sydney Basin, 4th Symposium. Department of Geology, University of Newcastle. pp. 61-62

BRYAN J. H. 1966. Geology of the Sydney 1:250 000 sheet. Geological Survey of New South Wales 1:250 000 Geological Series Explanatory Notes, 46 pp.

CARNE J. E. 1908. Geology and mineral resources of the western coalfield. *Memoir of the Geological Survey of New South Wales.* **6**.

CHESNUT W. S. 1982. Notes on the occurrence of lateritic gravels (?Rickaby's Creek Gravel) at the RAAF Base, Lapstone, NSW. Geological Survey of New South Wales Report GS 1980/473.

CLARK D. 2007. Temporal clustering of surface ruptures on stable continental region faults: a case study from the Cadell Fault scarp, south eastern Australia. Proceedings of the Australian Earthquake Engineering Society Conference, Wollongong, Australia, November 2007, pp17.

CLARK D. J., CUPPER M., SANDIFORD M. AND KIERNAN K., in press, Style and timing of late Quaternary faulting on the Lake Edgar Fault, southwest Tasmania, Australia: implications for hazard assessment in intracratonic areas. Geological Society of America Special Publication.

COLWELL J. B., COFFIN M. F. AND SPENCER R. A. 1993. Structure of the southern New South Wales continental margin, southeastern Australia. *BMR Journal of Australian Geology and Geophysics* **13**, 333–343.

CRONE A. J., DE MARTINI P. M., MACHETTE M. N., OKUMURA K., AND PRESCOTT J. R. 2003. Paleoseismicity of aseismic Quaternary faults in Australia: Implications for fault behaviour in stable continental regions. *Bulletin of the Seismological Society of America* **93**, 1913-1934.

CRONE A. J., MACHETTE M. N. AND BOWMAN J. R. 1997. Episodic nature of earthquake activity in stable continental regions revealed by palaeoseismicity studies of Australian and North American Quaternary faults. *Australian Journal of Earth Sciences* **44**, 203-214.

DAHLSTROM C. D. A. 1990. Geometric constraints derived from the law of conservation of volume and applied to evolutionary models for detachment folding. *AAPG Bulletin* **74**, 336-344.

DAVID T. W. E. 1896. Anniversary Address. *Journal of the Royal Society of New South Wales*. **30**, 33-69.

DAVID T. W. E. 1902. An important geological fault at Kurrajong Heights, N.S.W. *Journal of the Proceedings of the Royal Society of N.S.W*. **36**, 359-370.

DICKINSON J. A., WALLACE M. W., HOLDGATE G. R., GALLAGHER S. J. and THOMAS L. 2002. Origin and timing of the Miocene-Pliocene unconformity in southeast Australia. *Journal of Sedimentary Research* **72**, 288-303.

HACK J. T. 1973. Stream-profile analysis and stream-gradient index. *Journal of Research of the United States Geological Survey* **1**, 421-429.

HENRY H. M. 1987. Mellong Plateau, central eastern New South Wales: an anomalous landform. *Journal of the Proceedings of the Royal Society of N.S.W*. **120**, 117-134.

HERBERT C. 1989. The Lapstone Monocline - Nepean Fault; a high angle reverse fault system. In: R.L. Boyd and K. Allen (eds). Proceedings of the Twenty Third Newcastle Symposium: Advances in the study of the Sydney Basin, Newcastle, NSW, 217-224.

HILL K. C. AND RAZA A. 1999. Arc-continent collision in Papua New Guinea: constraints from fission track thermochronology. *Tectonics* **18**, 950-966.

MAUGER A. J., CREASEY J. W. AND HUNTINGDON J. F. 1984. Extracts and notes on the Penrith 1 : 100 000 sheet. *CSIRO Division of Mineral Physics - Report for National Energy Research Development and demonstration Program*. Report **81/1357.**

COLLINS C.D.N. AND DHU, T, 2003. Atlas of isoseismal maps of Australian earthquakes 1841 - 2003. Geoscience Australia Dataset, ANZCW0703006681.

PICKETT J. W. AND BISHOP P. 1992. Aspects of landscape evolution in the Laptsone Monocline area, New South Wales. *Australian Journal of Earth Sciences* **39**, 21-28.

PICKETT J. W. 1984. Pre-basalt topography on Mount Tomah, New South Wales. *New South Wales Geological Survey Quarterly Notes* **57**, 22–27.

PILLANS, B. 2003. Dating ferruginous regolith to determine seismic hazard at Lucas Heights, Sydney. In: Ian C. Roach, (Editor) Advances in Regolith: Proceedings of the CRC LEME Regional Regolith Symposia, 2003 CRC LEME, 324-327.

PULFORD A. 1997. Cenozoic landscape evolution of the east Australian highlands: constraints from Miocene basalts, Blue Mountains, N. S. W. Honours Thesis, Australian National University, Canberra (unpubl.).

RAWSON, G. A. 1990. Drainage modification associated with the Lapstone Structural Complex, New South Wales – Geomorphological evidence for neotectonism. Unpublished Masters thesis, University of Sydney, 179pp.

SAINT-BEZAR B., FRIZON DE LAMOTTE D., MOREL J. L. and MERCIER E. 1999. Kinematics of large scale tip line folds from the High Atlas thrust belt (Morocco). Reply. *Journal of Structural Geology* **21**, 691–693.

SANDIFORD M., 2003. Neotectonics of southeastern Australia: linking the Quaternary faulting record with seismicity and in situ stress: In: eds Hillis R.R. and Muller D, Evolution and dynamics of the Australian Plate. *Geological Society of Australia Special Publication* **22**, 101-113.

SANDIFORD M., WALLACE N. AND COBLENTZ D., 2004. Origin of the in situ stress field in southeastern Australia. *Basin Research* **16**, 325-338.

SCHMIDT P. W., LACKIE M. A. and ANDERSON J. C. 1995. Palaeomagnetic evidence fro the age of the Lapstone Monocline, NSW. *Australian Coal Geology* **10**, 14-18.

SINCLAIR KNIGHT MERTZ CONSULTING, 2005. Sydney Basin Regional Structural Framework and Structural Risk Analysis. SRK Project Code: SBA002.

SINGH G, OPDYKE N D AND BOWLER J M 1981. Late Cainozoic stratigraphy, magnetic chronology and vegetational history from Lake George, N.S.W. *Journal of the Geological Society of Australia* **28**, 435-452.

SUTHERLAND R. 1996. Transpressional development of the Australia-Pacific plate boundary through southern South Island New Zealand: constraints from Miocene-Pliocene sediments, Waiho-1 borehole, South Westland. *New Zealand Journal of Geology and Geophysics* **39**, 251-264.

VAN DER BEEK P., PULFORD A. AND BRAUN J. 2001. Cenozoic Landscape Development in the Blue Mountains (SE Australia): Lithological and tectonic Controls on Rifted Margin Morphology. *The Journal of Geology* **109**, 35-56.

WELLMAN P. and MCDOUGALL I. 1974. Potassium-Argon ages on the Cainozoic volcanic rocks of New South Wales. *Journal of the Geological Society of Australia* **21**, 247–272.

WELLMAN P. 1979. On the Cainozoic uplift of the southeastern Australian highland. *Journal of the Geological Society of Australia* **26**, 1-9.

ZEHNDER A. T. and ALLMENDINGER R. W. 2000. Velocity Field for the trishear model. *Journal of Structural Geology* **22**, 1009-1014.

Seismicity of the Sydney Basin Region

Gary Gibson, Seismology Research Centre, ES&S.

SEISMIC MONITORING IN THE SYDNEY REGION

Introduction

Our knowledge of past earthquakes in any region depends on the recorded history of the inhabitants, and on the recordings made by seismic monitoring instruments, especially those installed within the region. We have no information of any of the earthquakes that occurred in the Sydney region during the period of aboriginal habitation prior to European colonisation. The earliest known Australian earthquake was felt in Sydney on 22 June 1788, a few months after the colony was established. Until seismograph coverage was established, the location of larger earthquakes could be approximated by determining the location of maximum ground motion intensity, the earthquake depth estimated by the relative area that experienced high intensity relative to low intensity, and the magnitude estimated from the area or radius of perceptibility (McCue, 1980).

Purposes of Seismic Monitoring

Most seismic monitoring is done in order to investigate earthquake hazard. The dominant earthquake hazard is ground vibration, and it is this motion that is usually monitored. Other hazards include surface rupture, liquefaction, landslides and tsunami. Earthquake ground motion monitoring is used to determine information about the earthquake source (location, magnitude, mechanism, etc), seismic wave travel path (reflections, refractions, attenuation with distance), and the effects of the surface geology and topography at the recording site (amplification by resonance, attenuation of high frequency motion).

1. The Earthquake Source

The seismicity of an area includes the location of earthquakes within the area, their magnitude, and their recurrence rates. This includes delineation of active faults, if possible. Earthquake locations and origin times can be determined from measurements of the precise times that seismic waves from the earthquakes arrive at seismographs. A network of at least three seismographs, but preferably five or more, is required to locate the earthquakes that occur within the network. Earthquakes outside the network cannot be located as accurately.

Earthquake depths can only be determined accurately if there is a seismograph near to the epicentre, within a horizontal distance not exceeding about twice the earthquake depth. In the Sydney area earthquakes occur at depths from about 2 to 20 km.

2. The Seismic Wave Travel Path

The attenuation of seismic wave amplitudes with distance from an earthquake depends on the properties of the rocks within the earth's crust in the area, particularly by its temperature. Attenuation in cold, hard, old rock depends primarily on geometric spreading, while the reduction of amplitude with distance is higher in hot, soft, young rock. Absorption of energy within rocks is frequency dependent, and attenuation of high frequency motion is much more rapid than for low frequency motion.

3. The Site Effects

The effects of surface sediments and topography can significantly modify ground motion. Soft surface sediments give amplification of ground motion at their natural frequency by resonance, while reducing amplitudes at high frequencies by absorption. Site effects depend on near-surface unconsolidated sediments and on topography, and they can vary rapidly from place to place at scales

of tens to hundreds of metres. Areas with soft surface sediments and steep topography have a much higher earthquake hazard than experienced on a horizontal surface with hard rock outcropping.

Attenuation for earthquake waves travelling in the Palaeozoic bedrock beneath the Mesozoic sediments of the Sydney Basin is typical of attenuation in eastern Australia. However, the Sydney Basin sediments show higher than average attenuation, and this makes determination of local attenuation functions quite difficult, especially with limited data.

Seismographs in the Sydney Region

The first seismograph to be installed in New South Wales was a Milne instrument installed at the Sydney Observatory from 1906 to 1948. The Riverview Observatory installed its first seismograph in 1909, and seismic monitoring instruments are still being operated at this site. Most of the early seismographs were long-period instruments designed to record distant earthquakes, but with limited capacity for recording high frequency motion from local earthquakes.

One of the first seismograph networks in the world designed specifically to record local earthquakes was installed at five sites for the Metropolitan Water, Sewerage and Drainage Board of Sydney from 1958. The network was operated by the Australian National University in Canberra. In 1970 the network was reduced to four sites, and in 1983 radio telemetry was added to give central recording, although with limited dynamic range through use of a pen recorder, and very limited seismic frequency bandwidth.

Following the Newcastle earthquake in December 1989, Sydney Water upgraded the network. It adopted an integrated monitoring network design, incorporating both sensitive seismometers and strong motion accelerometers, fully based on digital data acquisition, with advantages as follows:

- common instrumentation, reducing operation and maintenance costs.
- strong motion reference sites, and even sites on structures, could act as normal seismograph sites that would not exceed full scale for large nearby events.
- combining strong motion bedrock sites with seismographs will eventually allow determination of a single consistent attenuation function for all levels of motion, and will significantly expedite collection of data for spectral attenuation functions. Attenuation functions inherently must use measurements from a wide range of earthquake magnitudes and distances.
- strong motion sites will be maintained regularly with seismograph maintenance, so instruments are much more likely to be working correctly for a large nearby earthquake.

In addition, high dynamic range instruments were used so that seismographs could measure larger earthquakes without going full scale, and strong motion accelerographs could trigger on smaller events. Six-channel instruments would give an overlap in the levels of motion recorded, increasing reliability and allowing system calibration checks.

The expanded network originally had instruments at 25 sites when fully installed by late 1993, operated by the Seismology Research Centre in Melbourne, and later reduced to 23 sites during 1998. About half of these are six-channel instruments with a triaxial seismometer and a triaxial accelerometer. There have been no moderate or large earthquakes in the Sydney area since the network was installed. Since 1992, one moderate magnitude distant earthquake has been recorded (at Ellalong).

Accelerographs in the Sydney Region

An SMA1 accelerograph was mounted in the nuclear reactor basement at Lucas Heights in about 1984. This was replaced by two digital accelerographs during 1989, one on the reactor structure and the other on bedrock nearby. They are intended to study the dynamic properties of the reactor structure and are in a noisy environment, so rarely trigger on small local earthquakes.

The combined seismograph and accelerograph network installed by Sydney Water in 1992, described above, has significantly improved strong motion monitoring in the Sydney area. In

addition, two strong motion accelerographs were installed in each of Sydney, Newcastle and Wollongong, as part of the Joint Urban Monitoring Project (JUMP), these instruments being operated by Geoscience Australia.

EARTHQUAKES IN THE SYDNEY REGION

Several catalogues of earthquakes in the Sydney area have been produced. The Australian National University produced printed monthly Bulletins from before 1967 to mid1993. The Bureau of Mineral Resources located and published locations on microfiche for many years, and after being renamed as the Australian Geological Survey Organisation published printed monthly bulletins from 1995 to mid-2000. This was replaced by an online access system for recent earthquakes.

After AGSO was renamed Geoscience Australia, the preferred solutions of the entire earthquake catalogue was placed online. This includes earthquake locations from other authorities when the Geoscience Australia seismologists consider those to be the preferred location.

The Seismology Research Centre in Melbourne has been operating seismographs for Sydney Water and other authorities in New South Wales since 1988, and produces three-monthly earthquake lists that include events in the Sydney region.

Local observatories often update their analyses for periods of months to a year after any event, as more data is gathered from remote instruments, and data are shared between observatories.

Internationally, preliminary epicentre determinations (PED) are published by the National Earthquake Information Centre (NEIC) of the US Geological Survey (USGS) with a delay of a few weeks after each event. The International Seismological Centre (ISC) then computes revised locations of all known events, using all available data, with a delay of about two years, publishing results on CD and online.

Since 2000, the author has been maintaining a consolidated earthquake catalogue of all Australian earthquake locations, including intermediate locations as data are accumulated, and locations from all authorities, both local and international. The preferred solution for each event is re-considered whenever new locations are added. Figures 1-5 have been produced using this catalogue.

The most significant known events in the Sydney area were:

1788 June 22, Sydney: The first recorded earthquake in Australia occurred on a Sunday afternoon, 1788 June 22, five months after the First Fleet landed. It was felt and heard by most people, apparently from the southwest, with a sound like a distant cannon, and visibly shaking trees. Hunter (1991) gives a number of references.

1872 October 18, Jenolan Caves, ML 5.5: An earthquake on Friday, 1872 October 18 at 0650 pm was felt from Jervis Bay in the south to Stroud in the north, and to Orange in the west. At Bathurst chairs were knocked over, candles shaken from tables and dishes smashed. The widespread distribution of low and moderate intensities suggests that the epicentre must have been in an unpopulated area, perhaps about the Jenolan Caves or north of Lithgow, or was deep beneath the surface.

1919 August 15, Kurrajong, ML 4.6: An earthquake occurred near Kurrajong on Friday 1919 August 15 at 0821 pm Sydney Standard Time. It was distinctly felt throughout Sydney and suburbs, though not noticed by all persons. It was described in detail by Cotton, 1921, and Drake, 1973, gave

a magnitude estimate of about ML 4.6. It was felt with Modified Mercalli intensity 5 at Kurrajong, on the Nepean River about 50 km north-west of Sydney. Highest intensities were reported from north and west of Kurrajong. The intensity in Sydney was about MM 3. It was felt by a few people at rest indoors in Newcastle. It was crudely located using intensity data near the north end of the Lapstone Fault, and may have been on either that fault or a related fault.

1961 May 21, Robertson, ML 5.5: An earthquake of magnitude ML 5.5 occurred near Robertson on 1961 May 22 at 0740 am AEST. This is about 60 kilometres south-west of Sydney. It has also been called the Bowral earthquake. The maximum intensities in the Robertson-Bowral area were about MM 7. The earthquake caused significant damage to buildings in the Moss Vale, Robertson and Bowral area, blocked the Macquarie Pass road with rockfalls, and caused some power failures. The intensity in Sydney was about MM 3. The epicentre was within a few kilometres of the present location of Wingecarribee Dam which was completed in 1974.

1973 March 9, Burragorang, ML 5.5: An earthquake of magnitude ML 5.5 occurred near the southern end of Lake Burragorang, about 30 km west of Picton on 1973 March 10 at 0509 am, AEST. This is about 70 kilometres WSW of Sydney. It has also been called the Picton earthquake. It caused about $A500,000 (1973 values) damage. It has been suggested that the earthquake could have been reservoir induced, but it is difficult to prove this (Drake, 1974). If this was the case, it is an example of delayed reservoir induced seismicity. The earthquake was probably at a depth exceeding 12 km, and occurred about 12 years after reservoir filling commenced.

1981 November 15, Appin, ML 4.6: An earthquake of magnitude ML 4.6 occurred near Appin on 1981 November 16 at 0358 am, AEST. This is about 50 kilometres south-west of Sydney. Intensities of MM 4 were felt over a broad area south-west of Sydney, but with only isolated values of MM 5 in the epicentral area. No damage was reported.

1985 February 13, Lithgow, ML 4.3: An earthquake of magnitude ML 4.3 occurred near Lithgow on 1985 February 13 at 0701 pm AEDT (daylight saving time). This is about 100 kilometres west of Sydney. Intensities of up to MM 7 were reported in the epicentral area, with minor damage to plaster, brickwork, tiles and chimneys, including several partly demolished chimneys. Objects fell off shelves in many parts of Lithgow. Total damage was estimated at A$65,000 (1985). The intensity in Sydney was very low, with only a few people reporting MM 2 to 3. The earthquake was felt much further to the west than to the east, suggesting that it may have been on a west-dipping fault.

1989 December 28, Newcastle, ML 5.6: The earthquake on Thursday 1989 December 28 at 1027 am AEDT was the first Australian earthquake confirmed to have caused fatalities. Thirteen people were killed by the earthquake, and there were hundreds of injuries. Extensive minor and moderate damage gave a total cost that exceeded A$1,500 million. This earthquake was centred off the north-east of the map in figure 1, and was felt over a radius of about 300 kilometres.

1999 March 17, Appin, ML 4.4: An earthquake of magnitude 4.4 occurred near Appin on Wednesday 1999 March 17 at 12:58 pm AEDT. The maximum reported intensity was of MM 5, although there were some reports of minor damage in the epicentral area. It caused some power failures, and was felt throughout the Sydney area.

Pre- and Post-1992 Seismicity

The quality of seismograph coverage of any area changes with time, and the general trend is for improvement with time. In the Sydney area, all events before 1960 were very poorly located using intensity data alone.

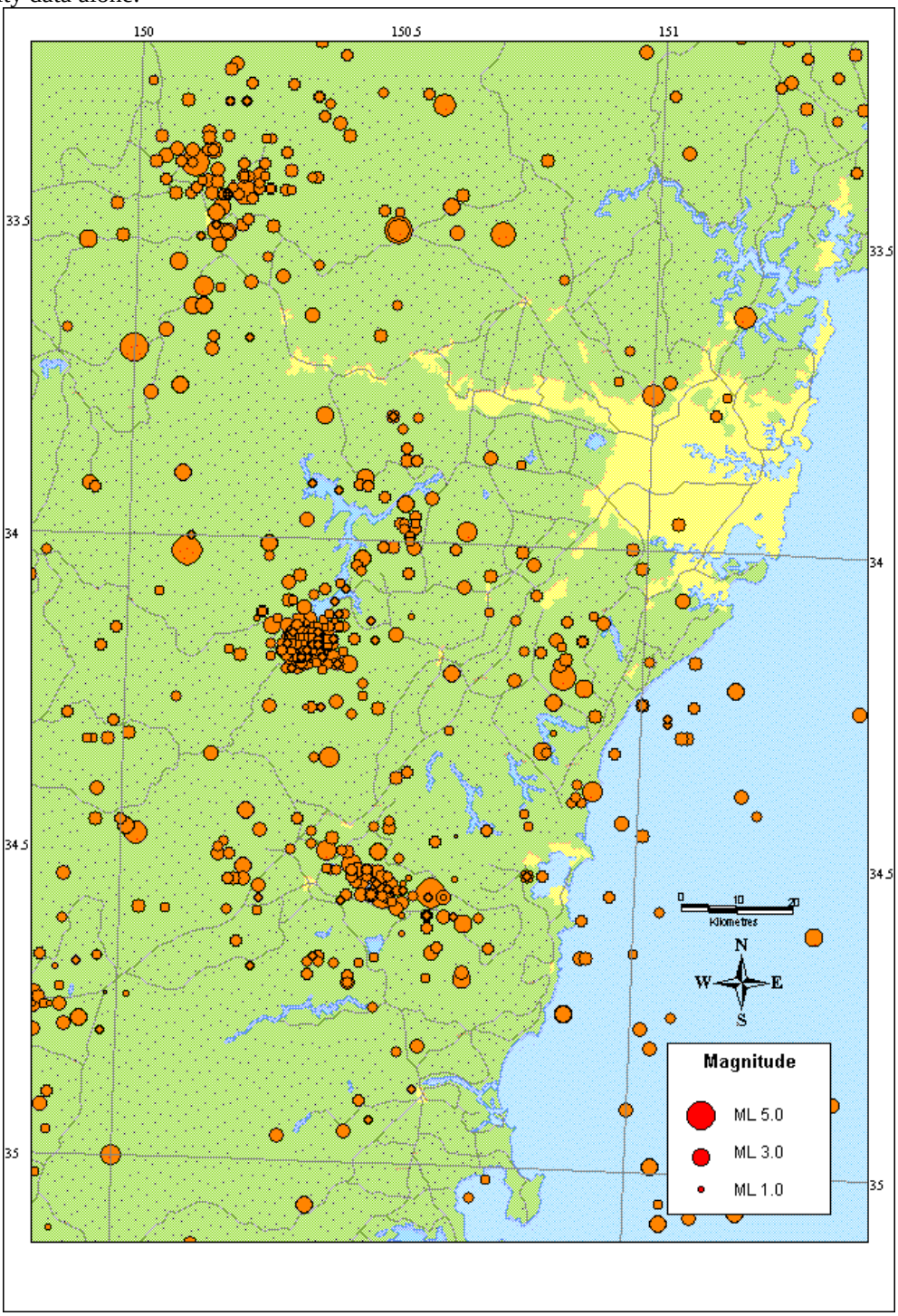

***Figure 1**: Sydney region earthquakes to 1992.*

From 1960 to 1991, there were only three to five seismographs in the area. Only smaller earthquakes within about 10 to 20 kilometres of these could be located with a well-defined depth estimate. The

instrumentation used had limited dynamic range so would go full-scale for even moderate magnitude earthquakes, so shear wave arrivals could not be read, and these events could not be located precisely. The instrumentation had very limited seismic wave frequency bandwidth, limiting timing precision and making earthquake magnitude estimates very difficult.

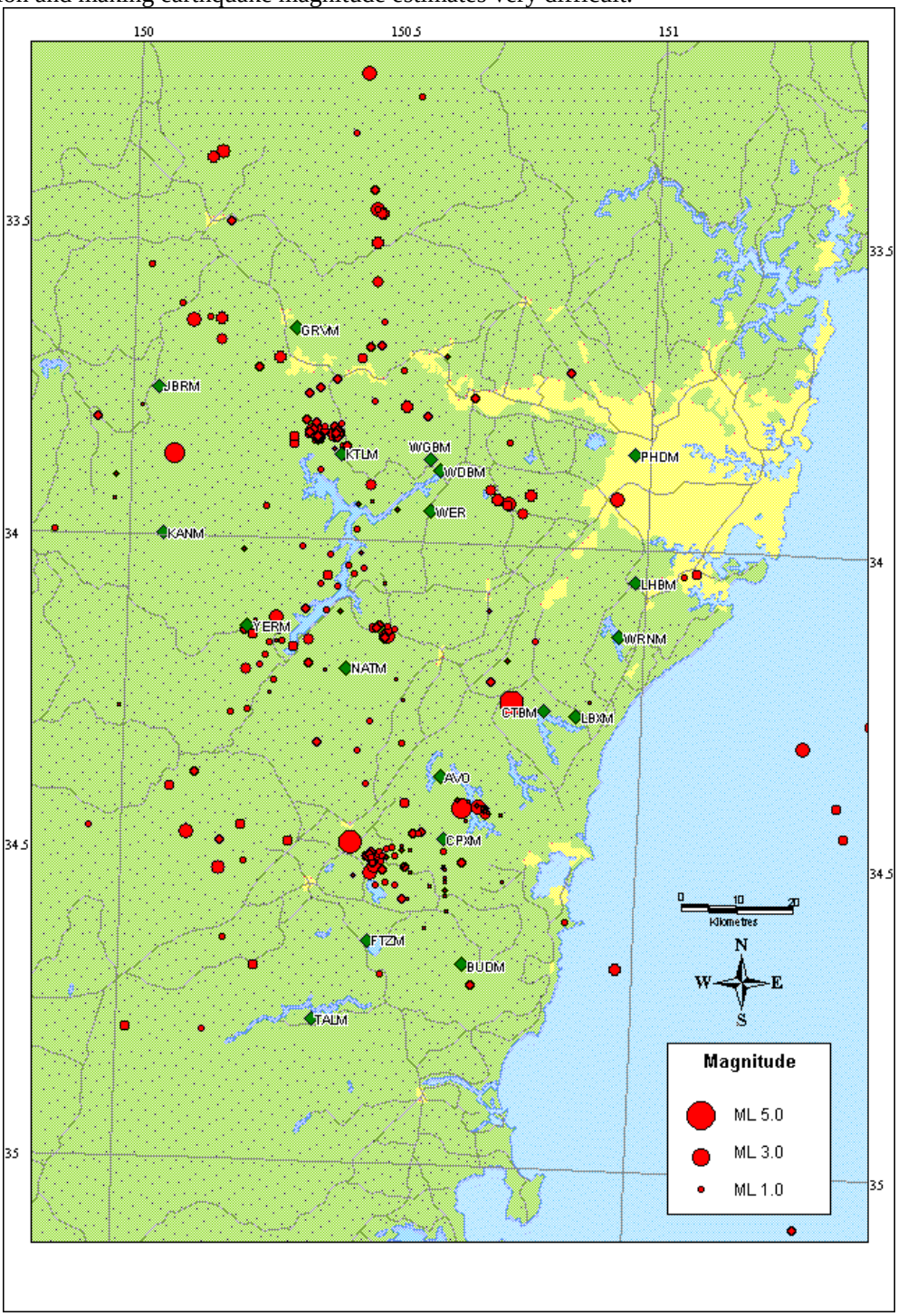

Figure 2: *Sydney region earthquakes, 1993 to 2005.*

Since 1992, most events larger than magnitude ML 1.5 can be located to a precision of a few kilometres or better, including depth. The distinctive seismic character of shallow events (earthquakes, blasts and coal mine collapses) within the Mesozoic sediments of the Sydney Basin

are very characteristic, making discrimination of earthquakes and blasts much easier. It is still possible that some shallow earthquakes have been mis-identified as a blast or coal mining collapse.

Sydney Region Earthquake Depths

Before 1992, earthquake depths were very difficult to determine with accuracy. For example, the Burragorang earthquakes of 1971 were located at all depths from near-surface to over 30 km, and appear in the cross-section as a vertical band. In reality the depths were probably only spread over a range of a few kilometres, probably at a depth of about 12 to 15 km. Some poorly constrained earthquakes before 1992 were assigned depths at the surface, while others were located at depths of 30 km or more. Earthquakes outside a network often locate too deep.

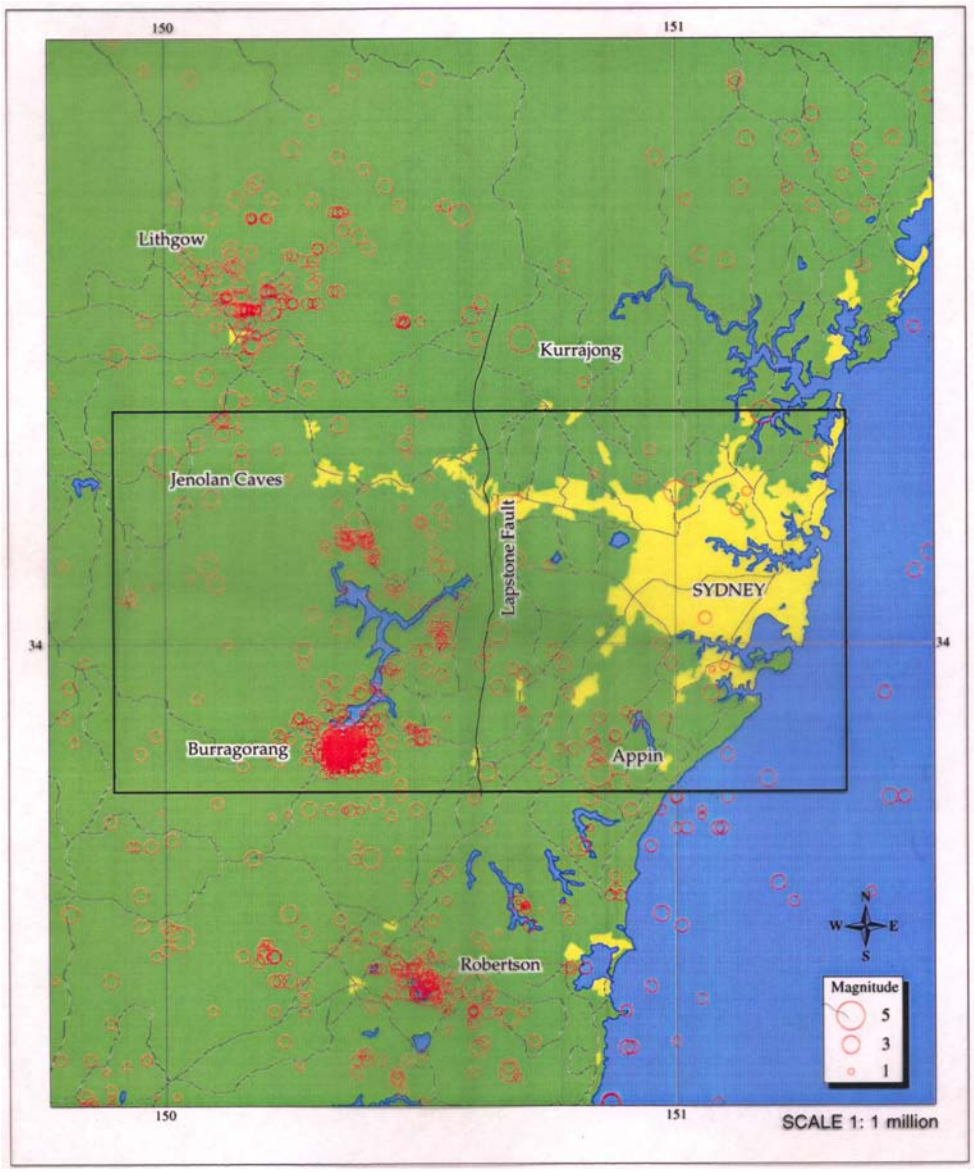

Figure 3: *Sydney region earthquakes with study area for sections delineated.*

Since 1992, there has been a significant improvement in earthquake location accuracy, especially for depths. Almost all of the events that were positively identified as earthquakes are near or west of the surface outcrop of the Lapstone Fault indicating that this fault system is active. The Lapstone Fault is the largest identified contributor to seismic hazard in the Sydney Region. Most of the earthquakes

in the Sydney area since 1992 were under the Blue Mountains. Most events have been located to a precision of a few kilometres or better, including depth. Although many near surface blasts and mine collapses have been recorded in coal mining areas, very few earthquakes appear in the top few kilometres. It is possibly that the Mesozoic sediments of the Sydney Basin are too weak to sustain very high stress. The deepest earthquakes that have been precisely determined are about 17 km deep.

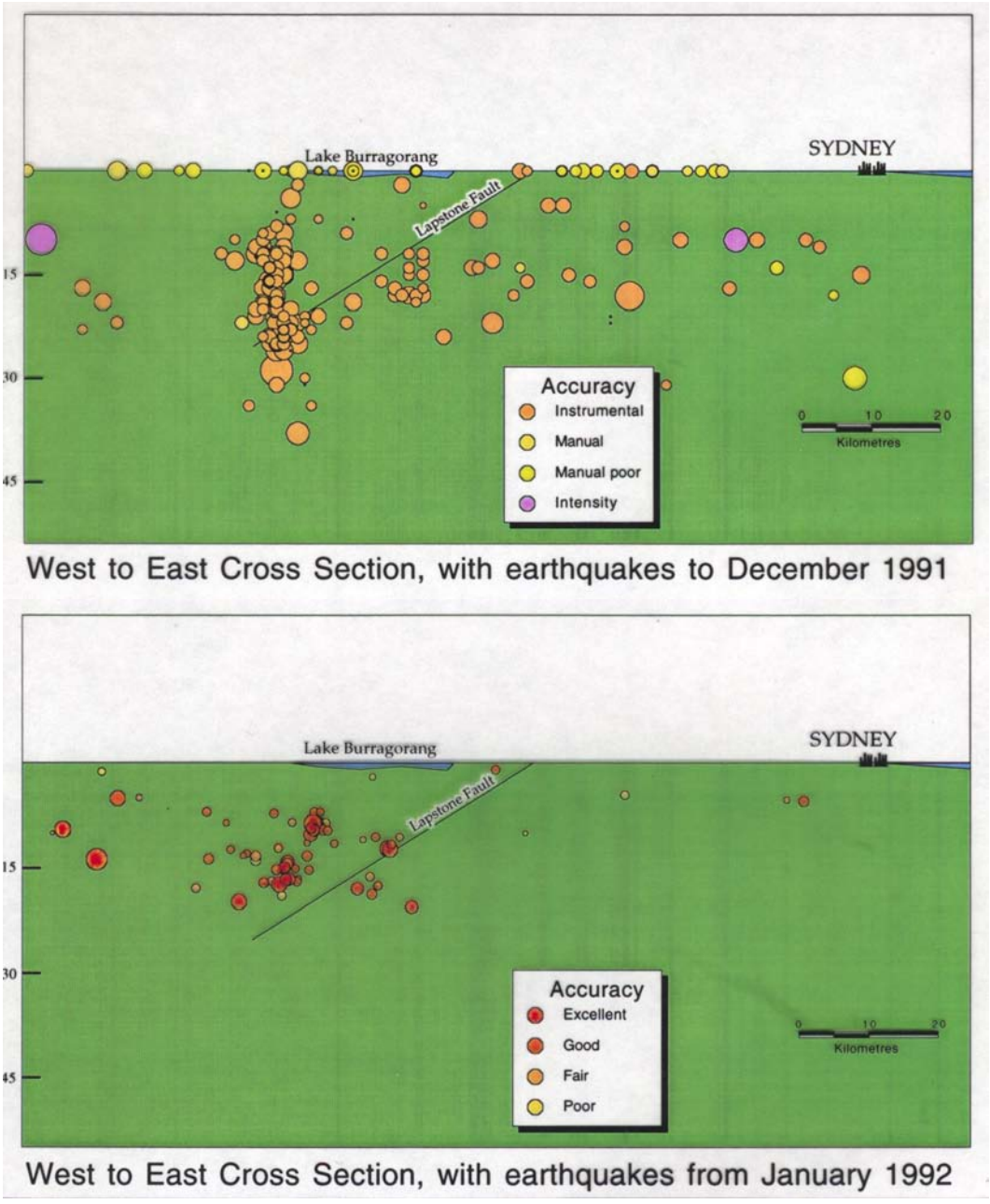

Figure 4: *Vertical sections with earthquakes before 1992 (top) and 1992 to 1998 (bottom)*

Although the overall rate of earthquake activity for the region is not altered significantly by the new data, a possible re-distribution is both reasonable in terms of geology and topography, and indicates that the Blue Mountains region has a higher level of earthquake hazard than the Sydney region. Although the level of activity under the Blue Mountains is above average by Australian standards, it is still far less than in the active earthquake areas of the world. The recording period is very short

when compared to the return period of large earthquakes, and earthquakes always cluster in space and time. There are still uncertainties regarding the activity to the south of the area, including the source of the Appin and Robertson earthquakes.

EARTHQUAKE HAZARD IN THE SYDNEY AREA

The most common measure of earthquake hazard at a location is a ground motion recurrence plot, either giving motion as a function of return period, or giving response spectra for one or more return periods. This is done using the Cornell method, where earthquake sources are defined and quantified, then attenuation functions are used to integrate probabilities of ground motion for all possible earthquakes in longitude, latitude, depth and magnitude.

The earthquake catalogue of known events is a key input, but when the duration of the catalogue is very much shorter than the average return period for medium to large earthquakes this gives a very limited sample of possible earthquakes. In stable continental regions like Australia the catalogue may have good coverage for 50 years and limited coverage for 100 or 200 years, while the average return periods for particular moderate to large earthquakes may be from thousands up to hundreds of thousands of years.

A seismotectonic model is used to include all possible earthquake sources. This usually consists of area or volume source zones within which it is assumed that earthquakes can occur at any point with the same probability. It is possible to include variations in probability within the source, and variation of the earthquake magnitude recurrence with depth can be included. As well as seismicity input, the seismotectonic model normally incorporates geological and geophysical data in the definition of the zones. Seismotectonic models with only area or volume source zones give a low-resolution average ground motion that only varies on a scale comparable to the size of the zones.

Since all shallow moderate to large magnitude earthquakes occur on pre-existing faults with rupture dimensions of kilometres or larger, it is possible to include active faults in the seismotectonic model, each with a specified location and earthquake magnitude recurrence rate. When an active fault is incorporated in the model, it is normal to reduce the earthquake activity rate in the local area or volume source zone by a compensating amount. As more and more active faults are delineated and quantified, the seismotectonic model gains in resolution, giving variations in estimated hazard depending on the proximity of faults.

Brown and Gibson (2000, 2004) have developed a series of seismotectonic models, designated AUS1 to AUS6, to compute ground motion recurrence as a measure of earthquake hazard. These are subject to continuous updating as more data comes available. Because earthquakes in Australia occur at a relatively limited rate, most of the model developments are currently the result of geological and geophysical inputs.

Figure 5 shows the earthquakes in the Sydney area to the end of 2001 and the source zones for model AUS5. In defining the source zones, the Sydney Basin was taken as a geological entity that is a significant feature on the scale of the upper crust, where earthquakes occur in this region.

The earthquake catalogue shows considerable variation in activity over the Sydney Basin, so it was divided into three zones. The high level of activity under the Blue Mountains in the south-west formed the West Sydney Basin zone. The Lapstone Fault, assumed to be a west dipping reverse fault, is along the eastern edge of the West Sydney Basin zone, and a high proportion of the West Sydney Basin activity may be on the Lapstone Fault.

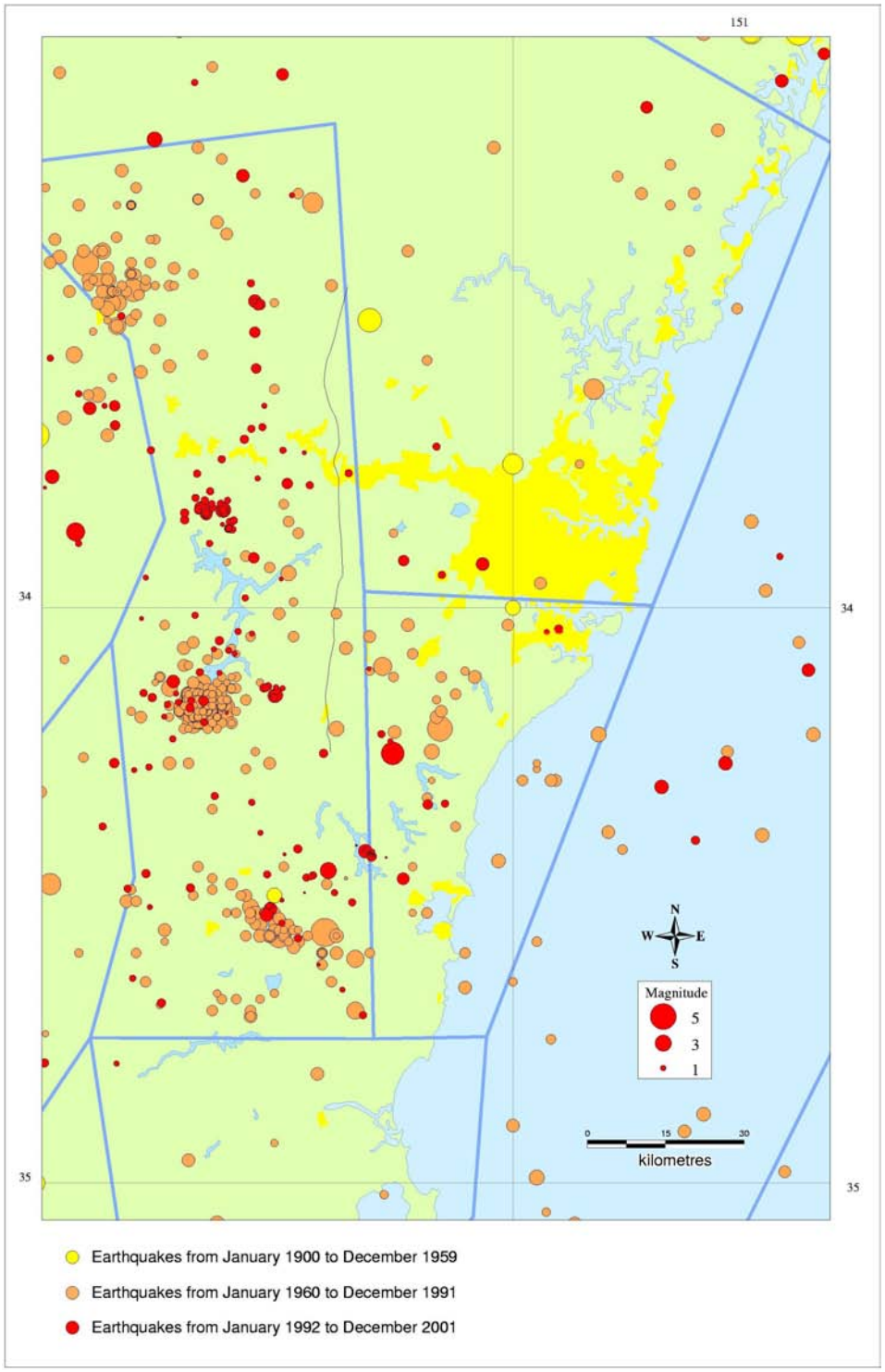

Figure 5: *Earthquakes in the Sydney area to 2001.*

The South Sydney Basin was defined by the moderate level of activity within the Sydney Basin south of Botany Bay in the Illawarra region. Although the Illawarra Scarp along the coast is largely an erosional feature, the earthquake activity in the Appin, Bowral and Robinson regions could easily be associated with a west dipping reverse fault that could be designated the Illawarra Fault, if it exists.

The North Sydney Basin was defined as the remainder of the Sydney Basin zone, characterised by a very low level of earthquake activity. Compared with other Australian cities, Sydney experiences very few local earthquakes that are less than magnitude 3 but which are felt over a limited area. The North Sydney zone might be considered as a downthrown region between reverse faults that are dipping away from the zone – the Lapstone to the west and the Hunter-Mooki Fault system to the northeast.

Note that the activity on a reverse fault is under the upthrown block, offset at distances up to 25 kilometres from the surface outcrop.

CONCLUSIONS

The higher density seismograph network operating over the past decade has significantly improved the resolution of earthquake locations in the Sydney region. The majority of earthquakes in the Sydney area are to the west, under the Blue Mountains, and probably on the active Lapstone Fault or related faults. The depth range of earthquakes under the Sydney Basin is limited, with few very shallow events in the Mesozoic sediments near the surface, and a maximum depth of about 20 km in basement rock.

It seems that attenuation for earthquake waves in the Sydney area is complicated by higher attenuation in the Mesozoic sediments of the Sydney Basin than in basement rocks. Earthquakes or blasts near the surface, including the only moderate magnitude earthquake in the area since the new network was installed (Ellalong near Cessnock, in 1994, magnitude ML 5.1), have near surface attenuation effects at both source and seismograph, so are difficult to analyse with present data. Some additional well-located events larger than about magnitude 3.0, particularly deeper events, will be required before local attenuation can be determined.

ACKNOWLEDGEMENTS

The author wishes to thank the many people involved in Australian seismograph monitoring who have contributed data over many years, especially staff from the Riverview Observatory, Australian National University, Seismology Research Centre, Sydney Water and Geoscience Australia. Lawrence Drake, David Denham and Kevin McCue have made significant contributions in analysis of the data.

REFERENCES

Brown, Amy & Gary Gibson, 2000: *Reassessment of earthquake hazard in Australia,* Proc 12th World Conf on Earthquake Engineering, Auckland, paper 751, 8 pages.

Brown, Amy & Gary Gibson, 2004: *A multi-tiered earthquake hazard model for Australia*, Tectonophysics, 390, 25-43.

Burke-Gaffney, T.N., 1951: *Seismicity of Australia,* Proc. Royal Soc. of NSW, Vol 85, 47-52.

Clarke, W.B., 1869: *On the Causes and Phenomena of Earthquakes, Especially in relation to Shocks Felt in New South Wales and in other Provinces of Australasia*, Trans. Royal Soc. N.S.W., 2, 51-86

Denham, D. (ed), 1973: *Seismicity and Earthquake Risk in Eastern Australia*, Bureau of Mineral Resources Bulletin 164, Aust. Govt. Publishing Service, Canberra

Denham, D., 1980: *The 1961 Robertson earthquake - More Evidence for Compressive Stress in Southeast Australia*, BMR Journal Vol 5, No 2, 153-156.

Denham, David, Günter Bock & Ron S. Smith, 1982: *The Appin (New South Wales) Earthquake of 15 November 1981*, BMR Journal Vol 7, No 3, 219-223.

Doyle, H. & R. Underwood, 1965: *Seismological stations in Australia*, Aust. Journal of Science, Vol 28, No 2, 40-43

Drake, Lawrence, 1974: *The seismicity of New South Wales*, Proc. Royal Soc. NSW, Vol 107, 35-40

Everingham, I.B., A.J. McEwin & D. Denham, 1982: *Atlas of isoseismal maps of Australian earthquakes*; Bureau of Mineral Resources Bulletin 214, Aust. Govt. Publishing Service, Canberra

Herbert, C., 1989: *The Lapstone Monocline - Nepean Fault - A High Angle Reverse Fault System*, Proc of the 23 Symposium, Advances in the Study of the Sydney Basin, Dept of Geology, University of Newcastle, 179-185.

Hunter, Cynthia, 1991: *Earthquake Tremors Felt in the Hunter Valley Since White Settlement*, Hunter House Publications, Newcastle, NSW, Australia, ISBN 0 646 01716 0

McCue, K.F., 1980: *Magnitude of some early earthquakes in southeastern Australia*, Search, 11, 3, 78-80.

McCue, Kevin (editor), 1996: *Atlas of isoseismal maps of Australian earthquakes, Part 3,* AGSO Record 1995/44, Canberra, ISBN 0 642 22350 5 X.

Rawson, A., 1989: *Fault-Angle Basins of the Lapstone Structural Complex - Geomorphological Evidence for Neotectonism*, Proc of the 23 Symposium, Advances in the Study of the Sydney Basin, Dept of Geology, University of Newcastle, 171-178.

Rynn, J.M.W., D. Denham, S. Greenhalgh, T. Jones, P.J. Gregson, K.F. McCue & R.S. Smith, 1987: *Atlas of isoseismal maps of Australian earthquakes, Part 2*; Bureau of Mineral Resources Bulletin 222, Aust. Govt. Publishing Service, Canberra

Notes on the Tectonic setting of, and Attenuation in, the Sydney Basin

KEVIN MCCUE[1]
AUSTRALIAN SEISMOLOGICAL CENTRE, PO BOX 324, JAMISON CENTRE ACT 2614, AUSTRALIA

TECTONIC SETTING OF THE SYDNEY BASIN

The Australian continent is an island of continental crust with a surrounding halo of oceanic crust within the Australian Plate everywhere except through the island of New Guinea (Doutch, 1982) where continental Australia collides with the Pacific Plate. The Sydney Basin is a Mesozoic Basin on the southeastern edge of the Australian continent about 2000 km from the nearest recognised plate boundary to the east stretching from northern New Zealand to Fiji (see Plate tectonic map in Figure 1 from Wikipedia).

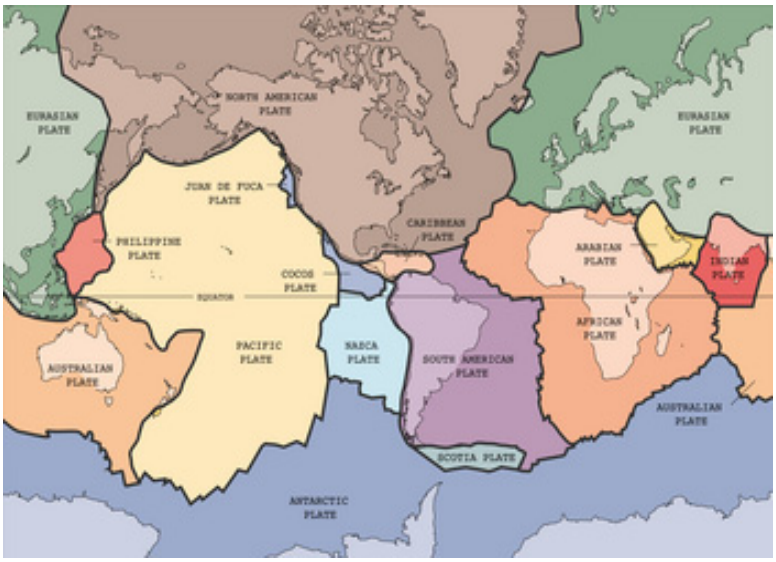

Figure 1 Tectonic plates showing the Australian continent's setting

The term intraplate is used here to identify areas not affected by interplate activity. The city of Auckland on the North Island of New Zealand is near the edge of the Australian/Pacific Plate boundary. It may not strictly be classified as interplate or intraplate because the plate boundary is wide and dips under the city, giving rise to the Recent volcanoes there. Across the Tasman Sea, the seismicity and earthquake hazard in the Sydney Basin are typical of eastern Australia as a whole. Earthquake epicentres do not correlate clearly with mapped faults or broad geological features and tend to be broadly diffused with embedded clusters through a 300 km wide area paralleling the southeast coast of Australia. Discrete areal zones have been defined by some authors (Brown and Gibson, 2000) for convenient hazard assessment but the history is very short, the first useful seismographs not installed until 1909 at Riverview Observatory so the zone boundaries will change as the seismicity patterns become better defined. There are many areas of continental Australia, particularly the western cratonic areas, that are more seismically active than the Sydney Basin.

The larger well-located Sydney Basin earthquakes actually occur in Lachlan Foldbelt basement underlying the Basin or near its interface with the Basin, the largest in the last 200 years, a modest

magnitude 5.6 event near Newcastle on 28 December 1989 (McCue and others, 1990). Parameters such as 'a' and 'b' of computed recurrence relations for identified seismic zones in the Sydney Basin are in the same range as those computed for other source zones throughout Australia (Brown and Gibson, 2000), they are essentially the same given the uncertainty in calculating them from the short period of instrumental data compared with the return period of potentially damaging magnitude 5^+ earthquakes.

A recognised measure of the hazard is the computed peak ground acceleration in a 475 yr period as shown on maps adopted by Standards Australia for incorporation into various editions of the Australian Loading Code (see for example McCue and others, 1993). Earthquake hazard in Australia is similar to that of other intraplate regions of the World, not negligible, but considerably lower than the hazard in any of the interplate regions (Giardini and others, 1999). By any recognised standard, the Sydney Basin setting is classically intraplate.

ATTENUATION IN THE SYDNEY BASIN

Valuable strong motion data have been collected in Australia over the last 15 years since the Joint Urban Monitoring Program to install accelerographs in urban areas with more than 50 000 people was initiated after the 1989 earthquake near Newcastle NSW. As yet there is insufficient data to determine attenuation rates in Western, Central or Eastern Australia, three regions that many expect should exhibit different rates of attenuation because of their different ages.

There is however a wealth of intensity information summarised in several hundred isoseismal maps for earthquakes throughout Australia (Everingham and others 1982, Rynn and others 1987 and McCue 1996) and Geoscience Australia Annual Seismological Reports post 1989). It is instructive to compare just two of these important earthquakes only weeks apart, one beneath the Sydney Basin sediments of Mesozoic age, and a similar sized event in southwestern WA in the Archaean craton (McCue and Gregson, 1993). The mechanisms of the earthquakes were very similar; thrusts with nodal planes dipping at intermediate angles under horizontal compression. Attenuation of seismic energy through the basin and craton might be expected to be as different as between any two geological settings in Australia. One factor which affects intensity estimates is time of day but both of these earthquakes occurred near midday local time so this factor can be discounted.

Pertinent details of the earthquakes are given in table 1 below along with characteristic measurements taken from the isoseismal maps, the equivalent circular radii of the areas enclosing intensities MM5, 4 and 3 or higher. It might seem surprising that the assigned maximum intensity is higher in Newcastle at MM8 than in Meckering MM6 at similar epicentral distances, especially given the shallower focus of the Meckering event. This is probably partly a result of good engineering practice. Following the magnitude Ms 6.8 earthquake that all but destroyed the township of Meckering in 1968, the town was relocated and rebuilt, the local council ensuring builders used earthquake design provisions for all new buildings. By comparison, no buildings in Newcastle had the benefit of incorporating earthquake design provisions, indeed most of the highly damaged buildings had severe flaws such as poor fastenings, missing beams, corroded wall connections and soft lower storeys. In addition the worst damage in Newcastle occurred in an area underlain by soft sediments, much of it hydraulic fill that no doubt contributed to the seismic load and assessed intensity.

Table 1: Parameters of the 1989 Newcastle NSW and 1990 Meckering WA earthquakes

PLACE	DATE	TIME	ML	DEPTH	ISOSEISMAL RADIUS*		
		UTC		km	MM5	MM4	MM3
					km	km	km
Newcastle NSW	28 December 1989	06:38	5.6	13 ± 2	105	185	300
Meckering WA	17 January 1990	23:26	5.5	6	25	150	260

* note that the scale bar of figure 9 in McCue and Gregson (1993) is incorrectly drawn.

The magnitudes measured by GA of the two earthquakes were similar, the Meckering event only 0.1 magnitude units smaller than the earlier earthquake at Newcastle. The table shows a much larger area of intensity MM5 in the Sydney Basin indicating that the focal depth of the WA earthquake may have been as shallow as 2 km or less which would support the lower peak intensity in Meckering but the MM5 radii also lend no support for an assumption of higher attenuation in the east relative to the west. The similar radii for the lower intensities clearly contradict the assumption of a higher attenuation in eastern Australia relative to the west, indeed, an opposite outcome might be deduced.

There are several isoseismal maps of other well documented pairs of earthquakes in the Sydney Basin and SW WA which could and should be analysed to check the universality of these observations.

CONCLUSIONS

Firstly, the Sydney Basin is a classic intraplate setting as measured by both the seismicity and hazard parameters. Secondly, the evidence from a comparison of the isoseismal maps of two very similar earthquakes on opposite sides of the continent challenges assumptions that the ground attenuation in the Sydney Basin is special or different from elsewhere in Australia.

REFERENCES

Brown, A., and Gibson, G., 2000. Reassessment of Earthquake Hazard in Australia. *12th World Conference on Earthquake Engineering.* Auckland NZ, Paper 0751, 7 pp.

Doutch, W., H., 1982 (Chairman). Plate-Tectonic Map of the Circum-Pacific Region, Southwest Quadrant. AAPG, Tulsa Oklahoma, USA.

Everingham, I.B., McEwin, A.J., and Denham, D., 1982. Atlas of isoseismal maps of Australian earthquakes. *Bureau of Mineral Resources, Australia*, Bulletin **214**.

Giardini, D., Grunthal, G., Shedlock, K., and Zhang, P., 1999. The GSHAP Global Seismic hazard Map. Annali di Geofisica, Vol 42, No. 6, pp 1225-1228.

McCue, K.F., Wesson, V., and Gibson, G., 1990. The Newcastle New South Wales, earthquake of 28 December 1989. *BMR Journal of Australian Geology and Geophysics*, **11**, 4, pp 559-568.

McCue, K., (compiler), Gibson, G., Michael-Leiba, M., Love, D., Cuthbertson, R., and Horoschun, G., 1993. Earthquake Hazard Map of Australia - 1991.

McCue, K., and Gregson, P., 1993. Australian Seismological Report, 1990. *BMR Record*, **1993/52**, 58pp.

McCue, K.F., (Compiler), 1996. Isoseismal Atlas of Australian earthquakes, Part 3. *AGSO Record*, **1996/44**.

Rynn, J.M.W., Denham, D., Grenhalgh, S., Jones, T., Gregson, P.J., McCue, K. and Smith, R.S., 1987. Atlas of isoseismal maps of Australian earthquakes. *Bureau of Mineral Resources, Australia*, Bulletin **222**.

Observations on faulting in the Sydney area reconciled with the seismicity rates: probabilistic fault rupture recurrence models

Kelvin Berryman, Terry Webb, Andrew Nicol, Warwick Smith, Mark Stirling
GNS Science, PO Box 30368, Lower Hutt, New Zealand
k.berryman@gns.cri.nz

ABSTRACT

New data pertaining to fault patterns, densities, and fault reactivation in the Sydney basin region provide a basis for reconciling fault activity with historic strain release manifest as earthquake magnitude and frequency. The dimensions of the faults infer associated earthquake magnitude. Site data on the size of reverse displacement on a reactivated, originally normal fault, combined with the scaling properties of earthquakes and other geological information, enable calculation of average subsurface single event displacements (SED's) for a range of fault sizes. At the same time, the rate of historical seismicity and expected maximum earthquake magnitude for the region have been used to estimate the rate at which seismic moment is released in the region. This paper reports on the new fault data from Sydney and presents a summary of modelled results for the frequency and magnitude of expected reverse fault earthquake rupture on reactivated normal faults in the 20-30 km wide coastal strip near Sydney.

Using the seismic moment release rate and the estimated number of faults that exist in the Sydney area we obtain a mean interval for recurrence of reverse faulting on any single structure as several million years. The associated earthquake magnitude distribution is in the range M 5.0-6.0 for the reverse faults in the coastal strip. The very long mean recurrence intervals that we obtain are a function of the low historical seismicity rate and the high density of fault structures in the Sydney Basin over which the seismicity could be distributed.

INTRODUCTION

Fault data from the southern coalfield and tunnel log data from the Sydney Basin provide new insights into fault occurrence in the Sydney basin so that historic seismic moment release can be assigned to structures with variable orientations and estimates of their rupture magnitude and frequency can be calculated. The data show that the c. 20-30 km wide coastal strip is divided by northwest-striking strike-slip faults, which are the largest structures. Between these faults there is a pervasive distribution of north- to northeast-striking dip-slip faults, most of which have net normal displacements. Distributed among the normal faults are some faults with net reverse displacement. Seismic moment release among dip-slip structures is assigned by proportion of the faults that have reactivated to have net reverse displacement.

To determine the fault dimensions and magnitude of an earthquake associated with a particular Single Event Displacement (SED) we need to use displacement-length and displacement-magnitude scaling relations. Two self-similar scaling relations have been adopted that embrace the likely range of earthquake stress drops expected for the Sydney Basin region. These relations are based on seismological data from low slip rate Eastern North America and low-to-moderate slip rate New Zealand regions. There are insufficient data to accurately define a relationship for continental Australia, let alone the coastal margin, for which stress levels are likely to be lower.

GEOLOGICAL SETTING OF THE SYDNEY REGION

Sydney is located in the Sydney basin (Herbert & Helby, 1980)(Figure 1), which is characterised by up to 5 km thickness of Permian and Mesozoic, terrestrial and marine sedimentary rocks. These rocks rest unconformably on Paleozoic rocks that are much more deformed. At the western margin of the Sydney basin Permian coal measures lap onto the Paleozoic rocks of the Lachlan Fold Belt. Sydney basin deposits consist of non-marine coal measures grading up into Triassic and possibly early Jurassic terrestrial and estuarine sandstone and siltstone (Herbert, 1980). The absence of younger Mesozoic rocks is attributed, by Ollier (1982) to uplift and doming as a precursor to the opening of the Tasman Sea which occurred from 80-55 Myr ago (Shaw, 1978). Thin Cainozoic-age rocks occur within the Sydney basin, most notably in the Penrith basin adjacent to the Lapstone Structural Complex (LSC) (Mauger et al., 1984) where several tens of metres of conglomerate, sand and clay represent ancient fluvial terrace and overbank flood deposits.

From a global tectonics perspective Australia is regarded as an intraplate setting, thousands of kilometres from an active plate boundary. However, as other areas on the margins of stable continental interiors such as eastern USA and India there are thick post-craton basins that are characterised by greater seismic activity than in the plate interiors. The Sydney area therefore is intraplate from a global tectonics point-of-view, but seismically more active than the continental interior, and with rock velocities and seismic attenuation that is more akin to active margin settings. Most earthquakes that occur within the Sydney Basin are within Paleozoic basement rocks that are located beneath the Mesozoic sediments, more than 3-4 km below ground surface. However, rare, shallow events such as the M_L 4.4 1999 Appin earthquake do occur within the Sydney basin sediments. Prior to the current study faults within the Sydney basin rocks were considered unusual,

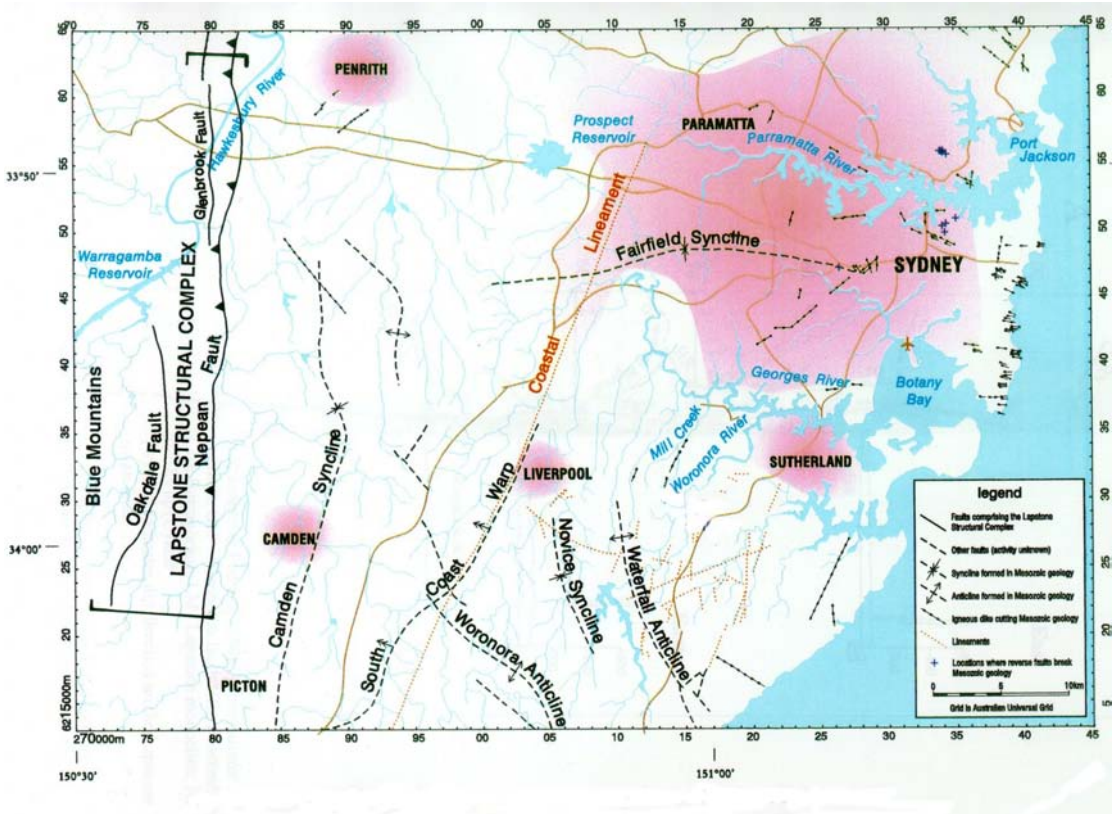

Figure 1 *Mapped structural features of the Sydney region prior to this study. Most structural data are from Herbert (1980), and Sherwin & Holmes (1986).*

with a compilation by Branagan et al (1988) listing only 16 occurrences of faults with a decimetre or more of displacement in Sydney basin rocks.

NEW FAULT DATA IN THE SYDNEY BASIN

In this paper we report on newly compiled data from the Southern Coalfield and tunnel log data from the Sydney Basin that provide new insight into the fault pattern, density and kinematics of the eastern, coastal, part of the Sydney Basin (Figure 2).

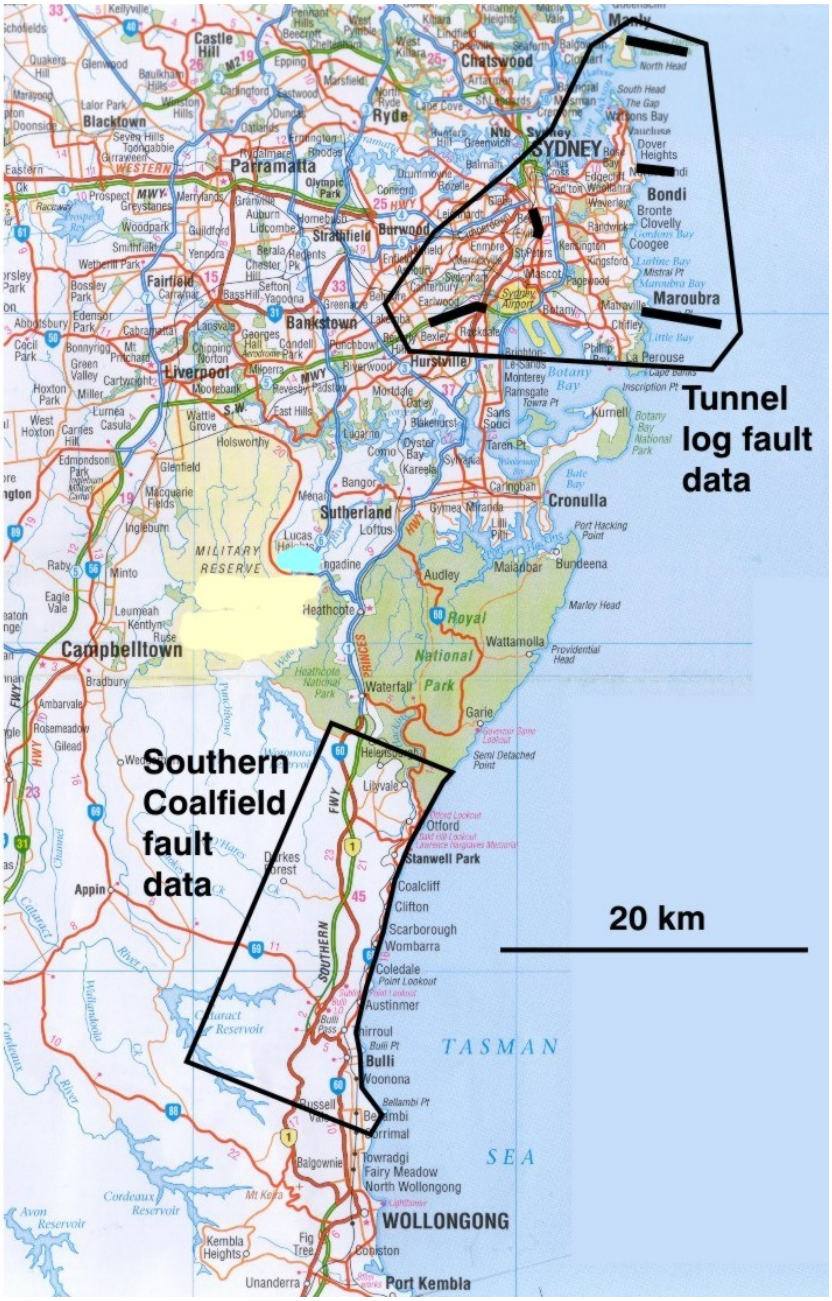

Figure 2 *Location of the Southern Coalfield and tunnels from which fault data have been obtained.*

Southern Coalfield data

The Southern Coalfield encompasses the southern section of the Sydney Basin south of Botany Bay. Fault data in this region were derived from coalmine plans on the top of the Bulli Seam and are two-dimensional (e.g. Figure 3). These data are used principally to calculate moment release for the fault population sampled so that moment rate can be partitioned between strike-slip and dip-slip structures. The faults in the Southern Coalfield are predominantly normal in their sense of slip and displace late Permian Illawarra coal measures. Faulting is to a large extent late Cretaceous and early Tertiary in age, representing the western margin of rifting associated with Tasman Sea opening from 80-55 Myr ago

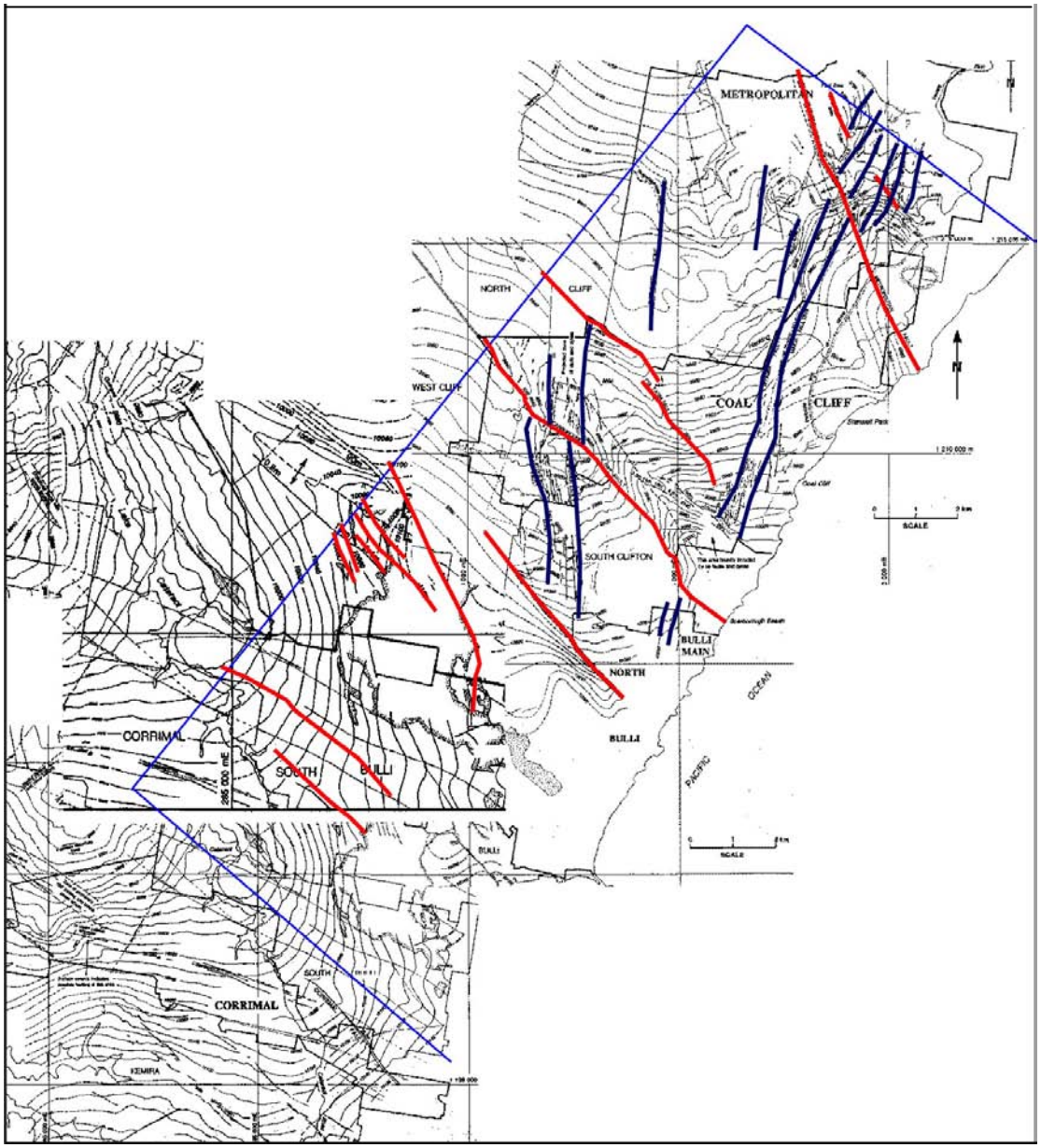

Figure 3 *Map of faults on the Bulli Seam in the coastal zone of the Southern Coalfield. Strike-slip faults are marked in red and dip-slip faults in dark blue. The blue rectangle outlines the 25 km by 10 km study area.*

The pattern of faulting for a 10 km × 25 km portion of the Southern Coalfield is shown in Figure 3. This region is part of the coastal zone which is bounded to the west by the South Coast Monocline. Faults in this region comprise two main sets that strike approximately northwest and north to north-northeast. The northwest striking faults are regional structures with typical trace lengths of 5 to >10 km, maximum apparent throws of 25 to 90 m (Lohe *et al.*, 1992), and predominantly strike-slip motion. The spacings of regional faults in this set are often 1–3 km. The more northerly striking fault set has predominantly dip-slip offsets and is dominated by two clustered fault arrays, which are spaced at 3–4 km (Figure 3.) and have a maximum length of 10 km. In the Wollongong–Port Hacking area there is a tendency for faults striking north-northeast to have displacements of less than 15 m, whereas faults striking west-northwest and northwest can reach 100 m in displacement (Sherwin & Holmes, 1986). The northwest striking faults appear to have accommodated the highest displacements and can be regarded as the dominant structures in the Southern Coalfield.

Although net displacements on the north-northeast striking fault sets are normal, small-scale field data indicates that many of these faults experienced late-stage reverse reactivation (Shepherd, pers. comm., 2002). A component of reverse displacement on north to north-northeast striking faults and sinistral strike-slip on northwest striking faults is consistent with contemporary strain data which are dominated by a northeast to east principal horizontal shortening direction (Hillis *et al.*, 1999). Thus both fault sets could be active in the contemporary strain field. Therefore, in our calculations of moment release rate we use both fault sets. Given that the northwest fault set is greater in number, in maximum apparent throw, and in trace length, we have assigned a greater component of the moment release to this set than to the more northerly-striking faults.

Northern tunnel log data

Some of the most complete fault data in the Sydney region, with respect to spacing, sense of slip, and displacement, are from tunnels, which, on the scale of the basin, produce one-dimensional samples of the fault population. Here we use data from six tunnels located in central and north Sydney trending in east-west (five tunnels including two from the M5 motorway) and north-south (one tunnel) directions (Figure 4). For each tunnel, fault locations, orientations, and net displacements were recorded. The fault data for these tunnels are summarised in Table 1. These data permit the spacing between adjacent faults to be estimated and these values were used for partitioning moment release among the dip-slip structures.

In each tunnel, faults were recorded where they offset beds within the Hawkesbury Sandstone Formation. A total of 133 faults were recorded in all tunnels with the main fault strikes being approximately north to northeast and northwest (Figure 5a). Approximately 128 faults have net normal displacement, while the remainder have net reverse displacement. Displacements range up to 9 m with most faults (110) carrying ≤ 1 m (Figure 5b).

Fault spacing was calculated for both reverse and normal faults and for northwest and north-northeast striking fault sets. We calculate an average normal fault spacing of 140 m. This value increases to 175 m if we consider only faults with a north to northeast strike. These results appear to be independent of tunnel trend.

Determining the spacing of faults that have experienced reverse reactivation is more difficult. This is because net displacements provide no indication of reverse movement on a reactivated fault if the magnitude of the reverse movement was less than earlier normal slip on the fault. Therefore, the maximum spacing for reverse faults is approximately 3.5 km, while the minimum could be as little as 180 m, the spacing of faults with net normal displacement. This lack of knowledge is handled as alternative branches with assigned weights in the probabilistic analysis.

Figure 4 *Locations of tunnels from which faults were recorded.*

Table 1 North Sydney Basin tunnel fault data

FAULT DATA	TUNNEL						SUMMARY	
	MALABAR	NORTH HEAD	BONDI OUTFALL	NEW S. RLY	M5 E-BOUND	M5 W-BOUND	TOTAL	MEAN
Logged distance (m)	4746	4120	1920	2230	2895	2973	18884	
Total offset (m)	25.4	29.6	12.0	18.3	11.4	6.1	103	
Mean fault spacing (m)	115.0	129.5	159.25	96.2	166.2	177.4		140.6
Throw (m/km)	5.4	7.2	6.3	8.2	3.9	2.0		5.5
N&NE fault spacing (m)	173.3	166.9	159.3	101.0	230.0	221.7		175.4
# of reverse faults	2	1	0?	1	1?	1	5-6	

A)

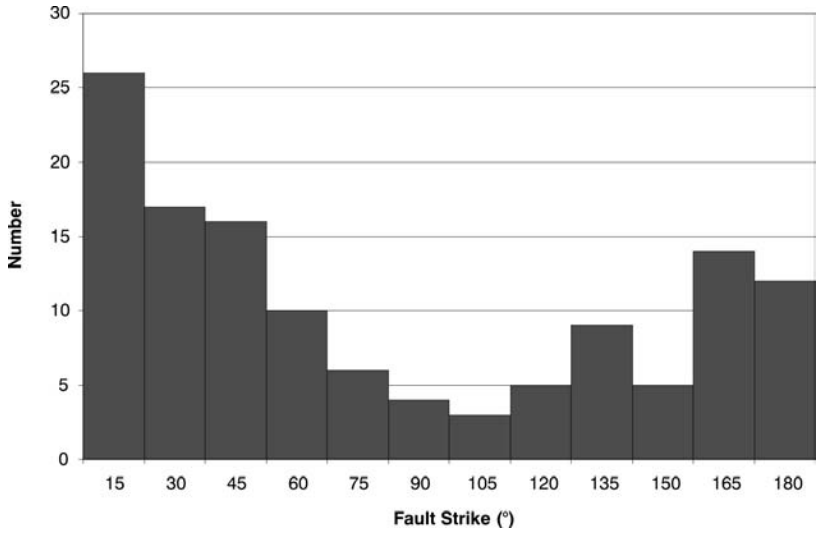

B)

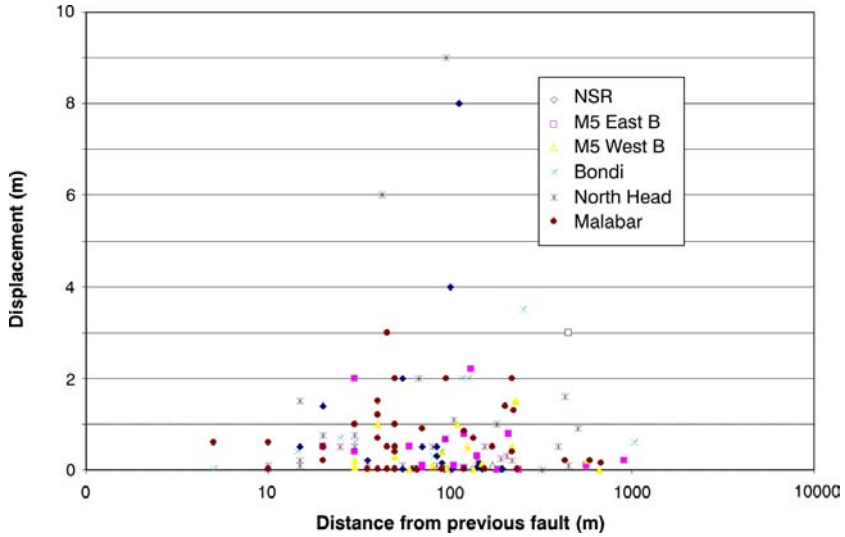

Figure 5 *Fault data from tunnels logs. a) Frequency histogram of fault strikes and b) Plot of fault displacement versus distance to closest adjacent fault.*

DERIVATION OF FAULT SCALING RELATIONS FOR THE SYDNEY REGION

In general, the parameters of earthquake rupture length, width, displacement, and seismic moment scale in quite predictable ways. These parameters can be related by scaling relations. Scaling relations enable the prediction of, for example, the length and magnitude of an earthquake rupture given its displacement. The observed field data in Sydney is fault offset and we have interpreted this in terms of a number of distinct earthquakes by using a displacement-length scaling relationship. A displacement-magnitude relationship is used to predict the range of mean magnitudes associated with our range of mean SED values

Many different earthquake scaling relationships have been developed over the past several decades, the most well-known of which are those derived by Wells and Coppersmith (1994). Their relationships are now recognised as having some limitations (e.g. Stirling *et al.*, 2002), the most significant for this study being that they are based on linear, rather than bilinear regressions. It has

been recognised for some time that large shallow earthquakes rupture the entire crustal thickness and are thus width-limited. Such earthquakes scale differently to smaller events (e.g. Scholz, 1982, Shimazaki, 1986). In this study, where displacements are relatively small and associated rupture widths and lengths are also modest, scaling relations that are self-similar, i.e. length, width, and displacement all increase in proportion to seismic moment, are appropriate. Seismologically based relations, rather than geological ones, are best in this situation as surface geological data are sparse for small earthquakes as few rupture to the surface.

The parameter that controls a self-similar displacement-length relationship is static stress drop (Mohammadioun & Serva, 2001). Stress drops, although certainly not a measure of absolute stress levels in the crust, are often used as a guide. A simple division between high stress drops for intraplate earthquakes compared with lower stress drops for interplate earthquakes has been recognised (Scholz *et al.*, 1986). Kanamori and Allen (1986) noted an almost equivalent difference between high stress drops for earthquakes occurring on crustal faults with long recurrence intervals *versus* low stress drops on short recurrence interval faults. These values have been determined from geological observations of large earthquakes world-wide.

For continental Australia we would expect high stress drops, it being a typical intraplate environment with relatively low rates of seismicity and long recurrence intervals. Early determinations of stress drops for continental Australian earthquakes by Denham *et al.* (1981) and Mumme (1984) found very low values of 10 bars or less. In these studies, rupture lengths were derived from aftershock distributions. In a following section we discuss how aftershock distributions systematically overestimate rupture lengths for world-wide data. It seems that for continental Australian earthquakes this effect is particularly pronounced. For example, in the Meckering earthquake, the secondary faulting, accompanied by aftershocks, was seen to develop over a period of weeks after the mainshock and, in one case, over 22 months (Gordon & Lewis, 1980). Seismological studies of the Meckering earthquake show that it was, in fact, a high stress drop event. Teleseismic body wave modelling by Vogfjord and Langston (1987) determined a source duration of 3–5 s, corresponding to a stress drop of ~100 bars. In their elastic dislocation modelling the subsurface fault length was assumed to be 20 km, significantly shorter than the curved 37 km length of the surface fault scarp. A detailed study of aftershock depths by Langston (1987) also concluded that the crust was very strong in continental Australia and that associated crustal stresses were high.

The Tennant Creek earthquake comprised three main events with each being associated with separate episodes of surface faulting (Crone *et al.*, 1992). Such an expansion of faulting with time would also be expected to be accompanied by an expansion of the aftershock distribution as observed in the Meckering earthquake. Such expansion is now understood in terms of stress triggering (e.g. King *et al.*, 1994) whereby the initial dislocation triggers slip on adjacent faults. The prevalence of such expansion or triggering is more an indication of high stresses within the crust rather than low stresses.

Other evidence that the crust in continental regions is in a critical state of stress comes from deep borehole data (Townend & Zoback, 2000, Zoback & Townend, 2001), which show that hydrostatic, rather than lithostatic, pore pressures exist in the brittle crust. The lower pore pressures mean that the crust is much stronger than it otherwise would be, and thus capable of withstanding high stress levels from tectonic driving forces. Areas of continental crust can thus behave as rigid plates over time scales of tens to hundreds of millions of years.

The Sydney Basin is more of a transition region between continent and margin, so we would expect stress drops to be a little lower than for a continental region. Rates of historical seismicity are low, so earthquake recurrence intervals will be long, again indicative of high stress drops (Kanamori & Allen, 1986).

Given that there is no Australian-specific scaling relation available, and few reliable determinations of stress drop, we need to use scaling relations from other similar tectonic environments. An appropriate self-similar seismologically based scaling relation for continental regions can be derived from the Eastern North America (ENA) data set of Somerville *et al.* (1987). Their data are earthquake source durations and seismic moments, measured by matching synthetic with actual seismograms. The source duration can then be interpreted in terms of rupture dimension. A self-similar regression of seismic moment on source duration, weighted according to the estimated uncertainties in both quantities, gives

$$\log (M_o) = 23.81 \pm 0.13 + 3.0 \log (\tau), \quad (1)$$

where M_o is the seismic moment in dyne-cm and τ is the source duration in seconds. To derive rupture length we follow Cohn *et al.* (1982), who show that the rupture duration that we measure is comprised of three terms: the time to rupture the fault plane, a travel time delay, and the rupture rise time. The time to rupture the fault is simply $L/0.8\beta$ for a unilateral rupture and $L/2/0.8\beta$ for bilateral, where β is the shear wave velocity and L the fault length. The travel time delay is zero, on average, for a unilateral rupture and $0.64\ L/2/\beta$ for bilateral. To estimate the rise time (slip duration) we use the moment-duration relation of Somerville *et al.* (1999, their Table 7):

$$\tau_r = 2.03 \times 10^{-9}\ M_o^{1/3} \quad (2)$$

and the corresponding moment-area (A) relation:

$$A = 2.23 \times 10^{-15}\ M_o^{2/3} \quad (3)$$

to get a rise time of $0.266\ L/\beta$ for unilateral ruptures and $0.266\ L/2/\beta$ for bilateral, with total rupture durations of $0.43L$ and $0.31L$ respectively, if $\beta = 3.5$ km/s.

It has recently been shown that earthquake ruptures tend to be unilateral, rather than bilateral (McGuire *et al.*, 2002). They found that 80% of ruptures tend to be unilateral and that this was true of both strike-slip and subduction zone thrust events. Given that duration, $\tau = 0.31L$ for bilateral ruptures and $\tau = 0.43L$ for unilateral, we use a linear combination of the logarithm of these factors to obtain a moment-length scaling relation that takes account of bilateral ruptures:

$$\log (M_o) = 22.63 \pm 0.13 + 3.0 \log (L), \quad (4)$$

where L is the rupture length in km and the uncertainty in the intercept value has been derived from the regression intercept uncertainty and an additional uncertainty related to the ratio of unilateral to bilateral ruptures. The scaling relation has a fixed slope of 3.0, in agreement with self-similar scaling, because the derived value was insignificantly different from 3.0.

We then use the relationship between seismic and geodetic moment:

$$M_o = \mu L W D, \quad (5)$$

(Aki & Richards, 1980), where μ is the crustal rigidity (3.0×10^{11} dyne/cm^2), W is the fault width, here taken to equal the length, and D is the average subsurface single event displacement, together with the definition of moment magnitude, M_w, as:

$$M_w = 2/3 \log (M_o) - 10.7, \quad (6)$$

(Kanamori, 1977), where M_o is in dyne-cm, to get

$$M_w = 2.08 \pm 0.17 + 2.0 \log (D), \quad (7)$$

Similarly we can also derive relationships between slip and length, this being a constant (for constant stress drop or self-similar scaling) such that

$$\log (D/L) = -3.85 \pm 0.13. \quad (8)$$

Following Somerville *et al.* (1987) we can then determine the static stress drop to be 120 bars. This would be regarded as a high static stress drop, in good agreement with that expected for intraplate regions such as ENA or continental Australia.

Given that we expect the stress regime in the Sydney Basin to be lower than a purely continental region, we need a lower stress drop scaling relation to use as an alternative to the ENA one. Teleseismic modelling of New Zealand earthquakes (Anderson *et al.*, 1993, Webb & Anderson, 1998, Doser *et al.*, 1999, and Doser & Webb, 2002) has produced a data set of seismic moments and source rupture durations equivalent to that of Somerville *et al.* (1987). The resulting scaling relation for a subset of these events that have occurred on or near low-to-moderate slip rate (<5 mm/y) faults is:

$$\log (M_o) = 22.33 \pm 0.05 + 3.0 \log (L), \quad (9)$$

from which we can similarly derive

$$M_w = 2.39 \pm 0.07 + 2.0 \log (D), \quad (10)$$

And

$$\log (D/L) = -4.10 \pm 0.05. \quad (11)$$

The static stress drop for the New Zealand relation is 60 bars, significantly lower than the ENA value, but higher than would be expected at a plate boundary (because earthquakes in low-to-moderate slip rate areas were selected). Given that the two scaling relations bracket the expected stress drop range for the Sydney Basin, when they are used together they should provide sound estimates of magnitude and rupture length from SED. We expect that the ENA stress drop is slightly more applicable than the low-to-moderate slip rate New Zealand environment.

Comparison of Scaling Relations with historical surface rupturing Australian earthquakes

As a check on the suitability of our ENA/NZ scaling relations we have plotted both fault length and displacement as a function of magnitude for all surface rupturing Australian earthquakes since 1968 (Table 2, Fig. 6). In terms of rupture length, there is very good agreement between the observed lengths and our weighted ENA/NZ relationship. The largest departures are for the Cadoux and Marryat Creek earthquakes, both of which appear to be unusually long.

Table 2 Parameters for historical surface-rupturing Australian earthquakes

NAME	YEAR	MONTH	DAY	HR:MIN	MS	MW	SURFACE RUPTURE LENGTH (KM)	DISPLACEMENT RANGE (M)
Meckering[1]	1968	Oct	14		6.8		20.0	0.4–2.5
Calingiri[2]	1970	Mar	10		5.1		3.5	0.04–0.4
Cadoux[3]	1979	Jun	2	09:47	6.0	6.1	14.7	0.2–1.4
Marryat Creek[4]	1986	Mar	30	08:53	5.8	5.7	13.8	0.1–0.7
Tennant Creek[5]	1988	Jan	22	00:35	6.3	6.3	10.2	0.1–0.8
Tennant Creek[5]	1988	Jan	22	03:57	6.4	6.3	9.8	0.1–1.2
Tennant Creek[5]	1988	Jan	22	12:04	6.7	6.6	16.0	0.2–1.8

[1]Vogfjord & Langston (1987), [2]Gordon & Lewis (1980), [3]Lewis *et al.* (1981), [4]Machette *et al.* (1993), [5]Crone *et al.* (1992).

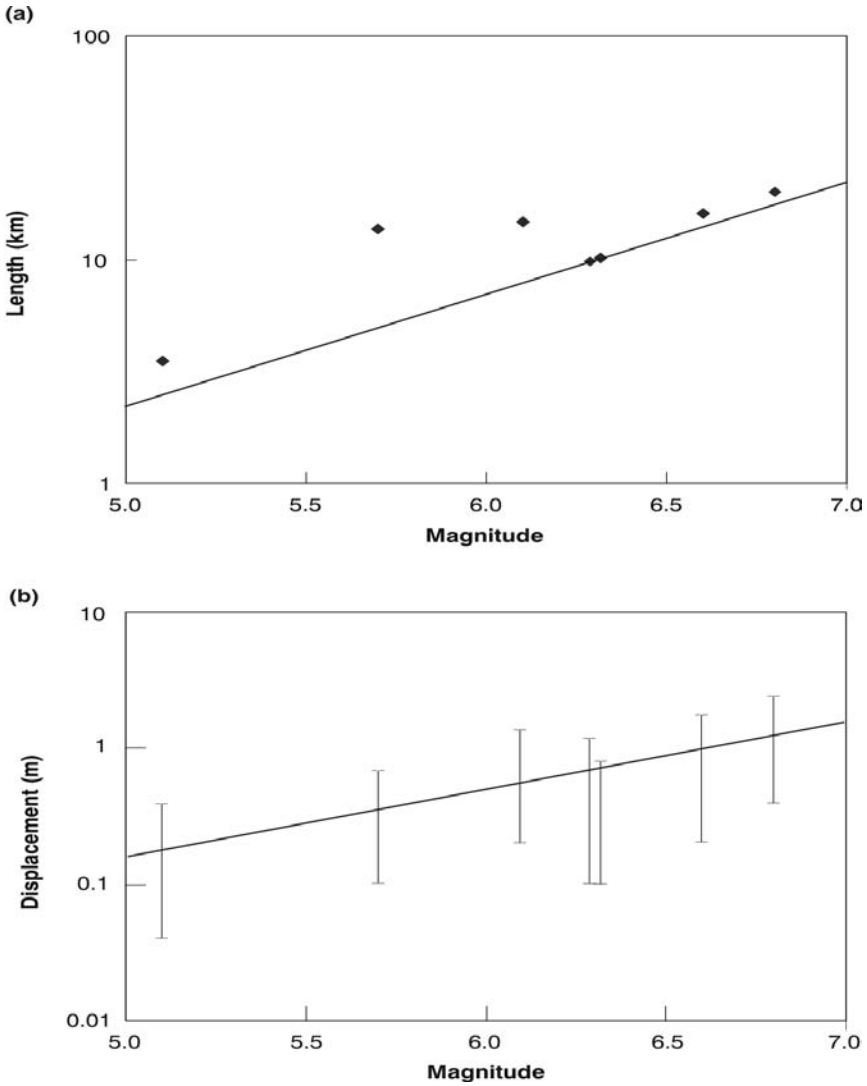

Figure 6 *Surface rupture data for historical Australian earthquakes (sources as in Table 2). Magnitude versus length data and a scaling relation based on a weighted average of Eastern North America and New Zealand relations. Magnitude versus range of observed displacements and an equivalent scaling relation to that used in (a).*

There is no reliable estimate of stress drop available for the Cadoux earthquake from either teleseismic body wave modelling or elastic dislocation modelling, it being too small to produce good quality data. The stress drop derived from the surface rupture length is ~28 bars (Denham *et al.*, 1987), although that study also cites overcoring and hydrofracturing measurements that show shallow stresses are high — in the 200–300 bar range. The study concludes that this area has comparatively high levels of crustal stress. The apparent low earthquake stress drops are thus most likely to be due to post-seismic fault expansion. There is even less seismological data for the Marryat Creek earthquake, again because of its small size. The most likely explanation for the long rupture length is, as for the other continental events, expansion of the surface fault extent due to stress triggering effects.

Observations of surface fault displacements vary significantly in size along strike. For the historical Australian surface ruptures we have plotted the range of observed surface displacements as a function of magnitude in Figure 6b. We have excluded very small values near to the ends of faults. Our weighted ENA/NZ scaling relation is completely consistent with these observations. Note that the uncertainties are far too great to be able to define a relationship in its own right.

DERIVATION OF FAULT PARAMETERS AND EARTHQUAKE SIZE FROM FAULT OFFSET

Well-determined reverse displacement of 35-50 cm has been observed in two exposures of a fault in the region and we use this range to explore the range of fault and earthquake parameters that are consistent with this. Scaling relations can also place some constraint on likely SED's. To get a surface rupture, we expect rupture widths greater than ~2 km, given that the top layer of crust is less seismogenic (based on local seismicity being distributed over the 2–18 km range and decreasing fault offsets towards the surface observed in coalfield data). A 2 km rupture width equates to a M_w4.9 earthquake with ~21 cm average subsurface slip. This equates to ~14 cm of surface slip, after a surface/subsurface slip correction of 0.67 has been applied (Stirling *et al*., 2002). On this basis, the 50 cm offset could comprise three SED's of ~17 cm, two of 25 cm, or one SED.

Work by Hecker and Abrahamson (2002) has shown that the distribution of slip at a point on a fault has a coefficient of variation (the standard deviation divided by the mean), ***C.V.***, of ~0.45 (for dip-slip faults). This is a statistical variability that may reflect true variability in the physical process and has been built into the probabilistic modelling.

Our aim is to determine mean recurrence interval using the rate of historical seismicity and observations of surface fault offsets. As part of this process we need to determine the geodetic moment, for which we need to know the average subsurface SED, not the surface SED, so that it can be compared with the moment release calculated from the seismicity, which is distributed in the 2–18 km depth range. The subsurface rupture lengths used above to calculate the subsurface SED were largely derived from aftershock distributions, which are known to overestimate rupture length. This effect is shown in Figure 7, where magnitude is plotted against subsurface rupture length for the Stirling *et al.* (2002) data set and for the seismological data set used in the derivation of the low-to-moderate slip rate New Zealand scaling relation. The New Zealand data have consistently shorter rupture lengths for a given magnitude than the Stirling *et al.* (2002) data. We have used regressions on the two moment-length data sets shown in Figure 7 to correct for the Stirling *et al.* (2002) rupture lengths being overestimated. The regression on the New Zealand data included a factor assuming 20% of the ruptures were bilateral.

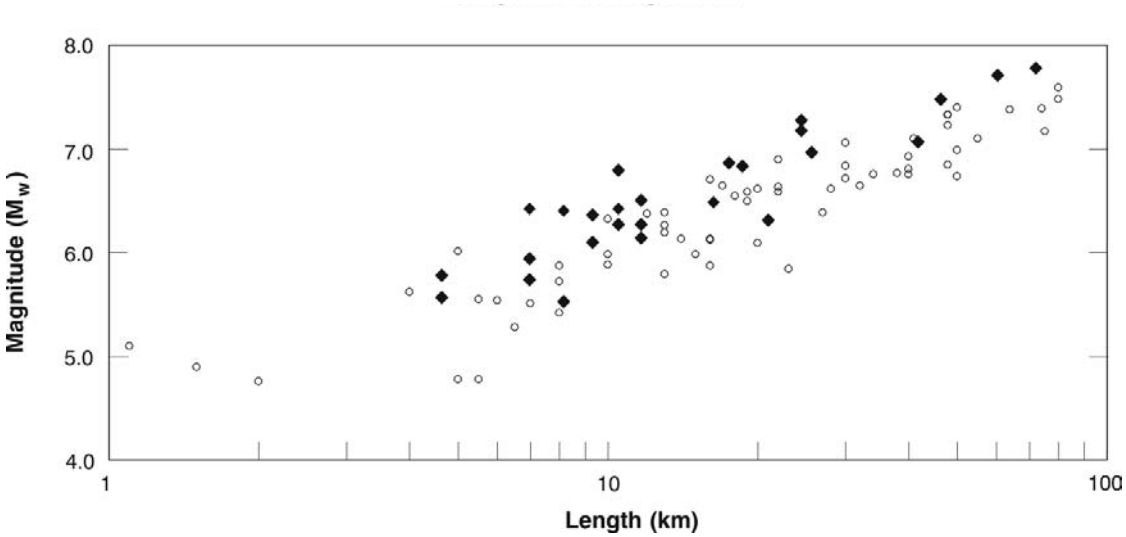

Figure 7 *Magnitude versus length data used to correct for the overestimation of rupture length. Open circles are for reverse, oblique-reverse, and rare strike-slip faults in regions of low slip rate from the world-wide database of Stirling et al. (2002). Solid diamonds are from New Zealand seismological data for earthquakes in regions of low-to-moderate slip rate.*

Next we provide a basis to calculate a distribution of possible characteristic magnitudes and rupture lengths associated with the SED's calculated for a fault. We bring more knowledge to bear on the problem by imposing constraints on allowable rupture lengths and widths. Fault scaling relations are required for determining magnitude and rupture length given SED. We have discussed the choice of suitable scaling relations for the Sydney Basin in the previous section. The relations for displacement-length are given by Equations 8 and 11, while those for displacement-magnitude are given by Equations 7 and 10.

Rupture lengths derived using Equations 8 and 11 have also been used to constrain allowable SED values in that earthquake rupture lengths are likely to be limited by the maximum fault length for the dip-slip fault zones (see section "New fault data in the Sydney Basin"). In general these zones are truncated by more dominant NW-SE oriented strike-slip faults. There is some possibility that an energetic rupture could jump across to a neighbouring zone, a classic example of this being the 1992 Landers, California, earthquake (e.g. Johnson *et al.*, 1994). To allow for such an eventuality we allow the maximum rupture length to be equal to the seismogenic thickness (18 km), i.e. to have an aspect ratio of 1:1, in 50% of cases. For the remaining cases, the maximum rupture length is limited to 10 km — the largest dip-slip fault zone length in the south Sydney Basin (see section "New fault data in the Sydney Basin"). When the rupture length calculated for a given SED value exceeds the allowable length as defined above, that particular branch of the probability calculations has been discarded.

Similarly, SED's associated with very short rupture lengths are also excluded. This is because very short ruptures will also have small widths (given that we are assuming 1:1 aspect ratios, suitable for dip-slip faults) and will thus not be capable of generating surface ruptures. Coalfield data show a decrease in total fault offsets towards the surface over depths of ~2 km, implying that surface ruptures are driven from depths greater than this. Seismicity is also sparse in the top 2 km, so within this depth range moderate to large earthquakes are very unlikely to nucleate. A minimum allowable width (and length) of 2 km has thus been used to exclude small SED values.

In order to determine the possible slip rate on any one of the faults we have identified in the region we need to know the long-term rate of background seismicity for the surrounding area, and derive slip rate from seismic moment release rate. For an area source zone, the seismicity is assumed to obey the Gutenberg-Richter relationship:

$$\log (N(m)) = a - bm, \qquad (12)$$

where $N(m)$ is the annual number of events of magnitude m or greater, and a and b are the rate and slope parameters (often referred to as a- and b-values).

Two area source zones have been defined for the region:

The East Sydney Basin area source from the Seismology Research Centre area source scheme (Gibson, pers comm., 1999). The seismicity parameters for this source are calculated from the post-1960 rate of M≥4 earthquakes recorded inside the zone.

A single large area source zone that was defined by Australia Geological Survey Organisation (AGSO) scientists (McCue pers comm., 2001). This zone encompasses eastern New South Wales, Victoria, and Tasmania, and the seismicity parameters are based on the 20th Century rate of M≥5 earthquakes recorded inside the zone. These earthquakes show a much more uniform spatial distribution than the smaller events that have occurred over Eastern Australia (e.g. in the East Sydney Basin). The large size of the zone also encloses enough M≥5 earthquakes to define statistically robust seismicity parameters.

The two source zones described above can be represented as alternatives in the probabilistic calculations, with their different rate parameters reflecting our limited knowledge of the spatial distribution of seismicity. The two alternative zones do not, however, adequately represent uncertainty in long-term variability in seismicity rates. Seismicity rates can vary in time, perhaps due to stress-triggering effects, for example. To reflect this we included the East Sydney Basin area source zone with a doubled seismicity rate as a third alternative. The seismicity data for each of our alternative models are presented in Table 3.

Table 3 Seismicity parameters for area source zones

	EAST SYDNEY BASIN	EAST SYDNEY BASIN (DOUBLED RATE)	AGSO LARGE AREA SOURCE ZONE
Cumulative a-value	2.0 (+0.12/–0.18)	2.3 (+0.12/–0.18)	5.4 (+0.12/–0.18)
b-value	0.93±0.11	0.93±0.11	1.14±0.08
Weight on logic tree	0.7	0.2	0.1

Figure 8 shows the normalised cumulative annual seismicity rates for the three models. The AGSO large area source zone has a higher rate of small earthquakes (M<~3.5), but due to its high b-value it contributes few large events compared to the other models.

An essential step towards obtaining slip rate is determining the moment release rate for the region. This is done by integrating over the magnitude distribution from the lower magnitude threshold up to the maximum magnitude, M_{max}, making use of the expression:

$$\log (M_o) = 1.5m + 16.05, \qquad (13)$$

(Kanamori, 1977). In general, the total moment release in an area is dominated by the largest events even though they are very infrequent. To determine a stable moment rate we need to truncate the

Gutenberg-Richter distribution at a maximum magnitude, i.e. integrate up to M_{max}. M_{max} for the area source zones has been set at M7.5 (Berryman & Stirling, 2003).

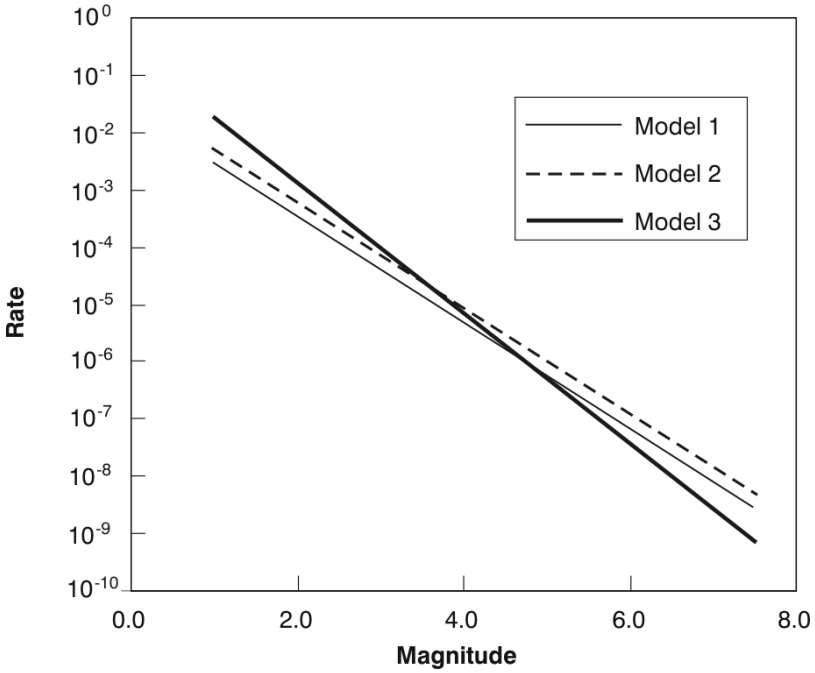

Figure 8 *Predicted cumulative earthquake recurrence rate as a function of magnitude for three source models. Model 1 is the East Sydney Basin, Model 2 is the East Sydney Basin with a doubled rate, and Model 3 is the AGSO large area source zone.*

The preceding steps allow us to calculate the moment release rate for the area of interest within the Sydney Basin. To determine the moment release rate of any particular fault in the study area we need to understand how the fault structures in the Sydney Basin accommodate regional strain. Given that strain rates are now very low (Tregoning, 2002), we can only estimate this from past faulting behaviour when the regional strain was east-west extensional, with the assumption that the behaviour will be similar now that the strain is reversed. We can also use more generic earthquake scaling properties to estimate proportions of moment release.

We have two sets of data that help us understand the fault structure of the Sydney Basin — that from coalfield data to the south and from tunnel logs in the north. The tunnel log data set is the more detailed and hence complete, but the tunnels are largely oriented east-west (Figure. 4) and are thus essentially a 1-D sample of the region. This means that north-south oriented dip-slip structures are well sampled, but northwest-southeast oriented strike-slip structures are not. If we were to partition the moment release rate according to the tunnel log data there would be a strong bias towards more moment release on the dip-slip structures because of the sampling bias. We therefore reject this approach. The coalfield data, however, are 2-D and are thus more useful for partitioning moment.

The coalfield data in the south show a pattern of major strike-slip faults dividing the region with dip-slip structures in between (Figure 3). We use the coalfield-based understanding of the Sydney Basin structure to partition the moment release rate between the strike-slip and dip-slip structures. We do this by calculating the total moment that has been released by the mapped structures using the data collated in section “New fault data in the Sydney Basin”. In practise, we do this in three ways because of other limitations in the collated data.

Firstly, we use the expression relating seismic and geodetic moments:

$$M_o = \mu A D \qquad (14)$$

(Aki & Richards, 1980) where μ is the crustal rigidity (3.0×10^{11} dyne/cm^2), A is the rupture area (in our case the fault length, L, times the width, W), and D is the average subsurface slip (in our case the recorded fault throw, although this is a minimum — see below). The results are shown in Table 4 ($L \cdot W \cdot D$).

Table 4 Proportion of moment release rate on dip-slip structures

	DIP-SLIP FAULTS AS INDIVIDUAL FAULTS	DIP-SLIP FAULTS IN ZONES
$L\ W\ D$	12%	18%
$L^2\ D$	7%	13%
L^3	16%	12%

In the above ($L \cdot W \cdot D$) treatment we have assumed a fault width of 18 km, i.e. steeply dipping faults going through the full seismogenic crust. An equally valid argument is to say that the mapped faults will have an aspect ratio of 1:1 (until L>18 km), and so we calculate the proportion of moment release accordingly. This is our second way of apportioning moment using the mapped structures and the results are also shown in Table 4 ($L^2\ D$). The values obtained are somewhat less than for the first ($L \cdot W \cdot D$) treatment.

A shortcoming of both the methods presented thus far is that the throws recorded for strike-slip faults in the coalfield data are just the vertical throw and do not represent the total offset. This may introduce a bias towards more moment release on the dip-slip structures. Our third approach is to assume self-similar scaling and to calculate the moment release rate according to L^3, thus avoiding the use of measurements of fault throw. The results (bottom row on Table 4) are comparable with the other approaches. All of the values in Table 4 have been used in probabilistic calculations.

Given that all the approaches we have used so far have some limitations, we also use more generic earthquake scaling properties to estimate moment release. In general, moment release in a region is dominated by the largest events. The moment release associated with the maximum magnitude earthquakes for the strike-slip and dip-slip structures can thus be used to estimate the proportion of moment release rate on dip-slip structures alone. We have already mentioned that the northwest-southeast oriented strike-slip faults are the longest structures in the region. We thus assume that the M_{max} already estimated for the region (M_w7.5) will occur on such a structure.

To estimate the M_{max} for the dip-slip structures we use the logic already developed on the other branch of the logic tree for the maximum likely rupture lengths (10 and 18 km), and use that to estimate M_{max}. The result is $M_w6.81\pm0.12$, giving proportions of moment release of 8% and 6% based on the ratio of mean and mean-plus-2-sigma M_{max} values respectively. We have used both in the probabilistic calculations.

Thus far we have obtained a range of 6–18% for the proportion of total moment released on the dip-slip structures, and conversely 82-94% on the strike-slip faults. Other information of relevance includes earthquake focal mechanisms. Studies by Denham (1980) and Denham *et al.* (1981) show a mixture of strike-slip and reverse focal mechanisms, in good agreement with our assumed model of a mixture of active strike-slip and dip-slip structures. Most of those focal mechanisms are, however, closer to the continental interior than our study area. While these data reinforce the suitability of our model, they are not sufficient to derive any accurate partitioning of moment release rate between strike-slip and dip-slip fault motion. This is because there are (i) too few events in an

equivalent tectonic environment and (ii), as already discussed, moment release rate is dominated by the largest events.

With the foregoing decisions and calculations we are able to calculate the moment release rate over all dip-slip structures in a 25 km × 10 km area. This moment release rate was based on the pattern of mapped strike-slip and dip-slip faulting in coalfield data in the South Sydney Basin. The tunnel log data for the North Sydney Basin is relatively complete for the dip-slip structures (Figure 5). These data show an average spacing of 5.7 faults/km. Reactivated reverse faults are also identified in the tunnel logs. These have an average spacing of 0.29 faults/km. Other dip-slip faults may also be reactivated, however, but if their net offset is still normal they will not be identified. We can thus partition the moment rate by using the dip-slip fault density measured in an east-west direction and assuming that these structures, or structures sub-parallel to them, accommodate all the necessary dip-slip motion within the 25 km × 10 km sample region.

Few of the tunnels in the north Sydney Basin have any significant north-south extent. The best example is the New Southern Railway tunnel, in which 89% of logged faults are in the NE-SW quadrant leaving only 11% as possibly being in the category of NW-SE oriented strike-slip faults. These data support our interpretation, based on the coalfield data to the south, that the strike-slip faults are fewer in number and more major through-going structures than the dip-slip faults.

In partitioning the moment release rate among the dip-slip faults consideration was given to the likelihood that already reactivated faults would take up future compressional stress or whether another of the normal faults will be reactivated with reverse slip for the first time. In the probabilistic calculations these decisions introduced large uncertainty to derived slip rate and recurrence estimates for the existing array of reverse faults.

In the final step on this part of the logic tree we need to calculate the slip rate for the reverse faults. Thus far we have determined the moment release rate on dip-slip structures and we understand the east-west density of those structures. As mentioned above, we assume that in the along-strike direction these structures continue, or are replaced by sub-parallel structures. This is a safe assumption because (i) dip-slip faulting has been shown to be pervasive throughout the region and (ii) tectonic strain needs to be accommodated over the whole length of the region. Effectively then, we can think of the dip-slip portion of the moment rate being released by an array of faults of length 25 km, width 18 km, at an appropriate density in the east-west direction. Slip rate for each of these faults can then be calculated using Equation 5, where $\boldsymbol{M_o}$ is replaced by moment rate and $\boldsymbol{D}$ is replaced by the slip rate. This slip rate is the average sub-surface rate, applies along the entire fault, and is thus the rate we need for any single fault.

In terms of the regional seismicity, the total moment release rate and slip rate for the fault array is made up of characteristic earthquakes on the any particular fault (whose length is calculated on the other branch of logic tree) plus a range of various-sized earthquakes over the rest of that fault array. These combine to produce the appropriate Gutenberg-Richter distribution of sizes and rates for the area.

Having calculated average subsurface SED (and the associated earthquake magnitude) and mean slip rate, then the mean recurrence interval for any fault of interest can now simply be calculated by dividing the individual SED values by the associated slip rate.

RESULTS

In this section we first present the results from our preferred model of rupture length, earthquake magnitude, slip rate, and surface rupture recurrence interval for distributions of surface SED. We then undertake sensitivity tests, varying certain model assumptions to judge the effect on the results.

Outputs from the preferred model

Typical outputs for a reverse fault in the 20-30 km coastal part of the Sydney basin with mean surface single event displacement of 30 cm from our preferred probabilistic model are summarised in Table 5, where we list the mean, median, 16th, and 84th percentiles for each quantity.

Table 5 Preferred values of logic tree output

	84%	MEDIAN	MEAN	16%
Surface SED (cm)	16	25	30	46
Subsurface SED (cm)	23	41	50	74
Rupture length (km)	2.5	4.0	4.9	7.5
M_w	5.0	5.5	5.5	6.0
Slip rate (mm/year)	0.00003	0.00015	0.00057	0.00082
Mean recurrence interval (Ma[1])	0.53	3.31	13.13	20.91

[1]Millions of years, the surface SED value in bold is the input parameter

Sensitivity tests

To investigate which of the input or derived parameters have the greatest effect on the target hazard parameters of rupture recurrence and associated earthquake magnitude, a series of sensitivity tests of the probabilistic model was carried out. For each sensitivity test the effect on mean recurrence interval is listed in Table 6.

In the section "Derivation of fault parameters and earthquake size from fault offset" we discussed the partitioning of moment rate between strike-slip and dip-slip structures in the Sydney Basin. For the preferred model, the majority of the moment rate was released on strike-slip structures. To put all the moment release on dip-slip structures is not a realistic option because strike-slip structures are largest in the region and in some cases also show signs of reactivation. The strike-slip structures are also well-oriented to slip in the current regional east-west compressive stress field. As a sensitivity test then, we put equal amounts of moment release on the strike-slip and dip-slip structures. The result is to significantly shorten the mean recurrence interval of surface rupture compared to the preferred model (Table 6), although the mean recurrence interval is still very long. The resulting mean recurrence interval distribution has been to move the distribution towards shorter recurrence intervals rather than change its shape. There is no effect on the magnitude distribution.

In the section "Derivation of fault parameters and earthquake size from fault offset" we discussed the partitioning of moment rate between the dip-slip structures in the Sydney Basin to obtain the slip rate of a reactivated fault. For the preferred model, slip was partitioned according to a mix of the fault density of reactivated reverse structures, and of all of the dip-slip faults. As a sensitivity test we used a fault density appropriate to just the logged reactivated reverse structures. This is quite an extreme test because faults are only logged as being reactivated if they have net reverse displacement. The resulting recurrence interval distribution is shortened by about a factor of 3, and the distribution is much more peaked. There is no effect on the magnitude distribution.

Table 6 Results of sensitivity tests on mean recurrence interval

	MEAN RECURRENCE INTERVAL (MA)			
	84%	**MEDIAN**	**MEAN**	**16%**
Preferred model	0.53	3.31	13.13	20.91
Equal moment rate on strike-slip and dip-slip structures	0.15	0.84	2.68	4.60
Moment rate distributed over only reactivated structures	0.19	0.72	1.46	2.41
Maximum allowable fault length 10 km	0.48	2.99	10.91	17.78
Maximum allowable fault length 18 km	0.53	3.52	14.01	22.42
Maximum magnitude 7.3	0.68	4.26	16.50	26.77
Maximum magnitude 7.7	0.40	2.57	10.48	16.43
10 bar scaling relation	0.17	0.98	3.54	5.77

In the section "Derivation of fault parameters and earthquake size from fault offset" we used a limit on maximum allowable rupture length to in turn limit the range of possible results from the probabilistic model. The preferred model allowed only 50% of rupture lengths in the 10–18 km range to be used and none greater than that. We have run two sensitivity tests on the rupture length limit, in the first allowing any rupture lengths less than 10 km and in the second allowing any rupture lengths less than 18 km. The effect on mean recurrence interval is small compared to the previous sensitivity tests (Table 6). The effect of allowing longer ruptures is to extend the tail of the mean recurrence interval distribution on the long recurrence side.

In the section "Derivation of fault parameters and earthquake size from fault offset" we used a maximum magnitude of 7.5±0.19 for the region to calculate moment release rate using the a- and b-values derived from historical seismicity. We have tested the sensitivity to this parameter by running models with the maximum magnitude set at 7.3 and 7.7 (a 1-sigma range). The results (Table 6) show only slight sensitivity to this parameter, with the effect being to move the distribution of mean recurrence intervals to shorter values if a larger maximum magnitude for the region is allowed. There is no effect on the shape of the distribution. The distribution of mean magnitudes is unaffected because that is derived from the SED distribution, not historical seismicity.

In the section "New fault data in the Sydney Basin" we chose two appropriate earthquake scaling relations to derive rupture length and magnitude from displacement. These relations encompassed the likely range of static stress drops expected for the Sydney Basin region, namely high values (in excess of 100 bars) expected in continental regions such as continental Australia and Eastern North America, and moderate values (~60 bars) derived from crustal New Zealand earthquakes in regions of low to moderate slip rate. Both of these relationships were derived using modern waveform modelling techniques. Before the advent of waveform modelling, some researchers attempted to estimate rupture lengths, and hence static stress drops, using aftershock distributions. This approach is now known to overestimate rupture length and underestimate stress drop. For example, stress drop values of ~10 bars have been determined in this way for continental Australia (Denham *et al.*, 1981; Mumme, 1984). We have used a 10 bar scaling relation in a sensitivity test. The results for this model (Table 6) show a significant shortening of mean recurrence interval, but there is little change in the shape of the distribution. The mean recurrence intervals are still long, even with this extreme test. The effect on the mean magnitude distribution is more marked with generally higher magnitude values (about half a magnitude unit) and a more sharply peaked distribution.

Summary of sensitivity analysis

The sensitivity tests show that the way in which moment rate is partitioned between strike-slip and dip-slip structures and how it is distributed over the dip-slip structures will have a direct effect on the mean recurrence intervals for surface rupture on any particular fault. However, in our tests of

these models mean recurrence intervals remain long. The parameters of allowable fault length and maximum magnitude have much less effect on the estimation of mean recurrence intervals than the partitioning and distribution of moment release rate. If extremely low values of stress drop were used in deriving scaling relations, mean recurrence intervals would be shortened significantly. Given that low published values of stress drop were derived some decades ago using a method that is now known to have some shortcomings, and more recent seismological data has been used to derive a high stress drop for a continental Australian earthquake, we do not consider a 10 bar stress drop option as viable.

CONCLUSIONS

The main conclusions as a result of this study are:

New data on the extent and density of faulting in the 20-30 km wide coastal part of the Sydney Basin has been obtained from coalfield and tunnel log data show that the region is divided by northwest-trending strike-slip faults. These are the largest structures and are thus assumed to be dominant. Between these faults there is a pervasive distribution of north- to northeast-trending dip-slip faults, most of which have net normal displacements. Distributed among the normal faults are some faults with net reverse displacements which we interpret as having sustained reverse faulting since a mid Tertiary inception of an approximately east-west compressive stress field across Australia.

By developing some fault scaling relations and linking these with the seismic moment release rate manifest as historic seismicity in the Sydney region a relationship between fault geology and seismicity has been achieved. This has been completed in a probabilistic framework such that uncertainty and sensitivity to model parameters can be assessed.

Two self-similar scaling relations have been adopted that embrace the likely range of stress drops expected for earthquakes in the Sydney Basin region. These relations are based on seismological data from low slip rate Eastern North America and low-to-moderate slip rate regions in New Zealand.

The outputs of the probabilistic modelling are mean and standard deviation recurrence intervals for surface rupture on the north- to northeast-striking reactivated faults and their associated earthquake magnitude. The mean recurrence interval is most sensitive to the way in which moment release rate is partitioned between strike-slip and dip-slip structures and the way in which moment rate is distributed over the dip-slip structures. In constructing the logic tree we have been careful to embrace the full range of likely values for these parameters so that the output distribution accurately reflects the uncertainty in knowledge.

The preferred result from the logic tree output is a recurrence interval for surface rupture of faults in the north- to northeast-striking array of 13 +7/-12 million years for the mean and one standard deviation range. The earthquakes associated with this faulting have magnitudes of $M_w5.5\pm0.5$ for the mean and one standard deviation range.

ACKNOWLEDGEMENTS

Norm Abrahamson, Paul Somerville, Dougal Townsend, & Russ Van Dissen were contributors to the project that this paper has been derived from. Keith Simpson and Peter Volk of Coffey Geosciences Pty Limited provided the Sydney Basin tunnel log data. John Shepherd of Shepherd Mining Geotechnics kindly provided information and personal observations on the Southern

Coalfield. Robert Langridge and Pilar Villamor provided useful review comments, and Carolyn Hume and Philip Carthew assisted with the production of the figures.

REFERENCES

Aki, K. & P. G. Richards (1980). *Quantitative Seismology: Theory and Methods*. W. H. Freeman, San Francisco, California.

Anderson, H., T. Webb, & J. Jackson (1993). Focal mechanisms of large earthquakes in the South Island of New Zealand, implications for the accommodation of Pacific-Australia plate motion. *Geophys. J. Int.*, 115, 1032–1054.

Berryman, K & M. Stirling (2003). Earthquake ground motions and fault hazard studies at the Lucas Heights research reactor facility, Sydney, Australia: evolution of methods and changes in results. Proceedings of International Symposium on Seismic Evaluation of Existing Nuclear Facilities, Vienna, Austria, 25-29 August 2003. IAEA-CN-106 publication.

Branagan, D. F., Mills, K. J., & A.R. Norman (1988). Sydney faults; facts and fantasies. *22nd Newcastle symposium on Advances in the study of the Sydney Basin, Newcastle, N.S.W., Australia, Apr. 15-17, 1988*; pp 111-118..

Cohn, S. N., T.-L. Hong, & D. V. Helmberger (1982). The Oroville earthquakes: A study of source characteristics and site effects. *J. Geophys. Res.,* 87, 4585–4594.

Crone, A. J., M. N. Machette, & J. R. Bowman (1992). Geologic investigations of the 1968 Tennant Creek, Australia, earthquakes — implications for paleoseismology in stable continental regions. *U. S. G. S. Surv. Bull.*, 2032-A, 51p.

Denham, D. (1980). The 1961 Robertson earthquake — more evidence for compressive stress in southeast Australia. *BMR J. Aust. Geol. & Geophys.*, 5, 153–156.

Denham D., J. Weekes, & C. Krayshek (1981). Earthquake evidence for compressive stress in the southeast Australian crust. *J. Geol. Soc. Aust.*, 28, 323–332.

Denham, D., L. G. Alexander, I. B. Everingham, P. J. Gregson, R. McCaffrey, & J. R. Enever (1987). The 1979 Cadoux earthquake and intraplate stress in Western Australia. *Aust. J. Earth Sci.*, 34, 507–521.

Doser, D. I., T. H. Webb, & D. E. Maunder (1999). Source parameters of historic (1918–1962) earthquakes, South Island, New Zealand. *Geophys. J. Int.* 139, 769–794.

Doser, D. I. & T. H. Webb (2002). Source parameters of large historical (1917–1961) earthquakes, North Island, New Zealand. *Geophys. J. Int.* (submitted).

Gordon, F. R. & J. D. Lewis (1980). The Meckering and Calingiri earthquakes October 1968 and March 1970. *Geol. Surv. W. Austr. Bull.*, 126, 133p.

Hecker, S. & N. Abrahamson (2002). Characteristic fault rupture: Implications for fault rupture hazard analysis. *PEER Lifelines Research Meeting* (notes).

Herbert, C. (1980). Depositional development of the Sydney basin. *In* Herbert, C & Helby, R. (editors). A guide to the Sydney basin. *Dept of Mineral Resources, Geological Survey of New South Wales, bulletin 26,* pp. 10-53.

Herbert, C. & R. Helby (editors) (1980). A guide to the Sydney basin. Dept of Mineral Resources, Geological Survey of New South Wales, bulletin 26.

Hillis, R.R., Enever, J.R., & S.D. Reynolds (1999). In situ stress field of eastern Australia. *Australian Journal of Earth Sciences* 46, 813-825.

Johnson, A. M., R. W. Fleming, & K. M. Cruikshank (1994). Shear zones formed along long, straight traces of fault zones during the 28 June 1992 Landers, California, earthquake. *Bull. Seism. Soc. Am.*, 84, 499–510.

Kanamori, H. (1977). The energy release in great earthquakes. *J. Geophys. Res.* 82, 2981–2987.

Kanamori, H. & C. R. Allen (1986). Earthquake repeat time and average stress drop. *Earthquake Source Mechanics,* S. Das, J. Boatwright, & C. Scholz (Editors). *American Geophysical Monograph* 37, 227–235.

King, G. C. P., R. S. Stein, & J. Lin (1994). Static stress changes and the triggering of earthquakes. Bull. Seism. Soc. Am., 84, 935–953.

Langston, C. A. (1987). Depth of faulting during the 1968 Meckering, Australia, earthquake sequence determined from waveform analysis of local seismograms. *J. Geophys. Res.*, 92, 11,561–11,574.

Lewis, J. D., N. A. Daetwyler, J. A. Bunting, & J.S. Moncrieff (1981). The Cadoux earthquake, 2nd June 1979. *Geol. Surv. W. Aust. Report*, 11, 133pp.

Lohe, E. M., McLennan, T. P. T., Sullivan, T. D., Soole, K. P., & C.W. Mallett (1992). Sydney Basin – Geological Structure and Mining Conditions, assessment for Mine Planning. CRSIRO division of Geomechanics, External Report 20.

McGuire, J. J., L. Zhao, & T. H. Jordan (2002). Predominance of unilateral rupture for a global catalogue of large earthquakes. *Bull. Seism. Soc. Am*. (submitted).

Machette, M. N., A. J. Crone, & J. R. Bowman (1993). Geologic investigations of the 1986 Marryat Creek, Australia, earthquakes — implications for palaeoseismicity in stable continental regions. *U. S. G. S. Bull.* 2032-B, 29pp.

Mauger, J.; Creasey, J.W.; & J.F. Huntington (1984). Extracts and notes on the Katoomba 1:100,000 Sheet, Sydney basin fracture analysis. CSIRO Division *of Mineral Physics.*

Mohammadioun, B. & L. Serva (2001). Stress drop, slip type, earthquake magnitude, and seismic hazard. *Bull. Seism. Soc. Am.*, 91, 694–707.

Mumme, I. A. (1984). The role of geological faulting in south-east Australia, and its bearing on the seismicity of the region. *Geol. Soc. Aust.*, 12, 389–391 (abstract).

Ollier, C.D. (1982). The great escarpment of eastern Australia: tectonic and geomorphic significance. *Journal of the Geological Society of Australia 29:* 13-23.

Scholz, C. H. (1982). Scaling laws for large earthquakes: Consequences for physical models. *Bull. Seism. Soc. Am*., 72, 1–14.

Scholz, C. H., C. A. Aviles, & S. G. Wesnousky (1986). Scaling differences between large interplate and intraplate earthquakes. *Bull. Seism. Soc. Am*., 76, 65–70.

Shaw, R.D. (1978). Sea floor spreading in the Tasman Sea: a Lord Howe Rise-eastern Australian reconstruction. *Bulletin of the Australian Society of Exploration Geophysicists 9:* 75-81.

Sherwin, L., & G.G. Holme (1986). Geology of the Wollongong and Port Hacking 1:100,000 Sheets 9029, 9129 Geological Survey of New South Wales Department of Mineral Resources.

Shimazaki, K. (1986). Small and large earthquakes: the effects of the thickness of the seismogenic layer and the free surface. *Earthquake Source Mechanics,* S. Das, J. Boatwright, and C. Scholz (Editors). *American Geophysical Monograph* 37, 209–216.

Somerville, P. G., J. P. McLaren, L. V. Le Fevre, R. W. Burger, & D. V. Helmberger (1987). Comparison of scaling relations of eastern and western North American earthquakes. *Bull. Seism. Soc. Am.,* 77, 322–346.

Somerville, P., K. Irikura, R. Graves, S. Sawada, D. Wald, N. Abrahamson, Y. Iwasaki, T. Kagawa, N. Smith, & A. Kowada (1999). Characterising crustal earthquake slip models for the prediction of strong ground motion. *Seis. Res. Let.,* 70, 59–80.

Stirling, M. W., D. Rhoades, & K. R. Berryman (2002). Comparison of earthquake scaling relations derived from data of the instrumental and pre-instrumental eras. *Bull. Seism. Soc. Am.* (in press).

Townend, J. & M. D. Zoback (2000). How faulting keeps the crust strong. *Geology*, 28, 399–402.

Tregoning, P. (2002). Plate kinematics in the western Pacific derived from geodetic observations. *J. Geophys. Res.*, 107, ECV 7-1–7-8.

Vogfjord, K. S. & C. A. Langston (1987). The Meckering earthquake of 14 October 1968: A possible downward propagating rupture. *Bull. Seism. Soc. Am.*, 77, 1558–1578.

Webb, T. H. & H. J. Anderson (1998). Focal mechanisms of large earthquakes in the North Island of New Zealand: slip partitioning at an oblique active margin. *Geophys. J. Int.*, 134, 40–86.

Wells, D.L. & K. J. Coppersmith (1994). New empirical relationships among magnitude, rupture length, rupture width, rupture area, and surface displacement. *Bull. Seism. Soc. Am.*, 84, 974–1002.

Zoback, M. D. & J. Townend (2001). Implications of hydrostatic pore pressures and high crustal strength for the deformation of intraplate lithosphere. *Tectonophysics*, 336, 19–30.

Ground motions in Sydney from an Earthquake on the Lapstone Structure

PAUL SOMERVILLE*,# AND ROBERT GRAVES*
*Pasadena Office, URS Corporation
Tel: 626-449-7650, Email: paul_somerville@urscorp.com
Deputy Director, Risk Frontiers
Tel: 02-9850-4416, Email: psomervi@els.mq.edu.au

INTRODUCTION

The Lapstone Structure is thought to be a north-striking fault that dips westward at a shallow angle. If an earthquake were to occur on this structure, the ground motions in the Sydney basin are expected to be stronger than predicted by empirical ground motion attenuation relations, due to two effects. First, rupture on the fault would be expected to occur at depth, and propagate up dip on the fault. This updip and easterly rupture propagation would focus energy toward the east into the Sydney basin, due to the rupture directivity effect. Second, this energy would become trapped within the thickening western margin of the Sydney basin, causing further amplification of the ground shaking level in the Sydney basin. We have used earthquakes in the Los Angeles region of California to illustrate the potential impact of these two effects on strong ground motion amplitudes.

RUPTURE DIRECTIVITY EFFECT

An earthquake is a shear dislocation that begins at a point on a fault and spreads at a velocity that is almost as large as the shear wave velocity. The propagation of fault rupture toward a site at a velocity close to the shear wave velocity causes most of the seismic energy from the rupture to arrive in a single large pulse of motion that occurs at the beginning of the record (Somerville et al., 1997). This pulse of motion represents the cumulative effect of almost all of the seismic radiation from the fault. The radiation pattern of the shear dislocation on the fault causes this large pulse of motion to be oriented in the direction perpendicular to the fault, causing the strike-normal ground motions to be larger than the strike-parallel ground motions at periods longer than about 0.5 seconds. To accurately characterize near fault ground motions, it is therefore necessary to specify separate response spectra and time histories for the fault-normal and fault-parallel components of ground motion.

Forward rupture directivity effects occur when two conditions are met: the rupture front propagates toward the site, and the direction of slip on the fault is aligned with the site. The conditions for generating forward rupture directivity effects are readily met in strike-slip faulting, where the rupture propagates horizontally along strike either unilaterally or bilaterally, and the fault slip direction is oriented horizontally in the direction along the strike of the fault. The conditions required for forward directivity are also met in dip slip faulting. The alignment of both the rupture direction and the slip direction updip on the fault plane produces rupture directivity effects at sites located around the surface exposure of the fault (or its updip projection if it does not break the surface).

Rupture directivity effects were clearly evident in the strong motion recordings of the 1994 Northridge, California earthquake, as illustrated in Figure 1. The top part of the figure shows the surface projection of the dipping fault plane, whose top edge (to the north) lies at a depth of 6 km and whose bottom edge (to the south) lies at a depth of 20 km. Rupture propagated updip from the hypocenter, shown by a star, which was located near the bottom edge of the fault. The recorded peak ground velocities were much larger over the top edge of the fault than above the epicentral

region, due to rupture directivity effects. Rupture directivity caused the largest intensities to occur to the north of the epicenter, shown by a star, as shown in the bottom figure.

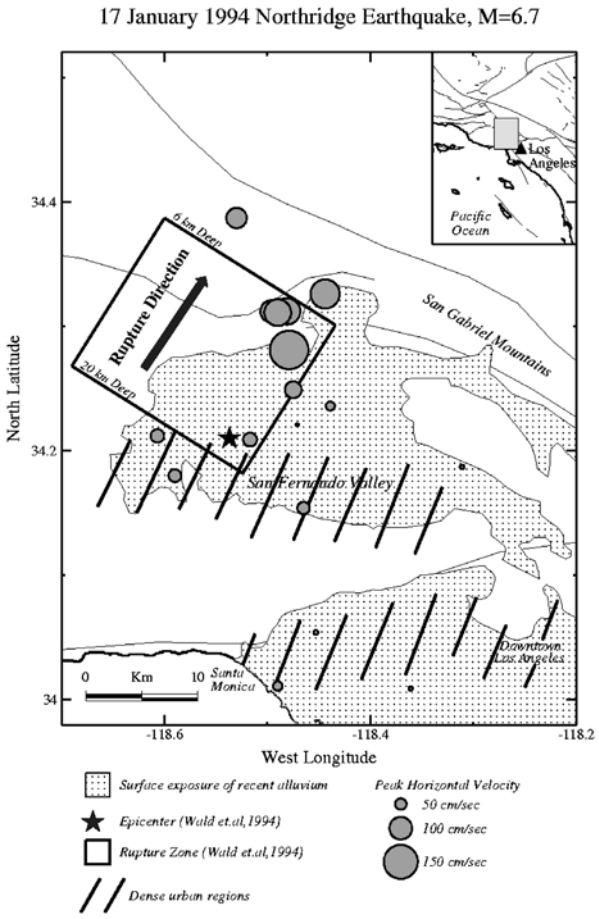

Figure 1. *Rupture directivity in the 1994 Northridge earthquake. Right: Surface projection of fault plane and recorded peak ground velocities. Below: Instrumental intensity map. (Source: TriNet). In both maps, the epicenter is shown by a star.*

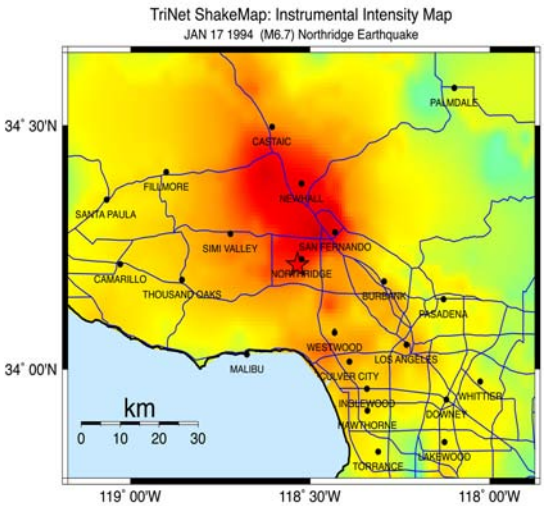

PERCEIVED SHAKING	Not felt	Weak	Light	Moderate	Strong	Very strong	Severe	Violent	Extreme
POTENTIAL DAMAGE	none	none	none	Very light	Light	Moderate	Moderate/Heavy	Heavy	Very Heavy
PEAK ACC.(%g)	*<.17*	*.17-1.4*	*1.4-3.9*	*3.9-9.2*	*9.2-18*	18-34	34-65	65-124	>124
PEAK VEL. (cm/s)	<0.1	0.1-1.1	1.1-3.4	3.4-8.1	8.1-16	*16-31*	*31-60*	*60-116*	*>116*
INSTRUMENTAL INTENSITY	I	II-III	IV	V	VI	VII	VIII	IX	X+

BASIN GENERATED WAVES

Many urban regions are situated on deep sediment-filled basins. A basin consists of alluvial deposits and sedimentary rocks that are geologically younger and have lower seismic wave velocities than the underlying rocks upon which they have been deposited. Basins have thicknesses ranging from a hundred meters to over ten kilometers. Conventional criteria for characterizing site response are typically based on the distribution of shear wave velocity with depth in the upper 30 meters as determined from field measurements. The response of this soil layer is usually modeled assuming horizontal layering, following the method illustrated on the left of Figure 2. The wave that enters the layer may resonate in the layer but cannot become trapped within the layer.

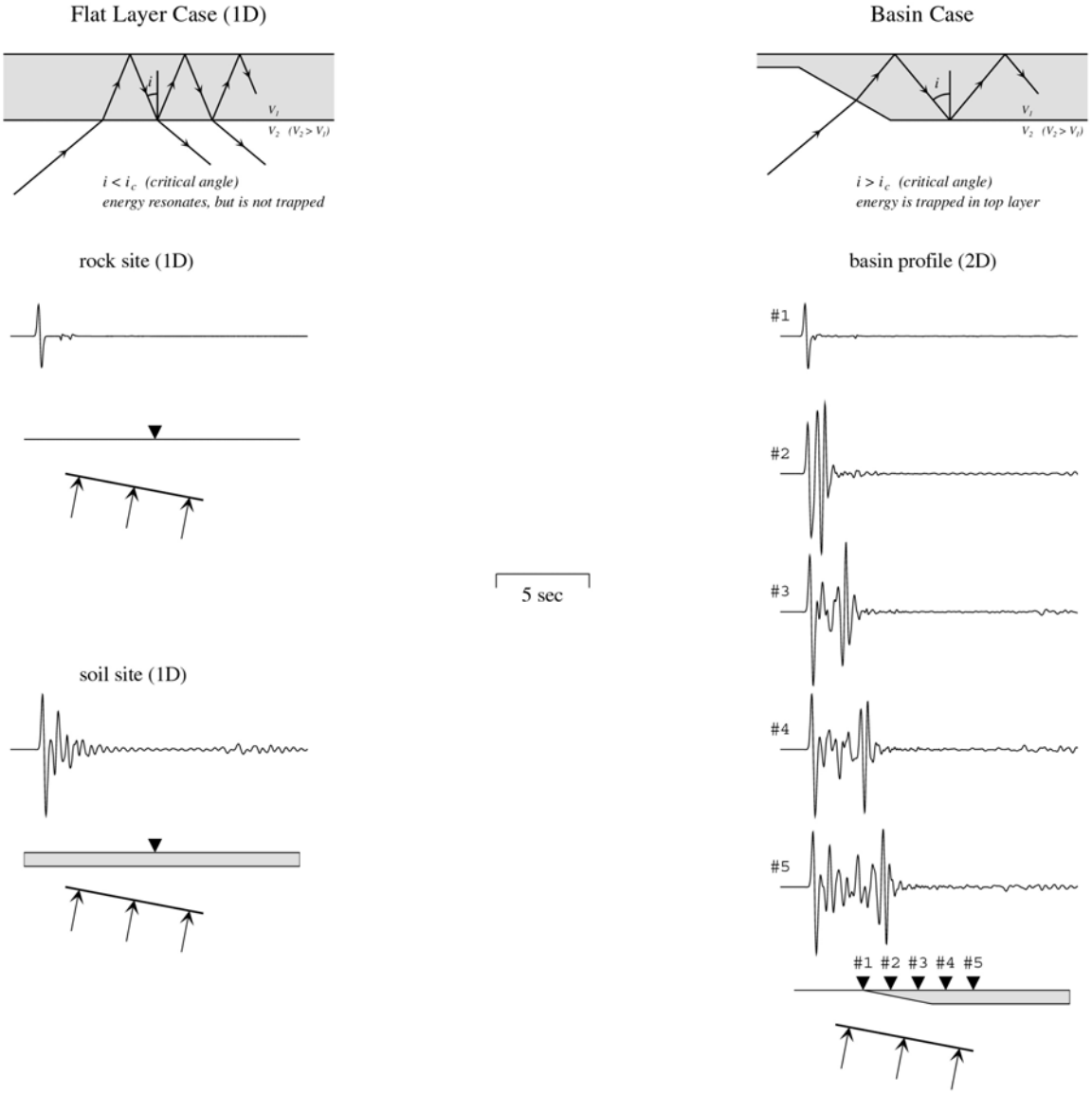

***Figure 2**. Schematic diagram showing that seismic waves entering a sedimentary layer from below will resonate within the layer but escape if the layer is flat (left) but become trapped in the layer if it has varying thickness and the waves enter it through its edge (right).*

However, at periods longer than one second, seismic waves have wavelengths that are much longer than 30 meters, and their amplitudes are controlled by geological structure having depths of hundreds or thousands of meters which in many cases, such as in sedimentary basins, is not horizontally layered. If the wave enters a basin through its edge, it can become trapped within the basin if post-critical incidence angles develop. The resulting total internal reflection at the base of the layer is illustrated at the top right of Figure 2. In the lower part of Figure 2, simple calculations of the basin response are compared with those for the simple horizontal layered model. In each case, a plane wave is incident at an inclined angle from below. The left side of the figure shows the amplification due to impedance contrast effects that occurs on a flat soil layer overlying rock (bottom) relative to the rock response (top). A similar amplification effect is shown for the basin case on the right side of the figure. However, in addition to this amplification, the body wave entering the edge of the basin becomes trapped, generating a surface wave that propagates across the basin. Most empirical ground motion attenuation relations do not distinguish between sites located on shallow alluvium and those in deep sedimentary basins, and tend to underestimate basin ground motions.

Recent work by Dolan et al. (2003) and Shaw et al. (2002) have identified the seismic potential of the Puente Hills Blind Thrust Fault system, which lies directly beneath downtown Los Angeles (Figure 3). The M_w 6.0 Whittier Narrows earthquake of 1987 evidently occurred on a segment of the Puente Hills Blind Thrust. The intensity distribution of this earthquake, shown in Figure 4, is dominated by strong intensity values south-southwest of the epicenter, due to the combined effects of rupture directivity to the south, and the trapping of this energy by the thickening Los Angeles basin.

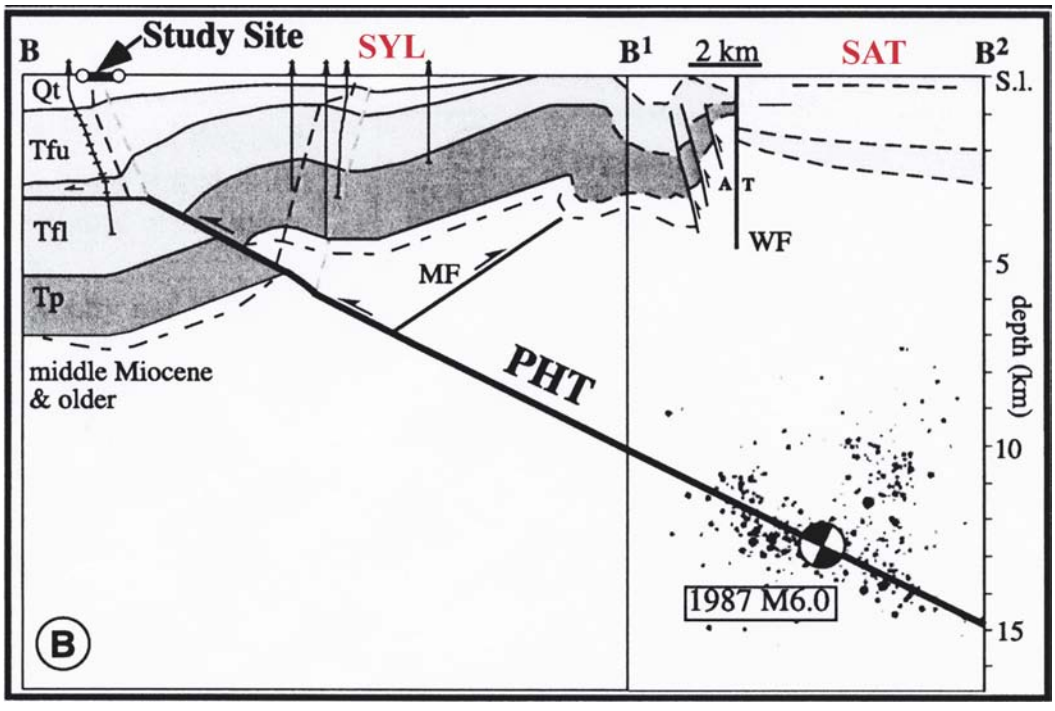

Figure 3. *South – North (B-B^2) cross section showing the Puente Hills blind thrust and the location of the 1987 Whittier Narrows earthquake. Downtown Los Angeles is located near "SYL." Source: Shaw et al., 2002.*

The rupture dimensions of the Whittier Narrows earthquake were approximately 10 km x 10 km. To assess the potential ground shaking hazard posed by a larger earthquake on the Puente Hills system, we examined a scenario where a "Northridge-type" earthquake occurs on the Los Angeles segment of the Puente Hills system. The Los Angeles segment of the Puente Hills system shares many of the characteristics of the fault that ruptured during the 1994 Northridge earthquake. Both are blind thrust faults with similar dimensions (20 km by 25 km), both dip at moderate angles (40 deg. for Northridge, 28 deg. for Puente Hills), and both terminate a few kilometers below the Earth's surface (6 km for Northridge, 3 km for Puente Hills).

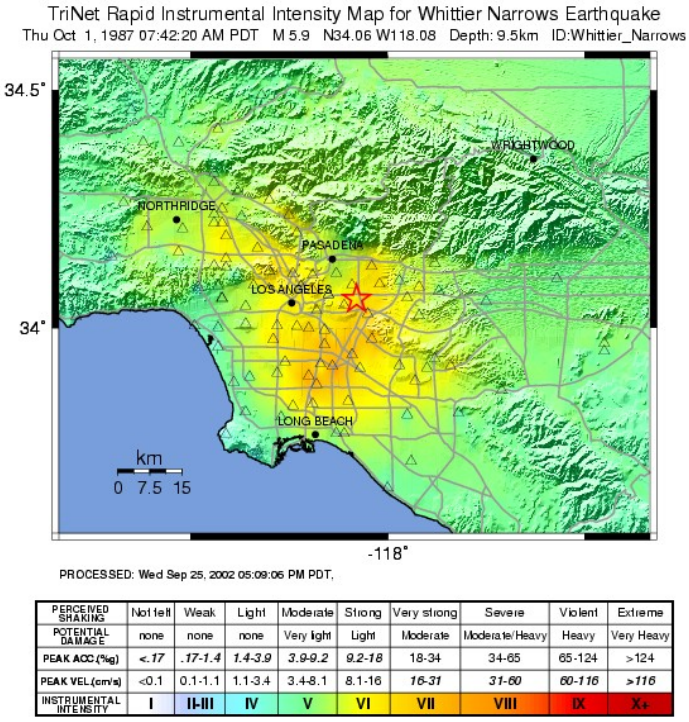

PERCEIVED SHAKING	Not felt	Weak	Light	Moderate	Strong	Very strong	Severe	Violent	Extreme
POTENTIAL DAMAGE	none	none	none	Very light	Light	Moderate	Moderate/Heavy	Heavy	Very Heavy
PEAK ACC.(%g)	*<.17*	*.17-1.4*	*1.4-3.9*	*3.9-9.2*	*9.2-18*	18-34	34-65	65-124	>124
PEAK VEL.(cm/s)	<0.1	0.1-1.1	1.1-3.4	3.4-8.1	8.1-16	*16-31*	*31-60*	*60-116*	*>116*
INSTRUMENTAL INTENSITY	I	II-III	IV	V	VI	VII	VIII	IX	X+

Figure 4. *Instrumental ground shaking intensity in the 1987 Whittier Narrows earthquake, whose epicenter is shown by a star. Source: TriNet.*

We calculated broadband (0-10 Hz) ground motions for this earthquake scenario using the hybrid simulation methodology of Graves and Pitarka (2004). The simulation covers an area 110 km by 150 km, which spans most of the greater Los Angeles metropolitan region. This region is divided into a uniform grid of sites with a spacing of 500 m, yielding a total of 66,000 sites. To obtain the full broadband response, the calculation is carried out independently in two frequency bands, and then summed together. At low frequencies ($f < 1$ Hz), motions are calculated deterministically using a finite-difference approach, which includes a detailed representation of the 3D subsurface structure throughout the model region. Nearly 400 million grid nodes are used to represent the FD model. The calculation is carried out on the HPCC Linux Cluster at USC and requires only about 8 hours to run using 120 CPU's. At high frequencies ($f > 1$ Hz), motions are calculated using a stochastic approach for each of the 66,000 locations. The model for earthquake rupture is taken from the description of the Northridge earthquake given by Hartzell et al. (1996).

The complexity of the propagating wave field is readily apparent in snapshots of the broadband (0-10 Hz) ground velocity simulated for the Puente Hills rupture scenario (Figure 5). Strong rupture

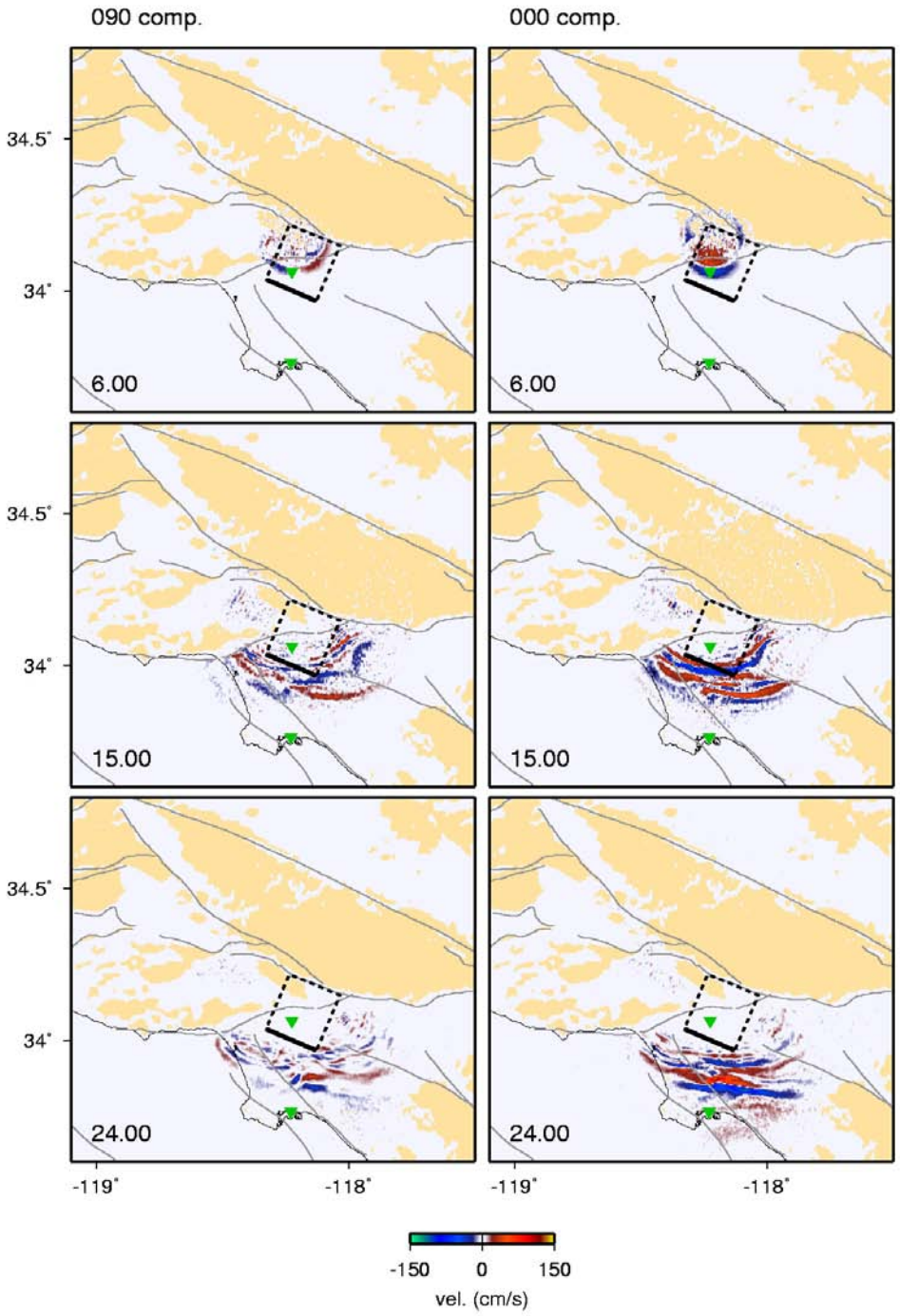

Figure 5: *Snapshots of the broadband (0-10 Hz) ground velocity for the N-S (left) and E-W (right) components of motion for the Puente Hills rupture scenario. Time (in sec) after earthquake initiation is indicated in the lower left of each panel. The black rectangle indicates the surface projection of the fault plane. Brown shading indicates surface exposure of more consolidated rock, white regions are primarily sediment filled basins. The green triangles denote locations for downtown Los Angeles (near top edge of fault) and Long Beach (south of fault). Strong rupture directivity channels large amplitude pulses of motion directly into the Los Angeles basin, which then propagate southward toward Long Beach as basin surface waves.*

directivity channels large amplitude pulses of motion directly into the Los Angeles basin, which then propagate southward as basin surface waves. This complexity is further apparent in comparing the broadband ground velocity time histories simulated at downtown Los Angeles and Long Beach (Figure 6). The waveform at Los Angeles is dominated by rupture directivity, which produces a strong, concentrated pulse of motion. At Long Beach, which is located across the Los Angeles basin from the rupture, the waveform is dominated by late arriving longer period surface waves. These surface waves are generated in the near fault region as the direct waves from the rupture are trapped within the sediments of the basin.

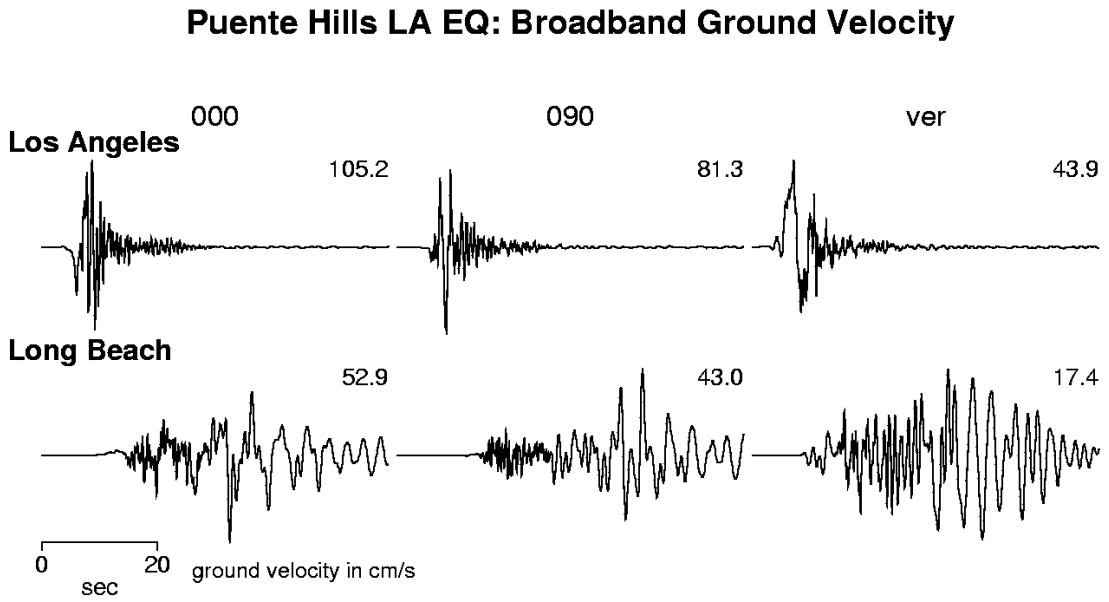

***Figure 6**: Broadband ground velocity time histories simulated at downtown Los Angeles (top) and Long Beach (bottom). The waveform at Los Angeles is dominated by rupture directivity, which produces a strong, concentrated pulse of motion. At Long Beach, which is located on the other side of the Los Angeles basin from the rupture, the ground motion is dominated by late arriving longer period surface waves. These surface waves are generated in the near fault region as the direct waves from the rupture are trapped within the sediments of the basin.*

The high density of sites used in the calculation allows us to construct detailed maps of various ground motion parameters. An example of this displays the peak ground velocity determined from the suite of simulated time histories (Figure 7). The largest motions occur along the top edge of the rupture plane, and are the result of rupture directivity effects. These strong pulses of motion are channeled directly into the sediments of the Los Angeles basin and become trapped as basin generated surface waves. These large amplitude surface waves travel southward across the basin, giving rise to an elongated pattern of elevated peak velocity that extends across the basin.

IMPLICATIONS FOR LAPSTONE EARTHQUAKE GROUND MOTIONS IN SYDNEY

The configuration of the Lapstone Structure and the Sydney Basin is equivalent to the configuration of the Puente Hills Blind Thrust and the Los Angeles Basin. Rotation of Figures 5 and 7 anticlockwise by about 110 degrees would orient the Los Angeles geometry to match the geometry in Sydney. The thick black line would represent the surface expression of the Lapstone Structure, and the dashed rectangular region to the left of this line would represent the surface projection of a Lapstone fault that dips to the west at a shallow angle. The region to the right of the thick black line

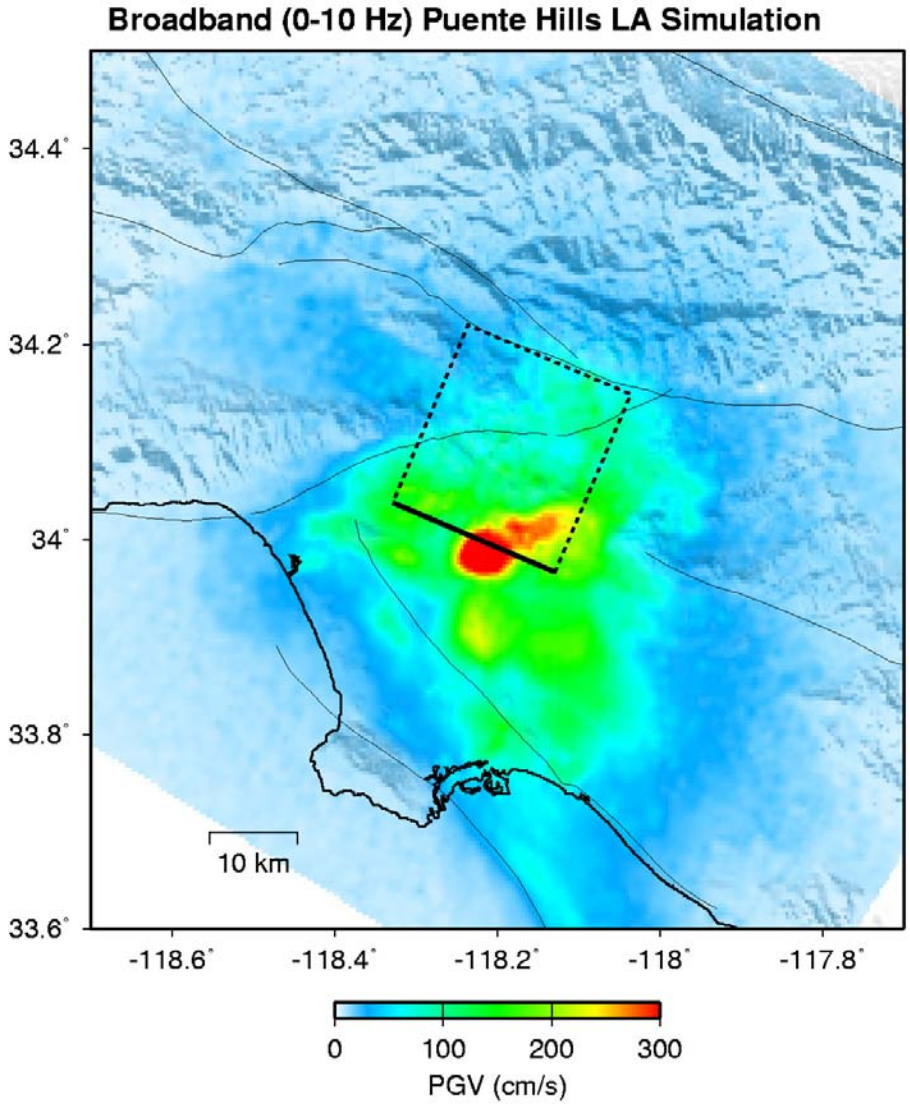

Figure 7: *Map of peak ground velocity from the broadband simulation of the Puente Hills rupture scenario. The largest simulated motions occur along the top edge of the rupture plane, and are the result of rupture directivity effects. These strong pulses of motion are channeled directly into the sediments of the Los Angeles basin and become trapped as basin generated surface waves. These large amplitude surface waves travel southward across the basin, giving rise to an elongated pattern of elevated PGV that extends across the basin. This pattern resembles the pattern of ground shaking intensity from the 1987 Whittier Narrows earthquake shown in Figure 4.*

would represent the Sydney Basin. Figures 5 and 7 show that the strongest ground motions would be located around the surface trace of the Lapstone structure, due to rupture directivity effects. They also show that there would be large ground motion amplitudes in the Sydney Basin, due to the trapping of these strong directivity pulses by the thickening edge of the Sydney Basin.

Particularly strong ground motion amplification can occur at the edge of a basin, if the basin has an abrupt edge caused by dip-slip faulting. The severe damage caused by the 1995 Kobe earthquake

occurred on the basin side of the fault, about 1 km from the fault that caused the earthquake. This narrow band of damage has been attributed to basin edge effects (Pitarka et al., 1998) caused by the abrupt change in depth to crystalline basement (about 1 km) that occurs across the fault. An abrupt increase in depth to bedrock across the Santa Monica fault caused a similar basin edge effect during the 1994 Northridge earthquake (Graves et al., 1998). If there is an abrupt increase in depth to bedrock across the Lapstone Structure, then it could cause basin edge amplification effects in a zone within a few km to the east of the Lapstone Structure.

REFERENCES

Dolan, J.F., S.A. Christofferson, and J.M. Shaw (2003). Recognition of paleoearthquakes on the Puente Hills Blind Thrust Fault, California. Science 300, 115-118.

Graves, R. and A. Pitarka (2004). Broadband time history simulation using a hybrid approach. Proceedings of the 13th World Conference on Earthquake Engineering, Vancouver, Canada, August 1-6, 2004, Paper No. 1098.

Graves, R. W., A. Pitarka, and P. G. Somerville (1998). Ground motion amplification in the Santa Monica area: effects of shallow basin edge structure, *Bull. Seism. Soc. Am.*, 88, 1224- 1242.

Graves, R.W. (1996). Simulating earthquake ground motions in 3D elastic media using staggered-grid finite-differences, *Bull. Seism. Soc. Am.* 86, 1091-1106.

Hartzell, S., Liu, P., Mendoza, C. (1996). The 1994 Northridge earthquake: investigation of rupture velocity, risetime, and high frequency radiation. J. Geophys. Res. 101, 20,091-20,108.

Pitarka, A., K. Irikura, T. Iwata and H. Sekiguchi (1998). Three-dimensional simulation of the near-fault ground motion for the 1995 Hyogo-ken Nanbu (Kobe), Japan, earthquake. *Bull. Seism. Soc. Am.*, 88, 428-440.

Shaw, J.H., A. Plesch, J.F. Dolan, T.L Pratt, and P. Fiore (2002). Puente Hills blind-thrust system, Los Angeles, California. Bull. Seism. Soc. Am. 92, 2946-2960.

Somerville, P.G., N.F. Smith, R.W. Graves, and N.A. Abrahamson (1997). Modification of empirical strong ground motion attenuation relations to include the amplitude and duration effects of rupture directivity, *Seismological Research Letters*, 68, 180-203.

Ground-motion attenuation modelling in southeastern Australia

TREVOR ALLEN, PHIL R. CUMMINS, TREVOR DHU
RISK RESEARCH GROUP, GEOSCIENCE AUSTRALIA

ABSTRACT

Ground-motion attenuation models have been derived for the southeastern Australian crust. These models employ both empirical and stochastic methods and are the first spectral ground-motion models to be based entirely on Australian ground-motion data. In the past, these studies have been hampered by a lack of quality ground-motion data given Australia's relatively low levels of seismicity.

Data recorded in the Palaeozoic crust of southeastern Australia (SEA) have been employed to derive empirical ground-motion attenuation models for the region. Empirical ground-motion models are derived for each of these datasets. These empirical models suggest that SEA has similar near-source attenuation with eastern North America for hypocentral distances less than 70 km.

Stochastic methods are employed to simulate ground-motions for larger earthquakes in regions where recordings from real events are not available. These models are largely based upon source and attenuation parameters derived from empirical studies. Spectral ground-motion predicted by these models are generally lower for SEA than ground-motion predicted by both eastern and western North American models, particularly at high-frequency (f > 2 Hz). Results from this study have significant implications for earthquake hazard and risk in Australia. They suggest that we are currently overestimating earthquake hazard in SEA. Furthermore, they suggest that we cannot simply rely on North American ground-motion models to predict earthquake ground-motions in Australia.

INTRODUCTION

It has long been recognised by engineers and seismologists alike, that the traditional measure of earthquake ground-motion, *peak ground acceleration* (PGA), is not a particularly good indicator for estimating structural damage (e.g. Hanks & McGuire, 1981). For this reason, frequency-dependent models are favoured to assess the degree of vulnerability a structure may be exposed to in earthquake hazard and risk studies. These models are referred to as *ground-motion attenuation models*.

Earthquake hazard and risk assessments in Australia typically adopt ground-motion models from other stable continental regions such as eastern North America (ENA) (e.g. Dhu and Jones, 2002; Jones *et al.*, 2005). However, there has been very little analysis undertaken to show whether ENA models (e.g. Atkinson & Boore, 1997; Toro *et al.*, 1997) are applicable to Australian conditions. Moreover, there has been some conjecture that ground-motion in some parts of Australia resembles that of active tectonic regions and may be better described by models such as Sadigh *et al.* (1997), developed for western North America (WNA). Uncertainties in the choice of attenuation model could potentially lead to undesirable outcomes, such as unrealistically high (or low) loading standards in the design and construction of critical infrastructure (e.g. large dams, power stations, hospitals, etc.). Furthermore, the choice of attenuation model has been demonstrated to have a significant impact on risk estimates in Australia (e.g. Patchett *et al.*, 2005).

Attenuation relations appropriate for the Australian crust have, in the past, been difficult to quantify owing to a lack of ground-motion data from moderate-to-large local earthquakes. Geoscience Australia (GA), in association with Environmental Systems and Services (ES&S) and the Australian National Committee on Large Dams (ANCOLD) have collaborated to assemble an Australian ground-motion database suitable for attenuation studies. The key focus of this project is to improve future earthquake hazard and risk assessments in Australia.

The present paper describes the development of the first spectral ground-motion attenuation models appropriate for the Australian crust. These models are based upon data recorded in the Palaeozoic crust of southeastern Australia (SEA) including some data recoded within younger the Sydney and Gippsland Basins.

AUSTRALIAN GROUND-MOTION DATA

Due to the development of much of the nation's infrastructure and higher than average earthquake activity, the seismograph network in SEA is well developed. Earthquake data used were recorded and located by the ES&S Seismology Research Centre, Melbourne, who have monitored earthquake activity in the region since the mid 1970's. Most of the earthquakes selected (80 in total) were well-located, having well-constrained focal depths. The events occurred from 1993 to 2004 and moment magnitudes range from $2.0 \leq \mathbf{M} \leq 4.7$. Data in this region has a good spatial distribution (to approximately 700 km) and comprises some 1220 ground-motion records.

EMPIRICAL GROUND-MOTION MODELS

The development of empirical ground-motion attenuation models for Australia largely follows the methods adopted by Atkinson (2004a) for ENA. Detailed analysis of the SEA dataset indicates that the decay of Fourier spectral amplitudes can be described by a trilinear geometrical attenuation model. The subsequent decay of spectral amplitudes can be approximated by the coefficient of $R^{-1.3}$ (where R is hypocentral distance) within 90 km of the seismic source. From 90 to 160 km, the SEA dataset indicates a zone whereby the seismic coda appear to be affected by crustal reflections and refractions. In this distance range, geometrical attenuation is approximately $R^{+0.1}$. Beyond 160 km, low-frequency seismic energy (i.e. f = 1 Hz) attenuates rapidly with R, having a geometrical attenuation coefficient of $R^{-1.6}$. Note that at present, we have not distinguished between attenuation models for Palaeozoic (e.g. Lachlan Fold Belt) and Mesozoic (e.g. Sydney and Gippsland Basins) crust, but rather have developed a combined ground-motion model. Developing models that describe the different geological terrains in southeastern Australia will be the scope of future work.

Fourier ground-motion models for SEA, WA (Allen *et al.*, in press) and ENA (Atkinson, 2004a,b) are compared for hypocentral distances at 1, 10, 50 and 100 km for an earthquake of **M** 4.5 (Figure 1). In general, we observe that SEA and ENA models are relatively consistent since the geometrical attenuation is the essentially the same over this distance range [geometrical attenuation for ENA is $R^{-1.3}$ for R < 70 km (Atkinson, 2004a)]. Owing to the higher geometrical attenuation observed in SEA for R > 70 km, the models differ considerably at larger distances (Figure 2). Low-frequency spectral amplitudes calculated for the WA model are observed to be significantly higher with increasing source-receiver distance than both SEA and ENA. Comparing spectral amplitude residuals (log observed less predicted) for the Atkinson's (2004a,b) ENA model further demonstrates the higher attenuation in SEA beyond the ENA postcritical distance of 70 km (Figure 3).

Given that we have no quality ground-motion records for earthquakes greater than **M** 4.7, these empirical models cannot be used directly to predict ground-motion for larger, potentially damaging

earthquakes. The source and attenuation coefficients evaluated in these studies, however, are used as key inputs to stochastic methods discussed below.

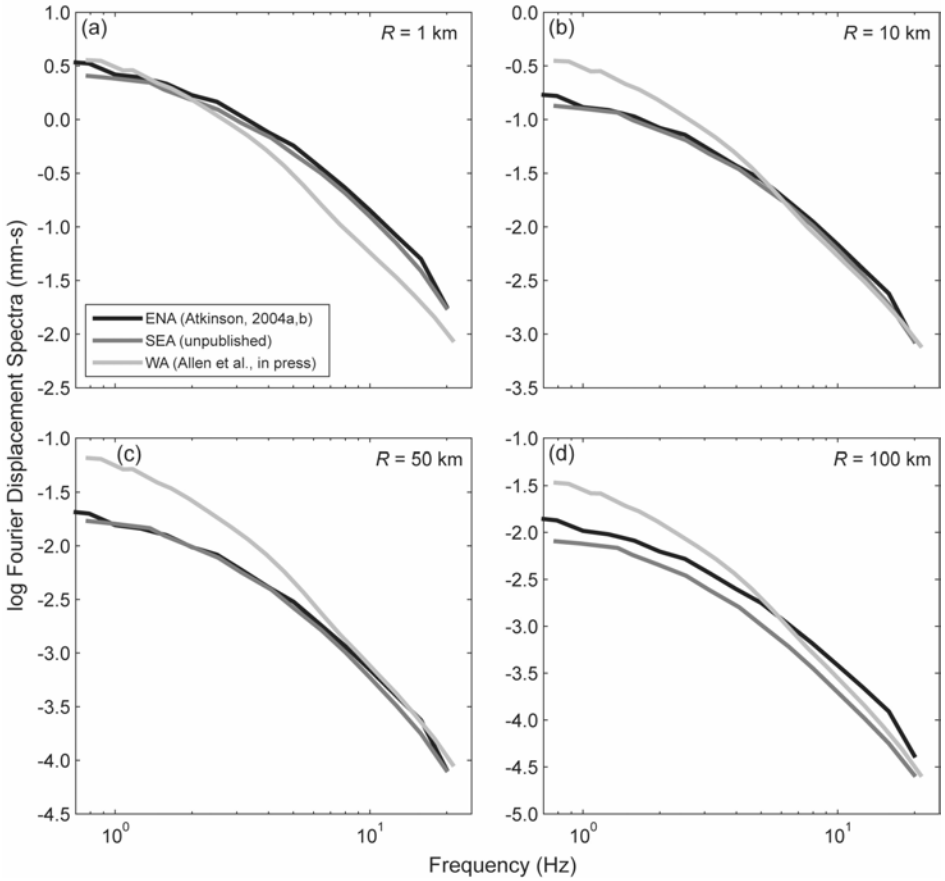

Figure 1: *Comparison of empirical Fourier displacement spectra at hypocentral distances of (a) 1, (b) 10, (c) 50 and (d) 100 km for an earthquake of **M** 4.5. Note that for all three models, source spectra (i.e. R = 1 km) converge at low-frequency indicating that estimates of M are consistent (a). In figures (b-d) we observe the effect of lower rates of attenuation in WA.*

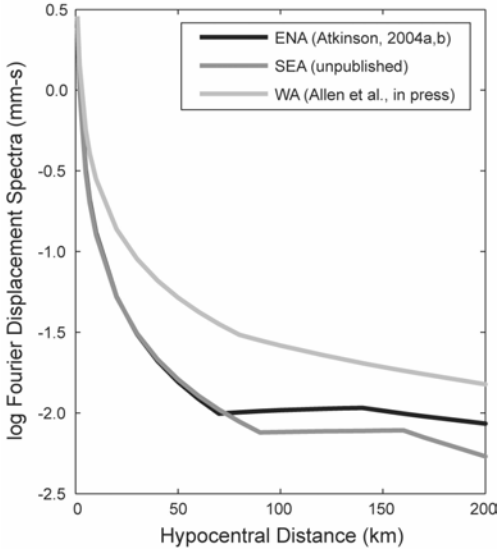

Figure 2: *Comparison of Fourier displacement spectra at a frequency of 1.0 Hz for hypocentral distances to 200 km for an earthquake of **M** 4.5. It can be observed that attenuation in SEA and ENA are very similar for R < 70 km. Beyond this distance we observe higher rates of ground-motion attenuation in SEA.*

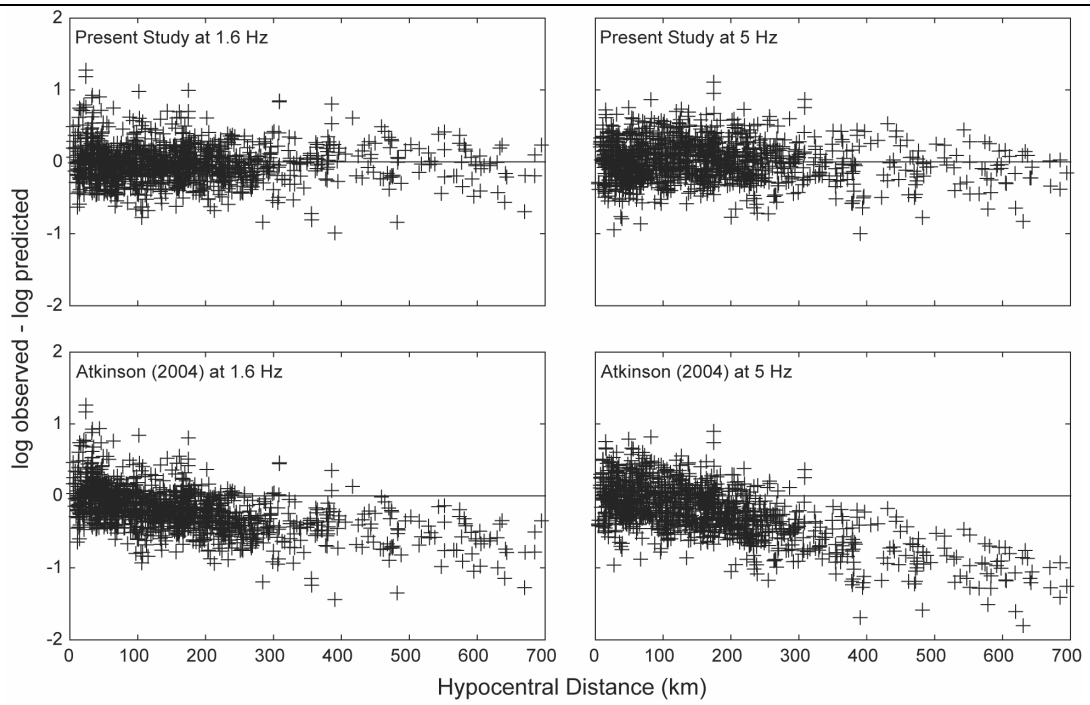

Figure 3: *Residuals of modelled SEA ground-motions plotted against hypocentral distance at 1.6 and 5 Hz. These data are compared with the Atkinson (2004a,b) attenuation model. At distances beyond the ENA postcritical distance of R = 70 km, the Atkinson (2004a,b) model overestimates ground-motions in southeastern Australia.*

STOCHASTIC GROUND-MOTION MODELS

The stochastic method is particularly useful for simulating earthquake ground-motions in regions of the world where recordings from large damaging earthquakes are simply not available (Hanks & McGuire, 1981; Boore, 2003). The method relies on an initial earthquake source model, based upon results from empirical studies.

We use software developed by Pacific Engineering & Analysis, El Cerrito, USA (Silva, 1987), to simulate ground-motions for a series of magnitude-distance bins. To accommodate uncertainty owing to the unpredictable nature of future events, model parameters are randomised about the base (mean) value a number of times for each magnitude-distance bin. For each randomisation, 5% damped Response Spectral Acceleration (RSA) are calculated. Subsequent regression analysis yields a stochastic ground-motion model that also incorporates estimates of uncertainty in the predicted ground-motion. Since the initial model parameters are based on ground-motion recordings on rock, our default attenuation model will be for rock sites.

Figure 4 shows the stochastic SEA rock ground-motion model compared to three North American models. Two of these were developed for the stable crust of ENA (Atkinson & Boore, 1997; Toro *et al*., 1997) and the other for seismically active Californian crust of WNA (Sadigh *et al*., 1997).

Near-source RSA indicate that the SEA rock ground-motion models have similar spectral shape to the Sadigh *et al.* (1997) model with low levels of high-frequency motion (and PGA) compared to the two ENA models (Figure 4a). As distance is increased from the source, we observe that all predictive attenuation models from North America overestimate ground-motion relative to the SEA model (Figures 4b-c), particularly at higher frequencies (f > 2 Hz). Two key points to consider is

that; 1) ground-motion in SEA appears to be consistently lower at almost all frequencies than in the highly deformed crust of WNA and; 2) low-frequency ground motion is similar to the Atkinson & Boore (1997) model near f = 1 Hz. This is of interest because empirical studies on both the ENA (Atkinson, 2004) and SEA datasets yield similar attenuation near 1 Hz (Figure 2).

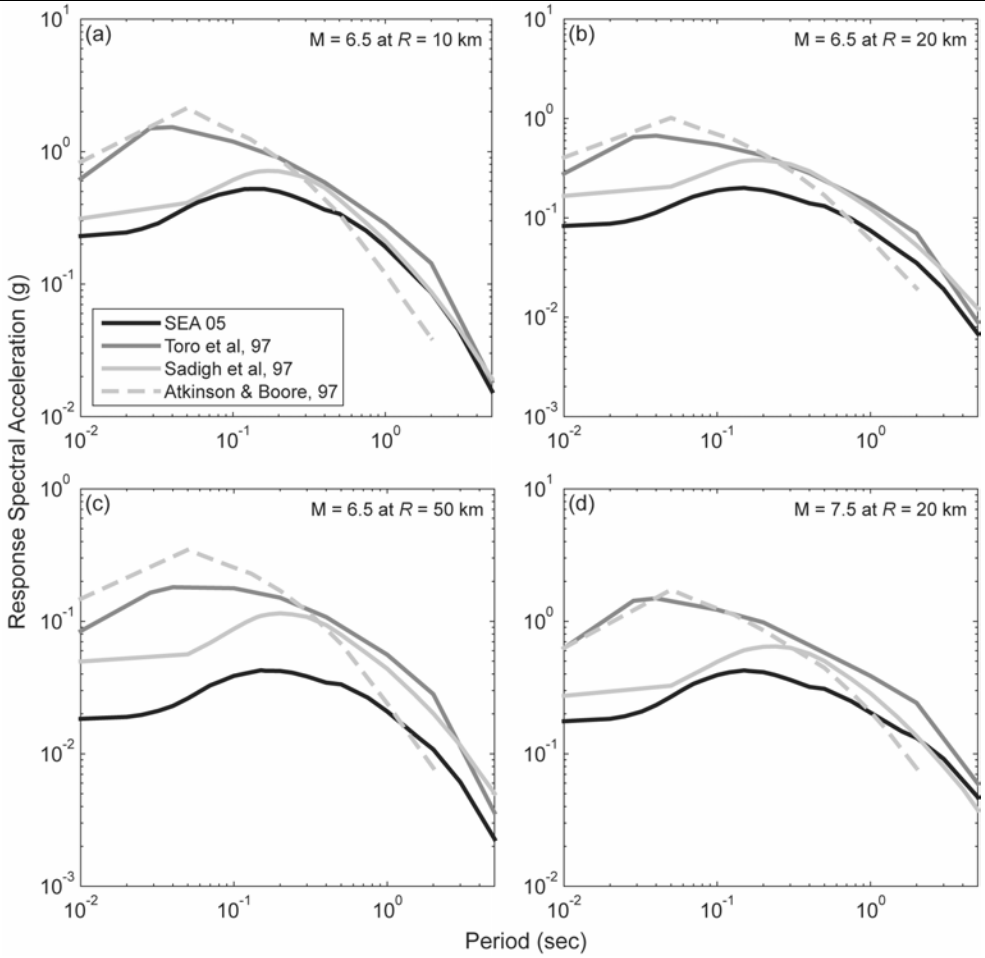

Figure 4: *Comparison of 5% damped RSA for the three North American ground-motion models and the stochastic SEA model. Near the seismic source (a), the SEA model is quite similar to the WNA model of Sadigh et al. (1997). With increased distance the SEA model appears to predict lower ground-motions at most frequencies greater than about 2 Hz. For lower frequencies, the SEA model similar to the North American models, particularly at shorter hypocentral distances. Each of the predictive spectral plots assume an earthquake focal depth of 8 km.*

IMPLICATIONS FOR EARTHQUAKE HAZARD

Results from the present study indicate that ground-motion attenuation in SEA is higher than previously assumed in many earthquake hazard and risk studies. Given earthquake hazard is defined as the probability of a certain level of ground-shaking being exceeded at a site within a certain time period, these results have a significant impact of the level of hazard that a structure may be exposed to. We suggest that earthquake hazard in SEA is currently being overestimated using current ground-motion relationships, particularly at frequencies greater than 1 Hz.

Although we have not been able to develop a reliable stochastic ground-motion model for WA at present owing to the anomalous nature of the WA dataset, results from empirical studies suggest that the attenuation of strong ground-shaking will be lower than in SEA. Consequently, we would expect to see larger ground-motions away from the fault rupture. Comparison of Fourier spectral models by Allen *et al.* (in press) indicate that at lower-frequency ground-motions ($f < 2$ Hz) attenuate less in WA than in ENA. In contrast, they observe lower levels in high-frequency motions relative to low-frequency motions. It may be that the use of current attenuation models actually underestimates hazard at low-frequencies in WA. Therefore, low-frequency ground-motions may be slightly higher than that of ENA models, but with diminished high-frequency motions. This is somewhat consistent to studies by Hao & Gaull (2004), who apply low-pass filters to ENA ground-motion models to fit observed ground-motion from WA.

CONCLUSIONS

This study presents the first ground-motion attenuation models that are appropriate for Australian crustal conditions. These empirical and stochastic models are based entirely on data recorded in Australia. We have not distinguished between attenuation models for Palaeozoic (e.g. Lachlan Fold Belt) and Mesozoic (e.g. Sydney and Gippsland Basins) crust, but rather have developed a combined ground-motion model for the whole of southeastern Australia. Developing models that describe the different geological terrains in the region will be the scope of future work.

Empirical attenuation models have been developed from two key datasets; one from WA and the other from SEA. In general we observe that ground-motion attenuates less in WA than in SEA, particularly at low frequencies. WA earthquakes, however, appear to have lower high-frequency motion relative to SEA earthquakes.

Given the difficulties associated in constraining reliable source and attenuation parameters for the WA dataset, development of stochastic ground-motion models concentrate on SEA rock sites. We observe that near the earthquake source, SEA RSA indicate similar spectral shape to the Sadigh *et al.* (1997) model developed for WNA with low levels of high-frequency motion (and PGA) compared to the two ENA models. As distance is increased from the source, we observe that all predictive attenuation models from North America overestimate ground-motion relative to the SEA model. These findings have significant implications for earthquake hazard and risk in this region. They suggest that by using North American ground-motion models, we are currently overestimating earthquake hazard in SEA. Consequently, we may be over-engineering infrastructure for strong ground-motion, particularly for frequencies greater than 2 Hz. More work is required to quantify these results, and also to develop useful models for both rock and soil sites. These models will provide a means to lower the uncertainty associated with Australian specific hazard and risk analyses.

ACKNOWLEDGEMENTS

The work detailed in this paper was done in collaboration, and with the financial support of the Australian National Committee on Large Dams (ANCOLD). We particularly acknowledge the efforts of Phil J. Cummins of ANCOLD, coupled with Wayne Peck and Gary Gibson of ES&S to gain support from Australian dam owners. We also thank Walt Silva and Nick Gregor of Pacific Engineering and Analysis for providing software and support for the development of the stochastic attenuation models.

REFERENCES

Allen, T.I., Dhu, T., Cummins, P.R. and Schneider, J.F. (in press). Empirical attenuation of ground-motion spectral amplitudes in southwestern Western Australia, *Bull. Seism. Soc. Am.*

Atkinson, G.M. 2004a. Empirical attenuation of ground-motion spectral amplitudes in southeastern Canada and the northeastern United States, *Bull. Seism. Soc. Am.* **94,** 1079-1095.

Atkinson, G.M. 2004b. Erratum to "Empirical attenuation of ground-motion spectral amplitudes in southeastern Canada and the northeastern United States", *Bull. Seism. Soc. Am.* **94,** 2419-2423.

Atkinson, G.M. and Boore, D.M. 1997. Some comparisons between recent ground-motion relations, *Seism. Res. Lett.* **68,** 24-30.

Boore, D.M. 2003. Simulation of ground motion using the stochastic method, *Pure Appl. Geophys.* **160,** 635-676.

Dentith, M.C., Dent, V.F. and Drummond, B.J. 2000. Deep crustal structure in the southwestern Yilgarn Craton Western Australia, *Tectonophys.* **325,** 227-255.

Dhu, T., and Jones, T. (Eds.) 2002. Earthquake risk in Newcastle and Lake Macquarie, *Geoscience Australia Record 2002/15*, Geoscience Australia, Canberra.

Hanks, T.C. and McGuire, R.K. 1981. The character of high-frequency strong ground motion, *Bull. Seism. Soc. Am.* **71,** 2071-2095.

Hao, H., and Gaull, B.A. 2004. Prediction of seismic ground-motion in Perth Western Australia for engineering application. *Proc 13th World Conf. Earthquake Eng.*, Vancouver.

Herrmann, R.B., and Kijko, A. 1983. Modeling some empirical vertical component Lg relations, *Bull. Seism. Soc. Am.* **73,** 157-171.

Jones, T., Middelmann M. and Corby, N. (Eds.) 2005. Natural hazard risk in Perth, Western Australia. 2005. Canberra, Geoscience Australia - Australian Government.

Patchett, A., Robinson, D., Dhu, T. and Sanabria, A. 2005. Investigating earthquake risk models and uncertainty in probabilistic seismic risk analyses, *Geoscience Australia Report 2005/02*, Geoscience Australia, Canberra.

Sadigh, K., Chang, C.Y., Egan, J.A., Makdisi, F. and Youngs R.R. 1997. Attenuation relationships for shallow crustal earthquakes based on California strong motion data, *Seism. Res. Lett.* **68,** 180-189.

Silva, W.J. 1987. State-of-the-art for assessing earthquake hazards in the United States; Report 24, WES RASCAL code for synthesizing earthquake ground-motions. *Department of the Army, US Army Corps of Engineers*, Washington.

Toro, G.R., Abrahamson, N.A. and Schneider, J.F. 1997. Engineering model of strong ground-motions from earthquakes in the Central and Eastern United States, *Seism. Res. Lett.* **68,** 41-57.

Landslides in the Sydney Basin: Is there a seismic link?

KERRIE M. TOMKINS, GEOFF S. HUMPHREYS, JOHN MACRIS AND PAUL P. HESSE
MACQUARIE UNIVERSITY, NORTH RYDE NSW 2109

ABSTRACT

Several large landslides have been found in the incised valleys of the Blue Mountains Plateau, located on the western margin of the Sydney Basin, where the valleys have cut into weaker strata of the Permian Shoalhaven Group. The landslides highlight the potential importance of mass movement processes in valley widening and hillslope denudation, yet the cause of failure in these valleys is unknown. The main triggers of landslides elsewhere (e.g. Europe, Asia and USA) are often earthquakes or severe rainfall events. In this paper we consider earthquakes as a possible trigger for the landslides and assess whether there is a seismic link between earthquakes and failure of the cliff lined upper slopes in the Blue Mountains Plateau. Seismic records for the Sydney Basin show a clustered distribution of earthquakes particularly in the south-west of the basin where several of the large pre-European landslides and smaller recent landslides have been found. The distribution of earthquakes and landslides indicates a possible seismic link. However, due to the difference in the time period of records (i.e. pre-European age of the older landslides versus the contemporary seismic record) and the impact of mining on the more recent landslides, we are not able to link earthquake events to failure. We suggest that the recorded earthquakes were not significant enough to trigger slope failure (maximum magnitude 5.6), but that the larger, older landslides may have been triggered by higher magnitude earthquake events.

Keywords: rock fall, dissection, landscape evolution, seismicity, Burragorang

INTRODUCTION

Examination of relief and geology maps of the Sydney Basin (Brunker and Rose, 1967; 1979) reveals several important features of the landscape: (i) a lower lying coastal sandstone plateau (Hornsby Plateau to the north and Woronora Plateau to the south) separated by a low relief basin on Wiannamatta Group shales (Cumberland Plain); (ii) a higher sandstone plateau to the west (Blue Mountains Plateau) bounded to the east by the Lapstone Structural Complex (LSC) (Branagan and Pedram, 1990); and (iii) deeply incised valleys that stem from the LSC to the west and south-west changing from narrow gorges to wide valleys upon intersecting the underlying Permian sediments.

The incised valleys of the Blue Mountains Plateau are the focus of this paper (Figure 1), especially those erosion processes that lead to valley widening once river incision has reached the Permian rocks. Recent investigations in the Nattai River valley, which drains into the Wollondilly River 55 km upstream of the LSC, suggests that valley widening, and presumably scarp retreat, is taking place by mass movement events, such as rock fall and debris flows (Tomkins *et al.*, 2004b). Previous mapping of the geology of the Wollondilly - Nattai area by McElroy and Relph (1958) indicates extensive areas of large scale surface slumping (landslides) but none of these have been confirmed. In contrast, landslides in Sydney Basin sediments have been identified along the Illawarra Escarpment near Wollongong where high relief coupled with high rainfall (1200 - 1500 mm a^{-1}) facilitates mass slope failure (Walker, 1963; Young, 1977). Further west, where rainfall is much lower (< 1000 mm a^{-1}), it appears that landslides have not been considered even though rock falls are omnipresent. However, the recognition of a large rotational landslide in the Wolgan valley to the north (Macris, 2002) has helped to change this perception.

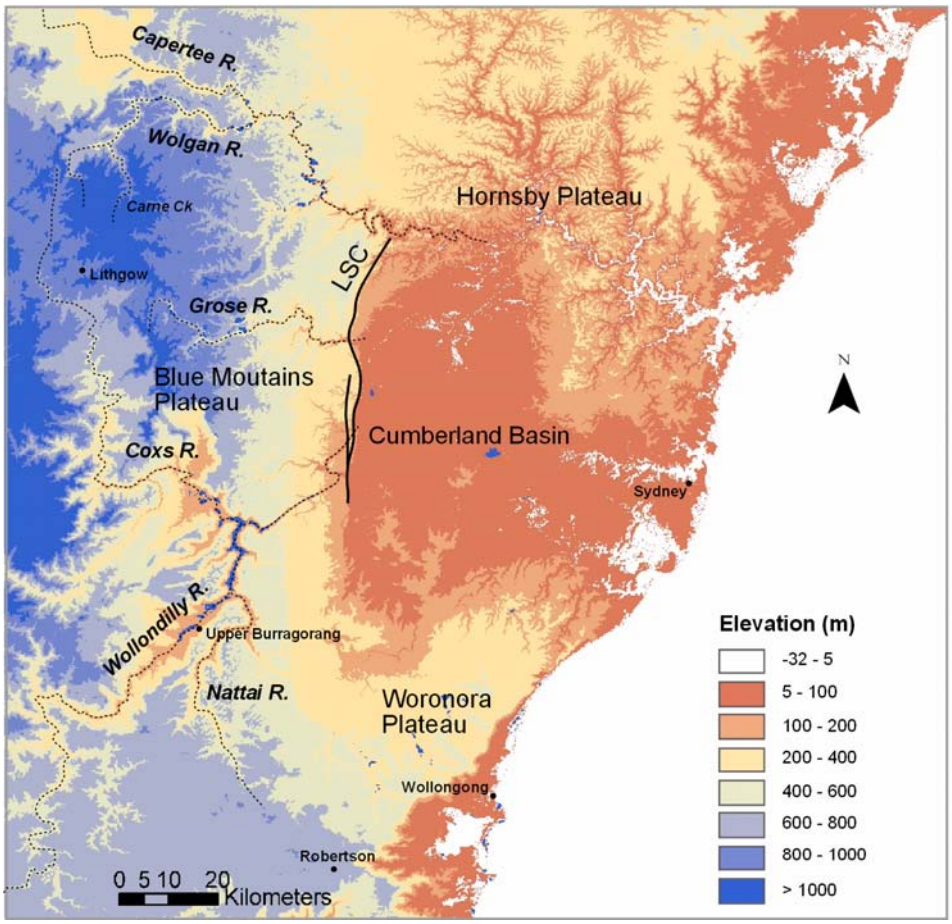

Figure 1: *Incised valleys of the Blue Mountains Plateau and locations mentioned in the text. Structure according to Bembrick et al. (1973).*

Landslide failure triggered by earthquakes has been widely reported internationally, especially in tectonically active regions (e.g. Keefer, 1984; Keefer, 1994; Dadson *et al.*, 2003). Despite being located on a plate centre, earthquakes have been recorded in Australia, although events are of a comparatively lower frequency and lower magnitude than those at plate boundaries (Sinadinovski *et al.*, 2000). McCue (1999) relates the distribution of earthquakes across Australia to the dominant north – south and east – west intraplate stress patterns (Figure 2) created through the northward movement of the Indo-Australian plate and the eastward movement of the Pacific plate. He shows the development of north-west and north-east oriented shear zones across the Australian continent, aligned to areas of seismicity, uplift and earlier volcanism. The centre of Australia is dominated by a north-west shear zone which extends from the east coast around Sydney. A north-east shear zone occurs parallel to the east coast and includes the south-eastern highlands. The Sydney Basin, and in particular the southern end of the Blue Mountains Plateau which includes the Nattai River, is revealed as an area of earthquake activity, the largest of which were recorded at Robertson in 1961 and Burragorang in 1973 with magnitudes of 5.6 and 5.5 respectively (Drake, 1976; Reynolds, 1976). The occurrence of earthquakes and intersection of shear zones across the Sydney Basin poses an important question. Could the landslides in the incised valleys of the Blue Mountains Plateau be

triggered by seismicity? In this paper we explore the spatial relationship between landslide occurrence and earthquakes to assess if such a link exists.

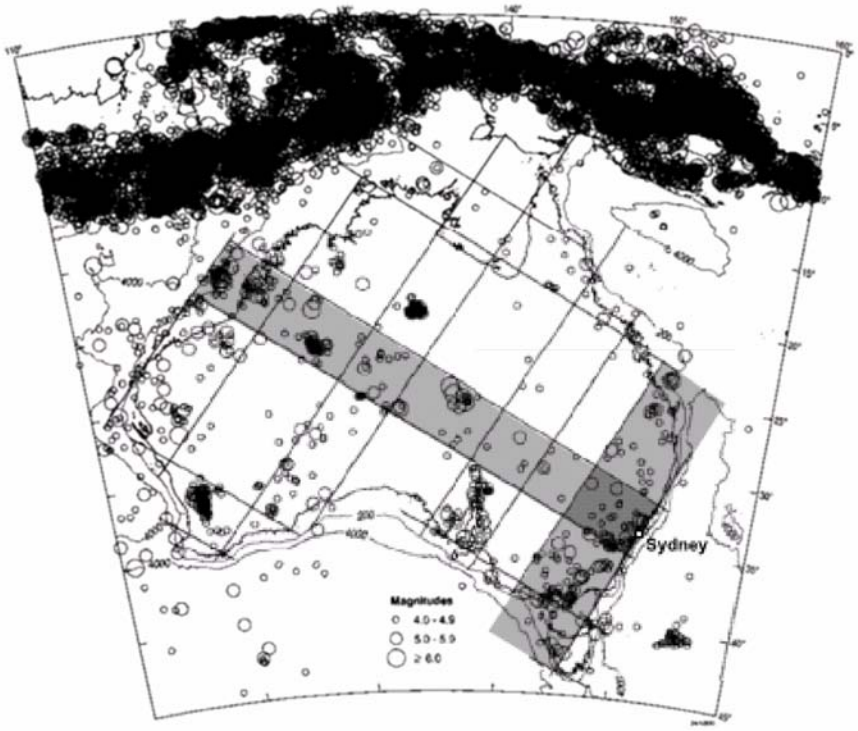

Figure 2: *Distribution of earthquakes across Australia (magnitude > 4) showing the relationship to north-west and north-east oriented shear zones. The Sydney Basin is located at the intersection of the central Australian (north-west) and east coast (north-east) shear zones (indicated by shading). (Source: McCue, 1999)*

LANDSLIDE OCCURRENCE AND DISTRIBUTION IN THE BLUE MOUNTAINS PLATEAU

Early geology reports from the Wollondilly and Nattai valleys comment on accumulations of large blocks of sandstones at the base of hillslopes, covered with debris and dense vegetation (Etheridge, 1893; McElroy and Relph, 1958). These blocks were sourced from the vertical cliff line above formed in the Hawkesbury and Narrabeen Group rocks. Reconnaissance investigations revealed that large mounds of blocks are widespread on the lower hillslopes and in the valley floor particularly along the lower Wollondilly and Nattai Rivers. Several large landslides were discovered in the Nattai and Wollondilly catchments which pre-date European settlement. For example, Tumbledown Landslide in the Nattai valley 5.5 km upstream of the confluence with the Wollondilly River, Bimlow Terrace on the Wollondilly River 5 km upstream of the confluence with the Coxs River and Lacys Landslide on Lacys Creek 10 km upstream of the confluence with the Wollondilly (Figure 1). Recent investigation of the Tumbledown Landslide found it to consist of a rock avalanche deposit of 1.5 M m^3 overlying an older, more extensive rotational landslide (Taylor, 2005). More recent smaller landslides along the Burragorang Walls at North Nattai have been associated with coal mining (Pells *et al.*, 1987; Cunningham, 1988). Mapping of the geology of the lower Wollondilly valley by McElroy and Relph (1958) shows additional areas of slumping which may represent landsliding but these areas are yet to be ground truthed.

Other large landslides in the Blue Mountains Plateau have been found in the Wolgan Valley along Carne Creek, a major tributary (Figure 1). The Carne Landslide is approximately 30 M m^3 and is

composed of Narrabeen Group sandstones sourced from the upper cliff line. Carne Creek has incised through into the Permian sediments which now form the valley floor and lower slopes. The landslide itself probably blocked Carne Creek, which is now manifested as an over steepened reach in the creek bed longprofile, with the drainage line pushed against the western valley side. The exact age of the landslide is unknown. However, material from a partly infilled depression in the toe-zone, but well away from any fluvial influence, was dated by Optically Stimulated Luminescence (OSL-SAR method using multiple grain quartz; University of Melbourne, Luminescence Laboratory) as 13.6 $\pm$ 2 ka, indicating at least a Late Pleistocene age for the landslide (Macris, 2002).

It is likely that large landslides are more widespread in the incised valleys of the Blue Mountains Plateau but have remained undiscovered due to the rugged terrain and difficulty of access. Air photo interpretation is hampered by a thick vegetation cover and also by "shadowing" from high cliffs and steeper valley sides. Thus known or strongly suspected landslides (e.g. Tumbledown, Lacys and Bimlow) were detected where the vegetation had been partly cleared and by way of drainage disruption and anomalous contouring on topographic maps (Rib and Liang, 1978).

SEISMICITY IN THE SOUTH-WEST SYDNEY BASIN

The distribution of earthquakes recorded in the Sydney Basin since 1872 is shown in Figure 3. There is a distinct cluster of earthquakes in the south-west of the basin at the location of the Wollondilly River (Warragamba to Upper Burragorang) and also on the western margin around Lithgow, and the southern margin near Mittagong and Wollongong. The south-west cluster, shown in more detail in Figure 4, includes 16 earthquakes and 291 aftershocks measured since 1960 (Table 1). The majority of the 16 earthquakes were between magnitude 1 and 3 and occurred at mid-crustal depths with the exception of 3 earthquakes which occurred at the surface and could be mining related (blasting). The largest earthquake was the Burragorang / Picton earthquake (M 5.5) which is discussed below.

The Burragorang earthquake (also known as the Picton earthquake) occurred on 9 March 1973 under the southern end of Lake Burragorang in the Wollondilly valley (Drake, 1974). The earthquake registered a magnitude 5.5 and was followed by 23 aftershocks which continued to occur for several months after the main shock (Mills and Fitch, 1977). The epicentre of the earthquake was located 6 km east of Yerranderie, although the area of seismicity extended in a north-west to south-east direction for 25 $\pm$ 4 km (MWSDB, 1974). The earthquake is thought to have resulted from movement along a steeply dipping thrust fault which extends 8 – 24 km depth below the surface within the Palaeozoic basement rocks, and approximately 8 km laterally along a north-west to south-east strike (Mills and Fitch, 1977). The earthquake was felt over an area of 60,000 km^2, however, structural damage in the township of Nattai 17 km north-east of the epicentre was reported to be no worse than at Wollongong 65 km away, suggesting that ground movement at the surface in the vicinity of the epicentre was probably minor (Denham, 1976).

DISCUSSION

The overlap in the distribution of earthquakes and landslides in the lower Wollondilly and Nattai valleys suggests a possible cause and effect link. Alternatively, it may be a coincidence given the presence of landslides in the Wolgan Valley to the north where very few seismic events have occurred since 1872. However, the problem with this analysis is that the Carne Landslide occurred well outside the modern seismic record and it is impossible to determine if seismicity was a trigger or contributing factor. Similarly, the ages of the Wollondilly and Nattai landslides are at least pre-European and therefore outside the period of record. The only landslides known to have occurred within the period of the seismic record are those at North Nattai, but these are attributed to ground subsidence caused by pillar extraction for coal mining (Pells *et al.*, 1987; Cunningham, 1988). Nonetheless analysis of the timing of failures at North Nattai (Pells *et al.*, 1987) shows some

possible overlap with recorded seismic events (Table 1) in 1973, 1976 and 1979, but not for the late 1965, December 1983 and early 1984 failures. Additionally, the Burragorang earthquake showed that moderate earthquakes can impact on structures tens of kilometres away, which suggests that slopes at or close to the angle of stability in neighbouring valleys might be affected. Therefore, we conclude that seismicity has been recorded within the areas where landslides occur, but we can neither confirm nor rule out a seismic link at this stage.

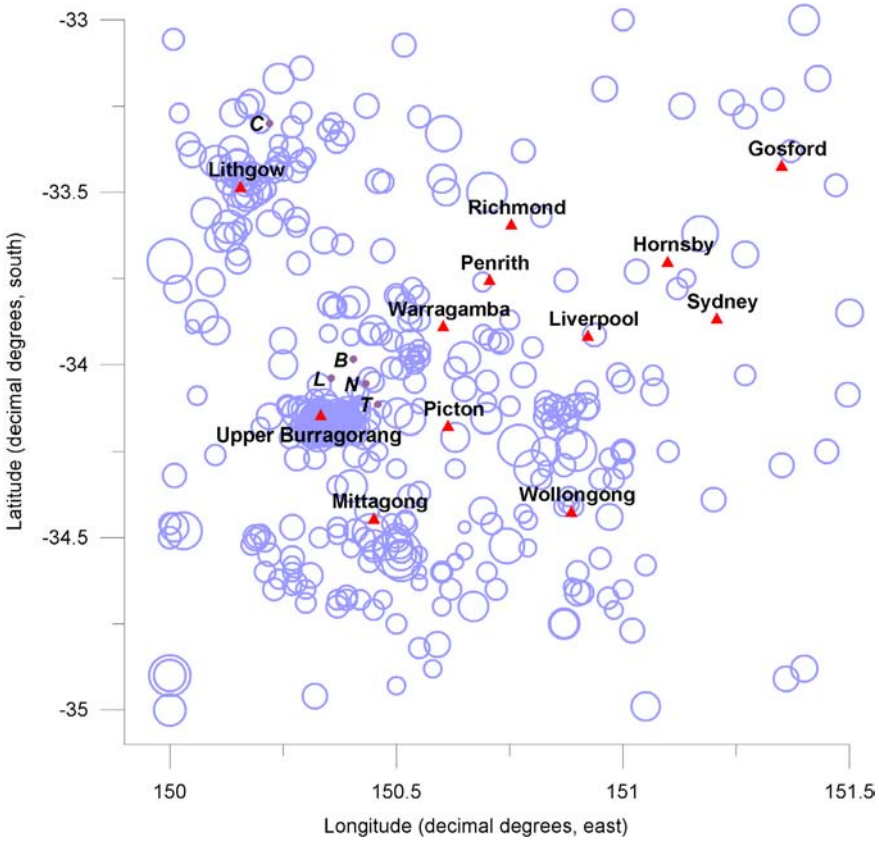

Figure 3: *Seismic events recorded in the Sydney Basin since 1872. Landslides indicated as C – Carne, B – Bimlow, L – Lacys, T – Tumbledown, N – North Nattai (Source: Geoscience Australia Earthquake Database http://www.ga.gov.au/oracle/quake/quake_online.jsp)*

The magnitude of earthquakes may be a key factor in determining if a landslide is triggered along the steep sides of the incised valleys in the Blue Mountains Plateau. Reynolds (1976) reports that a magnitude 5.5 earthquake is not likely to fracture hard rock at the surface or within 1 km of the epicentre, whereas a magnitude 6.5 earthquake is very likely to fracture hard rock at the surface. The strong joining patterning in the Triassic sandstones suggests that the vertical cliff lines could fracture and fail under a magnitude 6.5 earthquake or greater. Based on early records, Drake (1976) estimates that the return interval of a magnitude 5.5 earthquake in the south-west Sydney Basin is approximately 30 years, whilst the return interval of a magnitude 6.5 earthquake is approximately 300 years. More recent analysis of earthquake magnitude recurrence by Berryman and Stirling (2003) for the western Sydney Basin, which includes the LSC and Blue Mountains Plateau, indicates slightly longer return intervals. For example, a magnitude 6 earthquake is predicted to have a return of around 1,000 years and earthquakes of magnitude 7 to 7.5 may have return intervals of 10 – 25 kyr. Using the Tumbledown and Carne Landslides as indicators of the volume of rock that could be removed by landslides from the incised Nattai valley, the estimated return period of a 1.5 M m^3

landslide (Tumbledown) is around 1,000 – 2,500 years, which is consistent with the return period of an earthquake of magnitude 6 - 6.5 (see Appendix 1 for details). The estimated return period of a 30 M m^3 landslide (Carne) is around 20 – 50 kyr, which is consistent with the return period of an earthquake of magnitude 7.5 or greater. Therefore, it is possible that higher magnitude earthquakes may explain the occurrence of the larger, older landslides and the absence of earthquake induced landslides since European settlement where maximum recorded earthquake magnitude was 5.5 (Burragorang) and 5.6 (Robertson).

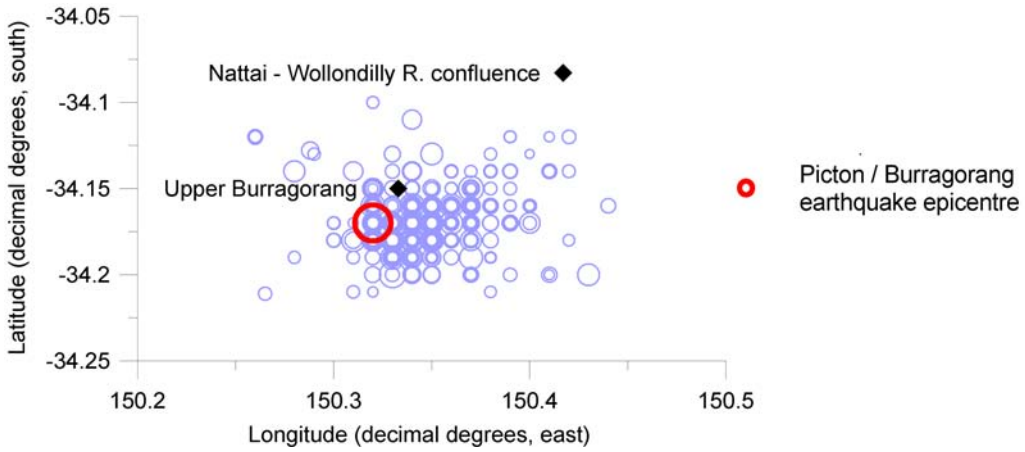

Figure 4: *Detail of the south-west cluster of seismic events (Latitude -34.1 to -34.25; Longitude 150.25 to 150.45) showing the location of the Burragorang earthquake epicentre. (Source: Geoscience Australia Earthquake Database http://www.ga.gov.au/oracle/quake/quake_online.jsp)*

Table 1: Timing, depth and magnitude of earthquakes within the south-west cluster (Latitude -34.1 to -34.25; Longitude 150.25 to 150.45) Source: Geoscience Australia Earthquake Database http://www.ga.gov.au/oracle/quake/quake_online.jsp)

DATE OF EARTHQUAKE	DEPTH (KM)	MAGNITUDE	NOTES
02/09/1960	10	1.7	
23/06/1962	0	1.9	
10/07/1962	8	3.2	
09/03/1973	21	5.5	Burragorang / Picton earthquake
09/03/1973 to 23/07/1973	Max 38	Max 3.9	Aftershocks
16/11/1974	0	1.2	
06/03/1975	0	1.5	
18/08/1976	16	2.4	
26/01/1978	17	2.3	
15/01/1979	24	2.8	
19/04/1979	20	2	
16/03/1982	23	2.2	
31/12/1982	19	2	
15/02/1986	24	1.7	
02/04/1987	22	2.7	
06/06/1996	20	2.5	
26/06/2001	10	1.9	

CONCLUSIONS

Landsliding may be an important process in valley widening and hillslope denudation of the incised valleys in the Blue Mountains Plateau, though the conditions or triggers of failure have not been determined. Earthquakes have been found to trigger landslides in Europe and elsewhere, and therefore warrant consideration. Analysis of seismic records for the Sydney Basin revealed a

clustered distribution of earthquakes particularly in the south-west of the basin at Upper Burragorang. The south-west cluster coincides with the occurrence of several large pre-European landslides. The age of the landslides however, precludes establishing a clear association. The only landslides to occur within the period of record do not show a consistent overlap in the timing of failure and are thought to be a direct response to underground coal mining. The largest magnitude earthquakes on record (5.5 and 5.6), however, may not have been significant enough to trigger slope failure. It may be that the larger, older landslides were triggered by higher magnitude events but we are unable to confirm this.

ACKNOWLEDGMENTS

This contribution forms part of a collaborative research program with the Sydney Catchment Authority (2003/28).

REFERENCES

Bembrick, C.S., Herbert, C., Scheibner, E., and Stuntz, J. 1973. Structural subdivision of the New South Wales portion of the Sydney - Bowen Basin. *Quarterly Notes of the Geological Survey of NSW* **11**: 1-13.

Berryman, K., and Stirling, M. 2003. Earthquake ground motion and fault hazard studies at the Lucas Heights Research Reactor Facility, Sydney, Australia: evolution of methods and changes in results. International Symposium on Seismic Evaluation of Existing Nuclear Facilities, Vienna. August 2003, 43-47.

Branagan, D.F., and Pedram, H. 1990. The Lapstone Structural Complex, New South Wales. *Australian Journal of Earth Sciences* **37**: 23-36.

Brunker, R.L., and Rose, G. 1967. Sydney Basin 1:500,000 Geological Sheet (Special). New South Wales Department of Mines, Sydney.

Cunningham, D.M. 1988. A rockfall avalanche in a sandstone landscape, Nattai North NSW. *Australian Geographer* **19 (2)**: 221-229.

Dadson, S.J., Hovius, N., Chen, H., Dade, W.B., Hsieh, M.-L., Willett, S.D., Hu, J.-C., Horng, M.-J., Chen, M.-C., Stark, C.P., Lague, D., and Lin, J.-C. 2003. Links between erosion, runoff variability and seismicity in the Taiwan orogen. *Nature* **426**: 648-651.

Denham, D. 1976. Effects of the 1973 Picton and other earthquakes in Eastern Australia. *Bulletin - Australia, Bureau of Mineral Resources, Geology and Geophysics* **164**: 15-27.

Drake, L. 1974. The Seismicity of New South Wales. *Journal and Proceedings of the Royal Society of New South Wales* **107**: 35-40.

— 1976. Seismic risk in New South Wales. *Bulletin - Australia, Bureau of Mineral Resources, Geology and Geophysics* **164**: 5-8.

Etheridge, R. 1893. Geological and ethnological observations made in the valley of the Wollondilly River, at its junction near the Nattai River, counties Camden and Westmoreland. *Records of the Australian Museum* **2 (4)**: 46-54.

Keefer, D.K. 1984. Landslides caused by earthquakes. *Geological Society of America Bulletin* **95**: 406-421.

— 1994. The importance of earthquake-induced landslides to long-term slope erosion and slope-failure hazards in seismically active regions. *Geomorphology* **10**: 265-284.

Lithografica Artistica Cartographica 1979. Sydney and Environs 1:200,000 raised relief map. Geo-Maps Company, Sydney.

Macris, J. 2002. Processes of Valley Slope Evolution; Evidence from the Western Blue Mountains, NSW. [Unpublished Honours thesis] Macquarie University, Sydney.

McCue, K. 1999. The cause of current Australian intraplate volcanism. ACES Inaugural Workshop, 31 January - 5 February 1999. Brisbane / Noosa, Queensland, Australia, 509-512.

McElroy, C.T., and Relph, R.E. 1958. Explanatory notes to accompany geological maps of the inner catchment, Warragamba storage. Department of Mines, Geological Survey of NSW, Sydney.

Mills, J.M., and Fitch, T.J. 1977. Thrust faulting and crust - upper mantle structure in East Australia. *Geophysical Journal of the Royal Astronomical Society* **48**: 351-384.

MWSDB 1974. Seismological investigations. Burragorang earthquake and aftershocks. Map and report. Metropolitan Water Sewerage and Drainage Board, Sydney.

Pells, P.J.N., Braybrooke, J.C., Mong, J., and Kotze, G.P. 1987. Cliff line collapse associated with mining activities. *in* Walker, B.F., and Fell, R., eds., *Soil Slope Instability and Stabilisation* Balkema, Rotterdam, 359-385.

Reynolds, R.G. 1976. Coal mining under stored water: report on an inquiry into coal mining under or in the vicinity of the stored waters of the Nepean, Avon, Cordeaux, Cataract and Woronora Reservoirs, New South Wales, Australia. Department of Public Works, Sydney.

Rib, H.T., and Liang, T. 1978. Recognition and identification. In *Landslides Analysis and Control*, Schuster, R.L., and Krizek, R.J., (eds). National Academy of Sciences, Washington; 34-80.

Sinadinovski, C., McCue, K., and Somerville, M. 2000. Characteristics of strong ground motion for typical Australian intra-plate earthquakes and their relationship with the recommended response spectra. *Soil Dynamics and Earthquake Engineering* **20**: 101-110.

Taylor, G.M. 2005. Landslides around Lake Burragorang: their characteristics, distribution and impact potential. [Unpublished Honours thesis] Macquarie University, Sydney.

Tomkins, K.M., Humphreys, G.S., Skeen, H.J., Taylor, G.M., Farwig, V.J., Shakesby, R.A., Doerr, S.H., Wallbrink, P., Blake, W.H., and Chafer, C.J. 2004b. Deciphering a colluvial mantle: Nattai catchment. SuperSoil 2004: Program and Abstracts for the 3rd Australian and New Zealand Soils Conference. University of Sydney, Australia, www.regional.org.au/au/asssi/supersoil2004.

van der Beek, P., Pulford, A., and Braun, J. 2001. Cenozoic landscape development in the Blue Mountains (SE Australia): Lithological and tectonic controls on rifted margin morphology. *The Journal of Geology* **109**: 35-56.

Walker, P.H. 1963. Soil history and debris-avalanche deposits along the Illawarra scarpland. *Australian Journal of Soil Research* **1 (1)**: 223-230.

Wellman, P., and McDougall, I. 1974. Potassium-argon ages on the Cainozoic volcanic rocks of New South Wales. *Journal of the Geological Society of Australia* **21 (3)**: 247-272.

Young, A.R.M. 1977. The characteristics and origin of coarse debris deposits near Wollongong, N.S.W., Australia. *Catena* **4**: 289-307.

APPENDIX 1. CALCULATION OF LANDSLIDE RETURN INTERVALS

The return intervals of the Tumbledown and Carne Landslides were estimated using the volume of the incised section of the Nattai valley as an indicator of erosion over time by landsliding. In doing so, we are assuming that landslides are the dominant erosional process leading to valley widening once a knickpoint has passed, and other processes such as slope wash have a negligible effect on erosion rates. The volume of the incised Nattai valley was determined by GIS (ArcMap, ArcHydro) using a 25 m digital elevation model, clipped to the top of the cliff line. The timeframe of valley erosion is indicated by Oligocene and Miocene basalts (Wellman and McDougall, 1974; van der Beek *et al.*, 2001) situated on the plateau in the Nattai and Grose River valleys which show that valley incision post-dates their extrusion.

Tumbledown Landslide	
Volume of Tumbledown Landslide	1.5 M m^3 = 0.0015 km^3
Volume of the incised Nattai valley	21.3 km^3
No. of landslides of this size required to erode the incised Nattai valley	14,200
Timeframe of erosion	14 – 34 Ma
Estimated return period of 1.5 M m^3 landslide	1,000 – 2,500 years

Carne Landslide	
Volume of Carne Landslide	30 M m^3 or 0.03 km^3
Volume of the incised Nattai valley	21.3 km^3
No. of landslides of this size required to erode the incised Nattai valley	710
Timeframe of erosion	14 – 34 Ma
Estimated return period of 30 M m^3 landslide	20,000 – 50,000 years

Ground movements and seismicity associated with underground coal mining in the Appin area

Peter Hatherly[1], Bruce Hebblewhite[2] and Greg Poole[3]

[1] School of Geosciences, University of Sydney, NSW, 2006
[2] School of Mining Engineering, University of NSW, 2052
[3] BHP Billiton, PO Box 514, Unanderra, NSW, 2526

INTRODUCTION

BHP Billiton commenced mining coal at Appin Colliery in 1962. Two other collieries, West Cliff and Douglas (formerly Tower) also now operate in the area. These collieries mine the Bulli Coal seam, a high grade coking coal which is at a depth of approximately 500 m. The mines use the longwall method. Panels of coal of dimensions about 250 m by 2 km are progressively extracted. To date an area of approximately 60 km^2 has been mined. Figures 1 and 2 show the locations of the mines.

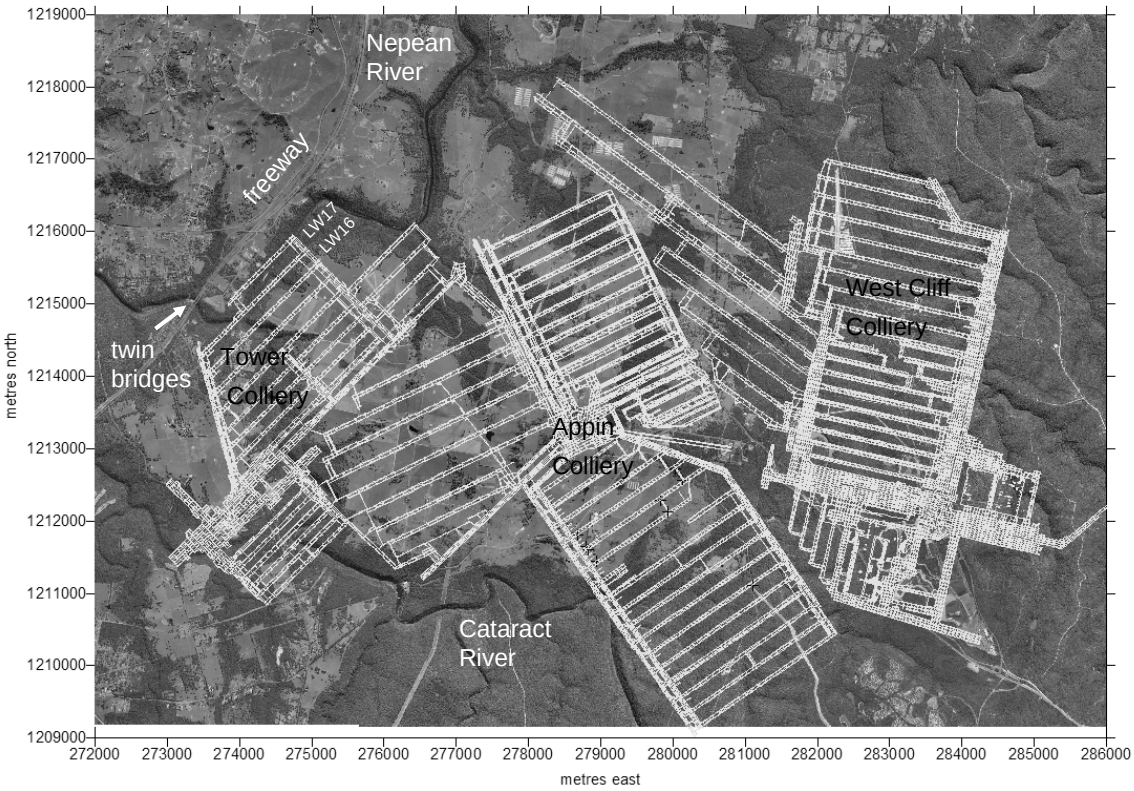

Figure 1. *Mine layouts for Appin, Tower and Westcliff Collieries as of 2005 superimposed on an aerial photograph. The freeway is part of the Hume Highway running between Sydney and Melbourne. Twin bridges cross the Nepean River gorge at the location shown. To the east of the bridge, the Nepean River joins the Cataract River and flows to the north east. Tower Colliery has mined beneath much of the Cataract River. Monitoring of the bridges was conducted during the extraction of Tower Colliery longwalls 16 and 17. Seismic monitoring was also conducted for some of this time.*

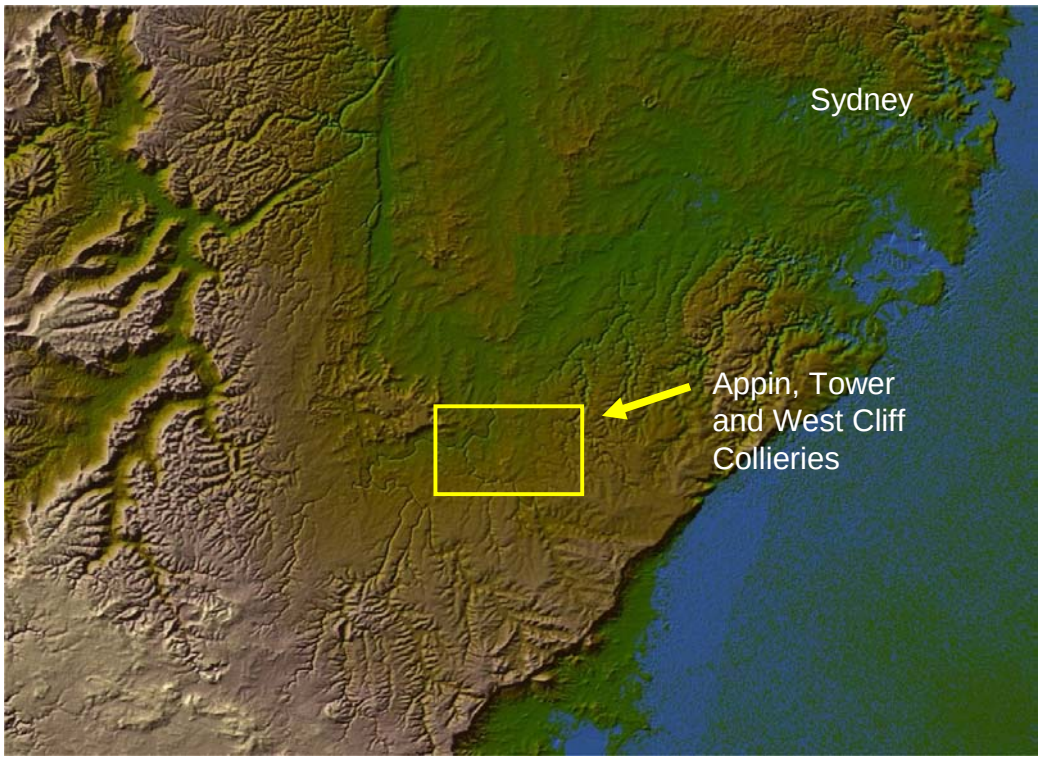

Figure 2. *Shuttle radar image showing location of Appin, Tower and West Cliff Collieries southwest of Sydney. The north-south trending Lapstone Structural Complex is evident to the northwest and continues to the west of the area of mining. Complex NW trending normal fault systems with throws of several tens of metres extend into the area from the coast. (Image compiled from http://jaeger.earthsci.unimelb.edu.au/Images/Landform/landform.html)*

Longwall mining extracts most of the coal seam. In response to the mining, the overlying strata fracture and displace (cave) into the void that is created. To a height of about 40 m above the seam, the strata are completely broken. For strata further from the seam, the displacements are progressively more elastic and the beds retain their integrity. At the ground surface, the subsidence is about 60% of the height of the extracted seam. For a 2 m thick Bulli seam, the subsidence is approximately 1.2 m. There may be some tensile failure at the ground surface, related to strata bending over extraction edges, but the cracking associated with this has limited depth extent.

To a certain extent, the movement of the overlying strata into the void left by the mining is mirrored in the underlying strata. Miners must therefore also manage movements and breakage in the underlying strata . In the Appin area, one consequence of this is that methane gas contained in underlying coal seams can make its way into the mine workings through fractures induced in the floor strata.

The caving associated with longwall coal mining also relaxes the strata in the vicinity of the mine. The extent of the relaxation is partly controlled by the nature of the strata but it is also related to the prevailing stress fields. In the case of the Appin area, the stress field is strongly deviatoric. At Tower Colliery, the ratio of the horizontal to vertical pre-mining stress is in excess of 3:1 with a predominant northeast orientation for the major principal stress direction (Hebblewhite, et al., 2000). At Appin and West Cliff Collieries, the major principal stress has a more easterly orientation (MacGregor, 2003).

In the late 1990's, Tower Colliery conducted longwall mining beneath sections of the deep (+50 m) gorges associated with the Cataract and Nepean Rivers, see Figures 1 and 3. As part of the mining of longwall panels 16 and 17 (see Figures 1 and 3), an extensive surface monitoring campaign was implemented in conjunction with the NSW Roads and Traffic Authority (RTA) and a Bridge Management Committee set up to assess the impact of this mining on the gorges and the Douglas Park bridges carrying the Hume Highway over the Nepean River. These bridges are over 600 m from the closest caving in longwalls 16 and 17 which were mined at a depth of about 450 m. Results of the monitoring are given in Hebblewhite et al. (2000).

Quite separately to the monitoring of ground surface movements, interest in the possibility that seismicity might also be occurring at this time was aroused following the chance recording of a seismic event during a conventional seismic reflection survey by BHP Billiton in July1998. This was followed by a magnitude 4.4 event on 17 March 1999 located just to the south of BHP Billiton's mines. Local residents were also reporting noticeable ground vibrations. BHP Billiton therefore undertook a preliminary program of seismic monitoring. Results are reported in Hatherly et al. (2000) and Vasundhara et al. (2000).

***Figure 3**. Detail of the Nepean and Cataract Rivers, longwalls 16 and 17 of Tower Colliery, the freeway, bridges and other infrastructure. Harris Creek flows south through a narrow ravine to the Nepean River. It is thought that difficult ground conditions in in-seam drill holes and mine headings in the northwest corner of LW16 are due to a northerly continuation of a north-south trending fault encountered further south in Tower Colliery. Black stars indicate locations of some of the seismic events detected during the period September 1999 to January 2000.*

In this paper, results of these two monitoring programs are summarized and we present some thoughts on the mechanisms that may be involved.

MONITORING OF THE DOUGLAS PARK BRIDGES

The monitoring program instituted by the Bridge Management Committee consisted of the following (Hebblewhite et al., 2000).

- GPS monitoring of targets across the terrain for horizontal movement.
- Conventional precise leveling and theodolite surveys in selected, accessible traverse lines across the overall terrain, gorges and adjacent to, and on the bridge, pier and foundation structures.
- EDM surveys on gorge closure at nominated cross gorge locations.
- Remote electronic monitoring of critical locations on the bridge decks, expansion gaps, bearing and other key structural locations.

The results of this study confirmed that although the bridge structure underwent some significant lateral movement towards the mining location, its serviceability was never compromised. In the vicinity of the bridges, the majority of the movement was of a regional 'rigid body' nature, with the bridge and the surrounds moving en-masse towards the mine. There was movement of 65 mm due to the mining of LW16 and a further 70 mm due to LW17. Directly above the longwall panels, subsidence was also observed as well as gorge closure and some degree of relative 'upsidence'. It is the large amounts of regional, horizontal ground movement, extending over quite considerable distances away from the mining that are of most interest in this paper.

SEISMIC EVENTS

The seismic monitoring was undertaken between August 1999 and June 2000 using 15 short period seismographs made available by the Australian National Seismic Imaging Resource (ANSIR). With no knowledge of where the seismicity, if any, would be located, the units were deployed across BHP Billiton's mining leases in the Appin area. The vertical component of the ground motion was mainly recorded.

From this program of monitoring, it was found that there were occasional seismic events that could be correlated over distances of about 6 km. The locations of these (see Figure 3) were found to be in the vicinity of Tower Colliery and the Nepean and Cataract River gorges. Some were also felt by residents.

The depths of the events are thought to have been less than 1 km. Their timing did not necessarily coincide with periods of active mining as is the case with the much smaller microseismic events caused by rock fracturing during longwall caving (see Hatherly et al., 2003, for example). However, by June 2000 when the mining of longwall 17 was completed, the seismic activity ceased.

DISCUSSION

Hebblewhite et al. (2000), discuss potential mechanisms for the observed subsidence and the lateral movement of the bridges towards the mine. To explain the lateral movement, three mechanisms were proposed.

- relaxation of strata in the direction of the principal horizontal stress towards the sides of the longwall panels,
- activation of geological structures, and
- the cantilevering of massive strata.

Unfortunately the measurements of ground movement did not extend far enough to the west to allow the extent of the zone of en-masse movement to be determined. In particular, it is not known how the ground moved west of Harris Creek, immediately to the west of the bridges (see Figure 3). This creek flows through a narrow ravine to its junction with the Nepean River and could well be located on a north trending geological fault inferred from the results of mine exploration.

Hatherly et al. (2000) also discuss the issues of triggered seismicity caused by mining as discussed by McGarr and Simpson (1997). Triggered seismicity is produced when an engineering activity such as mining and the filling of reservoirs causes small but sufficient changes to the overall stress field to facilitate ground movement. For example, around the mature coal mining areas of countries such as in Poland and Britain, there have been increases in the regional seismic activity. In the case of the Appin area, the Geoscience Australia website[1] also shows that there was a small cluster of small seismic events in the Appin area between 1971 and 1978 but at that time, the mining was not as extensive as at present.

There has been no mining north of LW17 since 2000, and the new Douglas Colliery is currently mining further to the east. The situation with regards to ground movement and seismic activity in the vicinity of the gorges of the Cataract and Nepean Rivers has stabilized. However, the question of exactly how the mining induced changes to the stress field interacted with the tectonic stress field in the period of 1999 to 2000 remains unanswered. If mining were to recommence in this area, the ground movements and seismic activity could well recommence.

ACKNOWLEDGEMENTS

This paper is published with the permission of BHP Billiton, Illawarra Coal. ANSIR is thanked for making available the short period seismographs.

REFERENCES

Hatherly, P., Poole, G., and Luo, X., 2000. Seismicity in the Appin area of NSW and its association with mining activities. V.H. Jensen and B. Butler, editors. Conference of the Australian Earthquake Engineering Society. 15-16 November 2000, Hobart, pp. 6-1 to 6-6.

Hatherly, P., Gale, W., Medhurst, T., King, A., Craig, S., Poulsen, B. and Luo, X., 2003. 3D stress effects, rock damage and longwall caving as revealed by microseismic monitoring. End of grant report. Australian Coal Association Research Program. Project C9021.

Hebblewhite, B., Waddington, A. and Wood, J., 2000. Regional horizontal surface displacements due to mining beneath severe surface topography. 19th Intl Conference on Ground Control in Mining, Morgantown, West Virginia, August 2000, pp. 149-157. (see also http://www.mines.unsw.edu.au/Publications/publications_staff/Paper_Hebblewhite_MineSubsidence_2001.htm)

McGarr, A. and Simpson, D., 1997. A broad look at induced and triggered seismicity. Gibowicz and Lasocki, editors, Rockbursts and Seismicity in Mines, Balkema, Rotterdam, pp. 385-396.

MacGregor, S., 2003. Definition of stress regimes at borehole, mine and regional scale in the Sydney Basin through breakout analysis. A.C. Hutton, B.G. Jones, P.F. Carr, B. Ackerman and A.D. Switzer, editors, Proceedings if the 35th symposium on "Advances in the study of the Sydney Basin", September 29-30, 2003 University of Wollonging, pp. 223-232.

Vasundhara, Watts, E., Hatherly, P., Poole, G. and Hebblewhite, B., 2000. Investigation of seismicity near Appin NSW, and its association with mining geology and tectonics. 19th Intl Conference on Ground Control in Mining, Morgantown, West Virginia, August 2000.

[1] http://www.ga.gov.au/oracle/quake/quake_online.jsp

Workshop Programme

10:00 – Welcome and introduction – Dan Clark (Geoscience Australia)

10:15 – Geological context of south–eastern Australian earthquakes – M. Sandiford (University of Melbourne)

10:45 – Summary of the 'inner Sydney Basin' geology and factors that relate to seismicity – David Branagan (University of Sydney)

11:15 – 11:30 morning tea

11:30 – Landslides and landform evolution in the Sydney Basin – Geoff Humphreys & Kerrie Tomkins (Macquarie University)

12:00 – Seismicity in the Sydney Basin and its relationship to active faulting – Gary Gibson (Environmental Systems & Services)

12:30 – 13:30 lunch

13:30 – A perspective of earthquake hazard in the Sydney area based on studies for the Replacement Research Reactor Project at Lucas Heights – Kelvin Berryman (Institute for Geologic and Nuclear Sciences, NZ)

14:00 – A brief field reconnaissance along the Lapstone Structural Complex – Dan Clark (Geoscience Australia)

14:30 – The way forward: quantifying the hazard from geologic sources (discussion)

15:00 – 15:15 afternoon tea

15:15 – Further discussion followed by summary and concluding remarks

The workshop will be concluded with a short presentation at ~16:00 by Mr. Dave Dobeson (science teacher in residence at Sydney University geology) entitled "Monitoring earthquakes in high-school science classrooms". Dave's talk will be followed by beverages and nibblies.

Participants list

Last Name	First Name	Organisation	Email
Allen	Trevor	Geoscience Australia	trevor.allen@ga.gov.au
Berryman	Kelvin	IGNS New Zealand	K.Berryman@gns.cri.nz
Blong	Russel	Benfield Australia Ltd	Russell.Blong@benfieldgroup.com, rblong@els.mq.edu.au
Branigan	David	University of Sydney	dbranaga@mail.usyd.edu.au
Clark	Dan	Geoscience Australia	dan.clark@ga.ov.au
Clarke	Geoff	University of Sydney	geoffc@mail.usyd.edu.au
Collins	Clive	Geoscience Australia	clive.collins@ga.gov.au
Dent	Vic	University of Western Australia	vic_dent@yahoo.com
Dhu	Trevor	Geoscience Australia	trevor.dhu@ga.gov.au
Dobeson	Dave	University of Sydney	
Fergusson	Chris	University of Wollongong	cferguss@uow.edu.au
Garratt	Jonathan	Roads and Traffic Authority NSW	Jonathan_GARRATT@rta.nsw.gov.au
Gibson	Gary	Environmental Systems & Services	gary.gibson@esands.com
Hatherly	Peter	University of Sydney	phatherly@geosci.usyd.edu.au
Hubble	Tom	University of Sydney	tom@geosci.usyd.edu.au
Humphreys	Geoff	Macquarie University	ghumphre@els.mq.edu.au
Langford	Rob	Geoscience Australia	robert.langford@ga.gov.au
McCue	Kevin	Australian Seismological Centre	asc@netspeed.com.au
McPherson	Andrew	Geoscience Australia	andrew.mcpherson@ga.gov.au
Murray–Wallace	Colin	University of Wollongong	cwallace@uow.edu.au
Ninis	Dee	Environmental Systems & Services	Dee.Ninis@esands.com
Pachette	Annette	Geoscience Australia	annette.patchette@ga.gov.au
Potter	Anna	Geoscience Australia	anna.potter@ga.gov.au
Sandiford	Mike	University of Melbourne	mikes@unimelb.edu.au
Sommerville	Paul	URSCorp	Paul_Somerville@URSCorp.com
Tomkins	Kerrie	Macquarie University	ktomkins@els.mq.edu.au